

SOLUTIONS TO SELECTED PROBLEMS IN MULTI-COMPONENT  
MIXED-BED ION EXCHANGE MODELING

By

EDWARD J. ZECCHINI

Bachelor of Science  
Rensselaer Polytechnic Institute  
Troy, New York  
1985

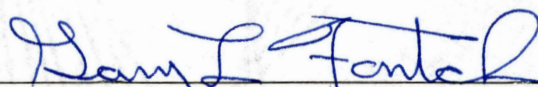
Master of Science  
Oklahoma State University  
Stillwater, Oklahoma  
1986

Submitted to the Faculty of the  
Graduate College of the  
Oklahoma State University  
in partial fulfillment of  
the requirements for  
the Degree of  
DOCTOR OF PHILOSOPHY  
July, 1990

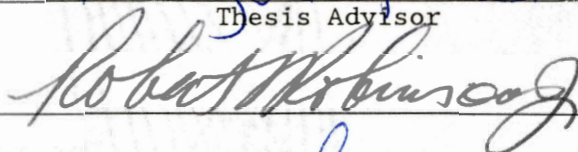
Sheet  
1990D  
Z420  
cop. 2

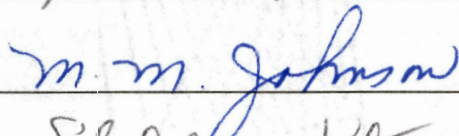
SOLUTIONS TO SELECTED PROBLEMS IN MULTI-COMPONENT  
MIXED-BED ION EXCHANGE MODELING

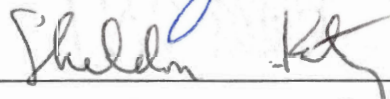
Thesis Approved:

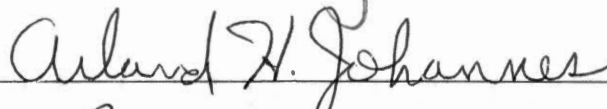


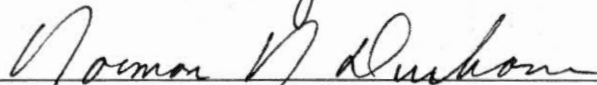
Thesis Advisor











Dean of the Graduate College

## PREFACE

This study involved addressing specific areas of multi-component mixed-bed ion exchange modeling at low concentrations. Film-diffusion control and bulk-phase neutralization were implemented to obtain rate expressions. A material balance framework was instituted in order to determine outlet-concentration profiles for mixed-bed ion exchange units. Amine cycle ion exchange and ternary cation exchange models have been compared to existing experimental data with mixed results. The model has been extended to handle six component exchange in neutral and pH adjusted water streams. The resultant model can accomplish the mixed-bed simulations necessary to optimize existing ion exchange columns.

I wish to express my deepest gratitude to my advisor Dr. Gary L. Foutch, for his irreplaceable assistance and total candor throughout the course of this study. I would also like to thank Dr. A. H. Johannes for his assistance and support without which this work would never have been accomplished. The aid of Dr. Sheldon Katz, Dr. M. M. Johnson, Dr. Jan Wagner and Dr. Robert L. Robinson, Jr., as committee members was paramount in the completion of this study.

I would like to thank Dr. Robert L. Robinson, Jr. and Amoco Foundation, Inc. for the fellowship which provided my financial support. This financial support provided me the ability to pursue this study.

Special thanks must be given to my parents Charles and Janette Zecchini, and my wife's, Thomas and Lois Hopkins, whose emotional support was unfailing throughout my time at Oklahoma State University. The patience, love, support, and above all, understanding that my wife, Cathy, provided during my tenure as a graduate student at Oklahoma State receive my undying gratitude. Without her, this work would never have been attempted, not to mention finished.

## TABLE OF CONTENTS

Chapter	Page
I. INTRODUCTION.....	1
Ion Exchange Kinetics.....	4
Mixed-Bed Ion Exchange.....	8
Mixed-Bed Modeling.....	10
Objectives.....	14
II. MIXED-BED ION EXCHANGE MODELING WITH AMINE FORM CATIONIC RESIN.....	16
Abstract.....	16
Introduction.....	16
Model Development.....	21
Assumptions.....	21
Flux Expressions.....	24
Particle Rates and Effective Diffusivities.....	25
Material Balances.....	27
Temperature Effects.....	29
Discussion.....	29
Rates of Exchange.....	32
Column Simulations.....	38
Conclusions and Recommendations.....	50
References.....	53
III. MULTI-COMPONENT UNI-VALENT MIXED-BED ION EXCHANGE MODELING IN NEAR NEUTRAL SYSTEMS.....	54
Abstract.....	54
Introduction.....	54
Model Development.....	59
Assumptions.....	59
Flux Expressions.....	61
Particle Rates.....	63
Material Balances.....	64
Discussion.....	65
Ternary Data.....	65
Exchange Rates.....	69
Column Evaluations.....	76
Conclusions and Recommendations.....	88
References.....	91

Chapter	page
IV. MULTI-COMPONENT MIXED-BED ION EXCHANGE MODELING IN AMINATED WATERS.....	91
Abstract.....	92
Introduction.....	92
Model Development.....	95
Assumptions.....	95
Flux Expressions.....	97
Rate Equations.....	99
Material Balances.....	99
Equilibrium Relations.....	100
Discussion.....	101
Ammonia.....	102
Morpholine.....	111
Conclusions and Recommendations.....	120
References.....	122
V. CONCLUSIONS AND RECOMMENDATIONS.....	123
BIBLIOGRAPHY.....	128
APPENDIXES.....	132
APPENDIX A - ANION FLUX EXPRESSIONS.....	133
APPENDIX B - TERNARY EXCHANGE EQUATIONS.....	142
APPENDIX C - PARTICLE RATES.....	150
APPENDIX D - COLUMN MATERIAL BALANCES.....	155
APPENDIX E - NUMERICAL TECHNIQUES.....	160
APPENDIX F - MODEL PARAMETER VALUES.....	164
APPENDIX G - COMPUTER CODE FOR CHAPTER III.....	166

LIST OF TABLES

Table	Page
Chapter II	
I. Selectivity Coefficients.....	19
II. Model Assumptions.....	23
III. Temperature Dependent Values.....	30
IV. Model Parameters.....	31
Chapter III	
I. Model Assumptions.....	60
Chapter IV	
I. Model Assumptions.....	96
Appendixes	
I. Comparison of Numerical Techniques.....	163



LIST OF FIGURES

Figure	Page
Chapter I	
1. Schematic Diagram of A Resin Framework.....	3
Chapter II	
1. Variation in Ionization Constants ( $K_b$ ) of Ammonia, Morpholine and Aminomethyl-Propanol.....	20
2. Ratio of Electrolyte to Non-Electrolyte Mass Transfer Coefficients for Sodium-Ammonium Exchange at Various pH's..	33
3. Ratio of Electrolyte to Non-Electrolyte Mass Transfer Coefficients for Sodium-Ammonium Exchange at pH = 9.4.....	34
4. Rate of Dimensionless Exchange of Sodium for Ammonium at Various pH's.....	35
5. Ratio of Electrolyte to Non-Electrolyte Mass Transfer Coefficients for Sodium-Morpholine Exchange, Various pH's, and Two Selectivities.....	36
6. Dimensionless Rate of Exchange of Sodium for Morpholine at Various pH's on AMBERSEP 252 ( $K = 2.1$ ).....	37
7. Dimensionless Rate of Exchange of Sodium for Morpholine at Various pH's on AMBERSEP 200 ( $K = 15.0$ ).....	39
8. Predicted Sodium Breakthrough for Ammonia Cycle Exchange with a Step Change in Inlet Concentration Compared to Bates and Johnson (1984), Experimental.....	40
9. Comparison of Time for 2 $\mu\text{g}/\text{Kg}$ Breakthrough Between this Model and Bates and Johnson (1984).....	42
10. Sodium Breakthrough Curves for Constant Feed Concentration, Ammonia Cycle Exchange at several pH's.....	43
11. Predicted Sodium Breakthrough for Ammonia Cycle Exchange at Various Cation-to-Anion Resin Ratios for pH 9.6.....	44

Figure	Page
12. Predicted Sodium Breakthrough for Ammonia Cycle Exchange at Various 25, 40 and 60°C for Temperature Independent Selectivity.....	45
13. Predicted Sodium Breakthrough for Morpholine Cycle Exchange at Various pH's and Conditions Equivalent to Figure 8.....	47
14. Comparison of Time for 2 µg/Kg Breakthrough for Ammonia Cycle and Morpholine Cycle Operation.....	48
15. Comparison of Sodium Breakthrough in the Morpholine Cycle for AMBERSEP 200 and AMBERSEP 252.....	49
16. Breakthrough Curves for Sodium and Chloride in the Morpholine Cycle at pH 9.6 for AMBERSEP 200 Cation Resin.....	51

### Chapter III

1. Comparison of Ternary Model Predictions with Omatete et al. (1980) Experimental.....	66
2. Comparison of Ternary Model Predictions with Dranoff and Lapidus (1961), Experimental.....	68
3. Ri Ratio for Sodium in the Ternary System: Sodium, Potassium, Hydrogen, at Various Potassium Resin Phase Loadings.....	70
4. Ri Ratio for Potassium in the Ternary System: Sodium, Potassium, Hydrogen, at Various Sodium Resin Phase Loadings.....	71
5. Dimensionless Rate of Exchange for Sodium in the Ternary System: Sodium, Potassium and Hydrogen.....	74
6. Dimensionless Rate of Exchange for Potassium in the Ternary System: Sodium, Potassium and Hydrogen.....	75
7. Five Component Breakthrough Curves for Sodium, Potassium and Chloride at a Cation-to-Anion Resin Ratio of 1/1.....	77
8. Five Component Breakthrough Curves for Sodium, Potassium and Chloride at a Cation-to-Anion Resin Ratio of 1/1.5.....	78
9. Five Component Breakthrough Curves for Sodium, Potassium and Chloride at a Cation-to-Anion Resin Ratio of 1.5/1.....	79
10. Five Component Breakthrough Curves for Sodium, Potassium and Chloride at a Cation-to-Anion Resin Ratio of 1/1.....	81
11. Six Component Breakthrough Curves for Sodium, Potassium, Chloride and Nitrate on a Type I Anion Exchange Resin.....	82

Figure	Page
12. Six Component Breakthrough Curves for Sodium, Potassium, Chloride and Nitrate on a Type II Anion Exchange Resin.....	83
13. Six Component Breakthrough Curves for Sodium, Potassium, Chloride and Nitrate on a Type II Anion Exchange Resin.....	84
14. Six Component Breakthrough Curves for Sodium, Potassium, Chloride and Nitrate on a Type II Anion Exchange Resin.....	85
15. Six Component Breakthrough Curves for Sodium, Potassium, Chloride and Nitrate on a Type II Anion Exchange Resin.....	86

#### Chapter IV

1. Hydrogen Cycle Operation Past the Ammonia Break for pH 9.6 and Cation-to-Anion Resin Ratio of 1/1.....	103
2. Hydrogen Cycle Operation Past the Ammonia Break for pH 9.6 and Cation-to-Anion Resin Ratio of 1/1.....	105
3. Outlet pH for Hydrogen Cycle Operation Past the Ammonia Break for pH 9.6 and Cation-to-Anion Resin Ratio of 1/1.....	106
4. Hydrogen Cycle Operation Past the Ammonia Break for pH 9.6 and Cation-to-Anion Resin Ratio of 1.5/1.....	108
5. Hydrogen Cycle Operation Past the Ammonia Break for pH 9.6 and Cation-to-Anion Resin Ratio of 2/1.....	109
6. Hydrogen Cycle Operation Past the Ammonia Break for pH 9.6 and Column Height of 10 cm, and a Cation-to-Anion Resin Ratio of 1/1.....	110
7. Hydrogen Cycle Operation Past the Ammonia Break for pH 9.6 and Cation-to-Anion Resin Ratio of 1/1 with a Square Wave Inlet Concentration Change.....	112
8. Hydrogen Cycle Operation Past the Morpholine Break for pH 9.6 and Cation-to-Anion Resin Ratio of 1/1.....	114
9. Outlet pH for Hydrogen Cycle Exchange Operation Past the Morpholine Break for pH 9.6 and a Cation-to-Anion Resin Ratio of 1/1.....	115
10. Hydrogen Cycle Operation Past the Morpholine Break for pH 9.6 and Cation-to-Anion Resin Ratio of 1.5/1.....	117
11. Hydrogen Cycle Operation Past the Morpholine Break for pH 9.6 and Cation-to-Anion Resin Ratio of 2/1.....	118

Figure

Page

12. Hydrogen Cycle Operation Past the Morpholine Break for pH 9.6 and Cation-to-Anion Resin Ratio of 1/1 with a Square Wave Inlet Concentration Change.....	119
---	-----

## NOMENCLATURE

- $a_s$  = interfacial surface area ( $L^2/L^3$ )
- $C_i$  = concentration of species  $i$  ( $meq/L^3$ )
- $C_i^*$  = concentration of species  $i$  in the resin ( $meq/L^3$ )
- $C_i^o$  = concentration of species  $i$  in the bulk ( $meq/L^3$ )
- $d_p$  = particle diameter (L)
- $D_i$  = diffusivity of species  $i$  ( $L^2/t$ )
- $D_{ei}$  = effective diffusivity for species  $i$  ( $L^2/t$ )
- $f_n$  = function evaluation  $n$  for Adams-Bashforth-Moulton Method
- $F$  = Faraday's constant (C/mol)
- FCA = anion resin volume fraction
- FCR = cation resin volume fraction
- $J_i$  = flux of species  $i$  in the film ( $meq/tL^2$ )
- $K_B$  = dissociation Constant for Base B ( $mol/L^3$ )
- $K_i$  = mass transfer coefficient (including flow) (L/t)
- $K_i'$  = mass transfer coefficient (excluding flow) (L/t)
- $K_B^A$  = resin selectivity for  $i$  compared to  $j$
- $K_w$  = dissociation constant of water ( $mol/l^3$ )
- $Q$  = capacity of the resin ( $meq/L^3$ )
- $R$  = universal gas constant

- $R_i$  = ratio of mass transfer coefficients  
 $T$  = temperature  
 $t$  = time (t)  
 $u$  = superficial velocity (L/t)  
 $x_i$  = bulk phase concentration fraction of species i  
 $y_i$  = fraction of species i on the resin  
 $Y_i$  = fractional concentration of species i based on the pseudo coion  
 $Z_i$  = charge on species i  
 $\delta$  = film thickness (L)  
 $\epsilon$  = void fraction  
 $\phi$  = electrical potential ( $\text{mL}^2/\text{tC}$ )  
 $\mu$  = viscosity of the bulk phase ( $\text{m/Lt}$ )  
 $\tau$  = dimensionless combined time-distance variable  
 $\xi$  = dimensionless distance variable

#### Superscripts

- $\circ$  = bulk phase value  
 $*$  = interfacial value  
 $'$  = overall value

#### Subscripts

- $A$  = species A  
 $B$  = species B / base B  
 $c$  = chloride  
 $h$  = hydrogen  
 $i$  = species i  
 $j$  = species j

n = sodium  
o = hydroxide  
p = pseudo component  
x = third cation  
w = water

## CHAPTER I

### INTRODUCTION

Ion exchange, as an applied process, is referenced as far back as the Old Testament of the Bible, Exodus 15:22-25. "When they came to Marah, they could not drink the water of Marah because it was bitter; therefore it was named Marah. And the people murmured against Moses, saying, What shall we drink? And he cried to the Lord; and the Lord showed him a tree, and he threw it into the water, and the water became sweet." Industrial applications began at the turn of the twentieth century. Increasing usage of ion exchange technology started in the late 1940's and continues to the present. The ion exchange process has advanced technologically, unfortunately fundamental studies and detailed modeling have fallen behind the technical applications.

The mechanics of ion exchange involves the usage of a fixed support with attached ionic species which can be interchanged with ions in a solution. The solid supports are referred to as ion exchangers. They contain charged species, i.e. sulfonate groups, that are permanently attached to the support structure. The attached groups attract oppositely charged ions, i.e. hydrogen, sodium, chloride, to achieve neutrality. The attracted species are mobile in that they can be replaced by a stoichiometric equivalent of like charged ions. This ability to change the species to which the fixed



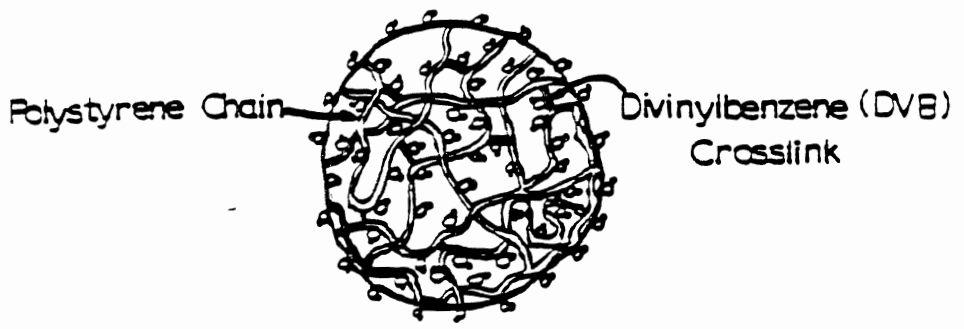
group is attached is the fundamental reason why these structures are of interest.

There are a number of applications for ion exchange. The most common application is in the purification of water. A typical ion exchanger is shown in Figure 1 (Struass and Kunin, 1980). The overall structure is typically a spherical bead consisting of polystyrene which is crosslinked with divinyl benzene to enhance rigidity. This polymeric support is referred to as a resin. The polymer has fixed groups attached to the polymer chains which bind an oppositely charged ion to achieve neutrality. An exchanger is classified as anionic or cationic depending on the nature of the mobile species. If the mobile ion is positively charged it is a cationic exchanger (or resin), if the mobile species is negatively charged it is an anionic exchanger (or resin).

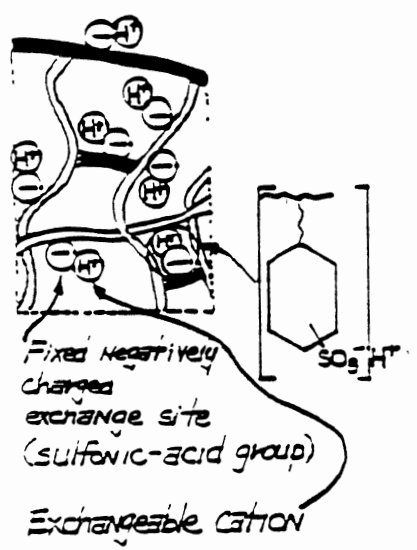
These exchangers can be used to remove cations, anions or both. One typical configuration is to use a fixed bed to exchange a given charged species. Units in series which first remove cations and then anions is one operational scheme. A second method is to mix anionic and cationic resins in the same unit. This is referred to as mixed bed ion-exchange (MBIE).

Ion exchange can be either an equilibrium or kinetic process. The characteristics of the resin, solution and operating conditions determine which process occurs. Equilibrium calculations, as in thermodynamics, determine the final conditions that can be achieved for a given case at low flow rates through a bed of packed resin. However, equilibrium does not indicate the time for reaction. The rate of approach to equilibrium is given by the kinetics. The

A Section of a Resin



Cation Resin



Anion Resin

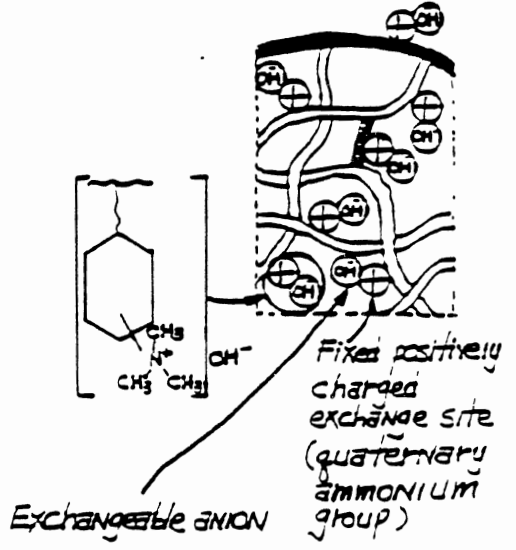


Figure 1. Schematic Diagram of A Resin Framework

kinetics can be described by identifying the rate determining step, where: 1) reaction rate, 2) particle diffusion, 3) film diffusion, and 4) combined film and particle diffusion, are the possible limiting steps. Film diffusion control is when ionic diffusion through an assumed liquid film surrounding the resin bead is the rate limiting step. Particle diffusion control is when the movement of ions within the particle framework is the slowest step. Combined film and particle diffusion is where each of the previously mentioned steps are important in determining the rate of exchange. These conditions differ from kinetic leakage. Kinetic leakage is when there is insufficient time allowed for exchange to approach equilibria. Haub (1984) and Yoon (1990) conducted extensive literature reviews of ion exchange equilibria, controlling steps, and kinetic models. In this dissertation only articles of particular importance to this work will be presented and discussed.

#### Ion Exchange Kinetics

In a packed column, the exchange characteristics can be estimated by using equilibrium calculations. Actual column performance can be predicted only by considering the kinetics governing the specific situation. Discovering the combination of rate limiting steps which govern any specific process is extremely important. The reaction of the exchanging species on the resin is almost never the rate controlling step. Therefore, most ion exchange is diffusion limited. This means that the movement of the charged species from the bulk phase through the liquid film, the movement through the particle structure, or both, are usually rate determining.

Since film diffusion and particle diffusion occur in series, the slower of the two will become the rate determining step. Particle diffusion is usually the rate controlling step for bulk phase ionic concentrations above 0.5 M, approximately. Concentrations lower than this tend to introduce film diffusion. It is possible for the process to fall into the area where the combination of film and particle diffusion must be considered. Yoshida and Kataoka (1988), Dadgar (1986) and Ahmad (1989) have considered regions in which both film and particle diffusion are important. Dranoff and Lapidus (1961) used a second order reaction scheme to determine the rates of exchange for a number of cases. The drawback to this method is the need to determine experimentally the reaction rate constants. The consideration of diffusion control allows for evaluation of the exchange process with information that is typically available in the literature. Ultra-low solution concentrations are almost exclusively film diffusion controlled processes, and therefore film diffusion is the focus of this work.

A large number of investigators have examined the film diffusion regime of ion exchange. Most have not accounted for the effect of the dissociation of water at these ultra-low concentrations. Helfferich (1965), Kataoka, et al. (1976a,b), and Wagner and Dranoff (1967) have considered situations where an acid or base is present to neutralize some of the species released from the resin. These studies have involved one or two coions (oppositely charged species) and for the most part binary exchange. There have been some studies involving ternary exchange, but these have dealt mostly with intra-particle diffusion.

Wildhagen, et al. (1985) have considered ternary film diffusion controlled ion exchange kinetics to determine the most appropriate effective diffusivity. This was limited to the case of one coion and no chemical reaction. They went on to define a new concentration variable based on one coion. The data to support the work from a binary standpoint is quite convincing. Unfortunately, additional ternary literature data were not considered and the experiments were limited to a thin fluidized bed with one set of ternary results. Omatete, et al. (1980a,b) considered ternary exchange from a theoretical standpoint, but the resultant model used correlations of overall binary mass transfer coefficients. These were for one specific system and included the presentation of only one set of ternary data. This is typical of the literature investigations in multi-component ion exchange. Much of the literature on ion-exchange kinetics is limited to single particle studies with one coion. These are theoretically interesting, but lack direct application to industrial needs, where column performance needs to be evaluated.

There are a number of references that have suggested the usage of the Nernst-Planck equation to describe film diffusion controlled ion exchange. Haub (1984) and Yoon (1990) have discussed many of these at length. Even so, there are a number worth mentioning here.

The process of ion exchange, as described earlier, involves the diffusion of a charged species. Typically, in most diffusion situations, Fick's Law is sufficient to describe the process. Ion exchange, because of the movement of electrical charges, is not well described by Fick's Law. It is necessary to incorporate the effect that individual moving electric charges have on each other. This can

be thought of as extending Fick's law to include an external force term. This is described by Bird, Stewart and Lightfoot (1960) as:

$$J_i = J_i^x + J_i^g$$

Where the superscript x denotes concentration driving force and g denotes an external force. This external force can be considered as an induced electrical potential. This is incorporated by using the Nernst - Planck equation. This equation is:

$$J_i = D_i \left[ \nabla C_i + Z_i \frac{F C_i}{R T} \nabla \phi \right]$$

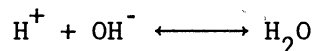
This has been shown experimentally to describe the process of diffusion limited ion exchange (Helfferich and Plesset (1958) and Kataoka, et al. (1968)). The major assumption of the Nernst-Planck equation is that the effect of one ion on another can be accounted for entirely by the electrical potential term, which arises due to differing ionic mobilities. This creates, what is referred to as, an induced electrical potential. There is no external electric field applied to the exchanger, only the induced potential created by ions moving at different rates on a microscopic level.

Film diffusion, as the name implies, assumes there is a liquid film that adheres to the particle surface. The Nernst-Planck equation describes the diffusion process, but a model is required to handle the film. There are a number of possibilities such as the hydraulic radius film model, boundary layer model and the static (Nernst) film model. Kataoka, et al. (1973), compared the hydraulic radius model and an effective diffusivity that accounted for the film thickness via the static film model. They determined that in the direction of favorable equilibrium, a maximum of 5 percent error arises from the

model where the effective diffusivity accounted for the film thickness. This was the method adopted by Haub (1984) for mixed bed ion exchange.

#### Mixed-Bed Ion Exchange

Mixed bed ion exchange (MBIE) is an intimate mixture of cationic and anionic resins used to deionize a contaminated liquid stream. MBIE is typically used where ultra-pure water is desired. The advantage of MBIE operating in the HOH cycle (cation resin in hydrogen form, anion resin in hydroxyl form) is due to the ion-exchange process being accompanied by a chemical reaction. This neutralization reaction is:



The net effect is to decrease the bulk-phase concentrations of hydroxide and hydrogen. This further effects the rate of exchange favorably because of the increased concentration driving force across the film for these ions. Most studies (Kataoka, et al. (1976, and 1977) and Smith and Dranoff (1965)) assumed that the reaction is irreversible and neglected the concentrations of  $\text{H}^+$  and  $\text{OH}^-$  after the exchange. Kataoka, et al. (1977) developed a model for the neutralization reaction occurring within the film surrounding the particle. This is based on the ability of the hydrogen (or hydroxide) ion to penetrate the film surrounding the anionic (cationic) resin. The larger the excess of hydrogen (or hydroxide), the further the ion penetrates. This reaction front is the point at which the solution is at neutral pH. These studies were limited to systems with

concentrations near the limiting value for film diffusion control, did not involve mixed-bed systems and were limited to binary exchange. The incorporation of these results within a mixed-bed model is essential but they must also be extended where possible to include multi-component exchange.

MBIE is particularly useful where ultra-pure water is desired. The Electrical Power Research Institute (EPRI) sets guidelines for ionic contaminants in boiler feed water for electric power plants. These guidelines are becoming more stringent because of improving technology and the effect that contaminants have on the boilers. The nuclear power industry also has two additional agencies (NRC and INPO) that have specific contaminant requirements that must be met in order to remain in operation. The power industry is an area where ion exchange is of major importance.

There is more than one cyclic operational choice for MBIE units. The hydrogen cycle (HOH cycle), uses cationic resin in the hydrogen form and anionic resin in the hydroxyl form to allow the water equilibrium reaction to consume excess hydrogen and hydroxide. Another choice, the Ammonia (or amine) cycle involves the addition of ammonia to the feed water to increase the pH of the water for corrosion control. The Ammonia cycle can take one of two forms; HOH cycle with ammonia present or operation with the cationic resin in the ammonia form. Both cycles are used industrially so modeling attempts should consider both methods.

Other pH control agents are available. Ammonia has been used historically because of its well known behavior and availability. Replacement of ammonia with a different weak base may improve overall



boiler performance as well as condensate polishing. Two alternative amines are morpholine and AMP (2-amino-2-methyl-1-propanol). EPRI has sponsored projects aimed at the evaluation of the best possible weak bases for addition to electrical power plant secondary cycle water (EPRI NP-5594, 1988). The trade offs in selecting alternative amines are several, not the least of which is additive toxicity. Models designed for ammonia operation should include the flexibility to consider alternative amines, where the physical properties are known.

The work conducted here is an attempt to advance the state of MBIE modeling and improve the understanding of the process. A theoretically based model will accomplish this by locating the areas where significant improvements can be made.

#### Mixed-Bed Modeling

Modeling of MBIE systems should improve the basic understanding of how certain system and ionic parameters effect the exchange process, and thereby allow for still more improvements in the technology. A model for hydrogen cycle MBIE at ultra-low concentrations in the range where the dissociation of water becomes important has been developed (Haub and Foutch, 1986a,b). Their model was limited to  $\text{Na}^+$  -  $\text{Cl}^-$  exchange in the hydrogen cycle at  $25^\circ\text{C}$ . The work by Haub and Foutch (1986a,b) was the first MBIE model at ultra-low concentrations. This model involved water equilibrium rather than assuming an irreversible reaction. The diffusion process around a given exchange particle was described by the Nernst-Planck equation. Overall column performance was obtained by solving the partial differential equations for the material balances on each

resin. A major improvement of this model is the separate material balance considerations for each resin. Previous work treated the mixture of anionic and cationic resin as a single salt removing substance. There are estimation methods still in use that require the determination of which species will break through first so that the overall system can be designed (Gottlieb, 1990). The effect of water dissociation can be seen when both resins are considered and the separation is accomplished. Extending this model to consider operation at other than 25°C was done by Divekar, et al. (1987). This required expressions for all of the physical properties used within the model as functions of temperature. The next extension of the model should consider operation with components different and additional to the four originally considered. Power plant concerns deal with the HOH cycles ability to remove ions other than Na<sup>+</sup> and Cl<sup>-</sup> only, and amine cycles.

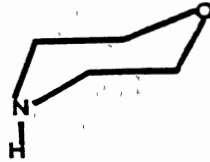
Hydrogen cycle operation produces neutral (pH = 7.0 at 25°C) ultra-pure water for electrical component processing or BWR (Boiling Water Reactor) nuclear electrical generation and some fossil fired electrical generating facilities. These applications typically require 18<sup>+</sup> megohm water in large quantities. The HOH cycle produces water of this quality.

The ability to measure ionic impurities has improved significantly in recent years with the development of on-line ion chromatography that allows parts per trillion (ppt) level analysis (Davis, 1990). This level of purification can only be achieved with a mixed-bed unit. The development of a model that can consider concentrations in this range for multiple species will allow for

improvements in operation and design of water polishing equipment.

The Divekar, et al. (1987) modification to the Haub and Foutch (1986) model can handle sodium and chloride contaminants at these ultra-low concentrations for a range of temperatures.

Amine cycle exchange is of interest to PWR (Pressurized Water Reactor) nuclear cycles and some fossil fired electrical generating facilities. The amine is added as a pH control agent to reduce corrosion products present in the secondary cycle. Industry guidelines recommend a feed water pH of 9.3 - 9.6 for non-copper alloys and 8.8 - 9.2 in the presence of copper alloys (EPRI NP-5056, 1987). These ranges have been maintained in the past by the addition of ammonia (for pH control) and hydrazine (for oxygen scavenging) to the boiler feed water. Recently, the possibility of using amines to replace ammonia has been considered. Currently, the most popular of these alternative amines is morpholine. The chemical structure of morpholine is:



King (1988) conducted a survey of the various alternative amines for pH control in secondary chemistry. The expanding usage of morpholine requires the development of new MBIE models to address morpholine and other alternative amines. Operating a MBIE unit with a pH control agent can be accomplished by two methods. The first is to operate in the HOH cycle, remove the amine as well as the other contaminants from the water, and then redose the feed water with the amine. The other method is to operate in the amine cycle (amine form cation resin) and

regenerate the MBIE unit as needed or on a regular schedule. This eliminates the necessity of redosing the feed water.

Operation in the HOH cycle with redosing has certain drawbacks. Redosing can be costly and leads to significant sodium slippage off of the mixed-bed polisher when the capacity has been consumed by the amine (Darvill, et al. 1986). The alternative is to convert the cation resin to the amine form and thereby remove the need to add more amine to the boiler feed water. Plant tests in the hydrogen cycle led Darvill, et al. (1986) to adopt mixed-bed polishing in the morpholine cycle. They found that, in the absence of condenser leaks, the morpholine cycle could be sustained for long periods of time. This cycle also has the ability to handle condenser leaks due to the favorable selectivity for sodium. Currently, the only model designed to handle MBIE in one of these cycles is that developed by Bates and Johnson (1984). This is a mass action equilibrium model that does not consider diffusional rate control. The model operates by the selection of an empirical plate height to match the data. This model should run into problems in situations where the selectivity is favorable for sodium with high cation-to-anion resin ratios. This is due to the effects shown by Haub (1984) and Yoon (1990) where the species that break through first are not easily determined. Also, the Bates and Johnson model assumes that all of the hydroxyl ion present is due to the dissociation of ammonia. This reintroduces the assumption that the unit is a single salt removing substance which is not true. The release of hydroxyl ions due to a different rate of anion exchange should be considered. These limitations do not retract from the ability of the Bates and Johnson model to operate effectively

in the ammonia cycle, where unfavorable sodium selectivity is encountered, due to the very low breakthrough limits for sodium. Any model should be able to consider operation in any amine form as well as the ammonia cycle.

### Objectives

There are a number of specific concerns that this dissertation will address. Extending the modeling effort begun by Haub and Foutch (1986a,b) to consider other and multiple ions while retaining the temperature flexibility is the focus of this work. The consideration of various amine cycles is one portion, and operation in the amine form or the HOH form are both addressed.

The format followed in this dissertation is to present the material as a series of articles, each covering a specific topic. Detailed developments will be presented in the appropriate appendix.

The first article will address the development and evaluation of a model designed for amine cycle MBIE. This model was developed to handle the operating conditions of MBIE with an amine form cationic resin. The model was constructed to allow consideration of any amine, provided that the necessary physical properties are known. The model will be compared with the model developed by Bates and Johnson (1984) and tested with operational data available from the literature.

The second article will address the general topic of multi-component HOH cycle exchange in neutral systems ( $\text{pH} = 7.0$ ). This is an extension of the HOH cycle model developed by Haub and Foutch (1986a,b). Temperature effects are included throughout the development. Some of the temperature dependent properties have been

fit exclusively for the limited temperature ranges that MBIE units typically experience ( $20^{\circ}\text{C}$  to  $90^{\circ}\text{C}$ ). The model will be compared with the limited amount of ternary exchange data that is available.

The final article addresses multi-component operation in other than neutral systems. Specifically, the operation of a MBIE unit with an aminated feed water stream in the HOH cycle. The characteristics of this development allow extending the MBIE unit operation past the amine break and switching over into the amine cycle. The reason for this type of operation is to minimize the initial treatments required.

There is a need for a model which predicts amine cycle ion exchange behavior because of the increasing usage of alternative amines. Alternative amines are a new area for power facilities as well as resin manufacturers. The ability to model these systems will enable design engineers and manufacturers to improve process and resin characteristics and thereby improve overall performance.

Facilities operating MBIE units typically experience ionic contaminants other than sodium and chloride. These other species have different properties and the ability to predict their fate within the bed is essential for an industrially useful model. The extension of previous binary exchange work to consider ternary systems should address these needs. A general ternary MBIE model to address uni-valent exchange operation in neutral systems will be presented.

Operation at other than neutral conditions is of growing importance as purification of streams maintained at a specific pH is necessary. The third article is directed at the operation of a MBIE unit with a pH control additive through the amine break. After the amine break, the unit may either be removed from service or allowed to operate in the amine cycle.

## CHAPTER II

### MIXED-BED ION EXCHANGE MODELING WITH AMINE FORM CATION RESINS

#### Abstract

A model for the operation of a mixed bed ion exchange (MBIE) unit with the cation resin in the amine form is developed. The model considers film diffusion limited exchange with bulk phase neutralization and correction for amine and hydroxide concentrations. The effect of pH and inlet concentration on the ratio of electrolyte to non-electrolyte mass transfer coefficients is addressed. The results for ammonia cycle exchange compare favorably with those of Bates and Johnson (1984). Amine cycle operation with morpholine is addressed. The evaluation of other alternative amines is possible, provided that the necessary physical property data are available.

#### Introduction

Electrical power generating facilities encounter the problem of corrosion of metallic surfaces due to contaminants present within the feed water system. The suspended and dissolved solids present in the water are removed by a series of filtrations and ion exchanges. Ion exchange removes ionic contaminants from the water by passing the water through a packed bed of ion exchange resins. Combining the

purification steps with a pH adjustment agent further reduces the corrosion of process equipment.

One method for improved corrosion control is the introduction of a weak base into the water stream to increase the pH. This in turn reduces the amount of corrosion that occurs on the metallic surfaces. This base has historically been ammonia. In recent years alternatives to ammonia have been considered. One of the alternatives that is experiencing increasing usage is morpholine ( $C_4H_8ONH$ ).

The major factors that affect the selection of a weak base are; 1) dissociation constant, 2) distribution coefficient, 3) degradation characteristics, and 4) toxicity. The dissociation constant reflects the extent to which the base ionizes when dissolved in water. The larger the dissociation constant the more effective the weak base is at pH control. The distribution coefficient is defined as the ratio of the base in the steam phase to the water phase, when two phases are present. A low value for the distribution coefficient is desirable to provide decreased corrosion rates in process equipment where two phase operation occurs (Sawochka, 1988). The base must also be thermally stable because of the wide range of process conditions that it will experience. Some bases are unstable under certain conditions and the effects of their degradation products must then be considered. Finally, the base should not be toxic since material handling is necessary and spills may occur.

Water stream purification must be considered when evaluating an amine. The most important factor is the selectivity coefficient for sodium over the amine on the cationic resin. The selectivity coefficient relates the interfacial and resin phase concentrations as:



$$K_B^A = \frac{C_B^* \bar{C}_A}{\bar{C}_B C_A^*} \quad (\text{eq. 2-1}).$$

Where the bar denotes resin phase and the \* denotes interfacial concentration. If this value is less than one, then the resin tends to prefer ion B, the opposite is true if it is greater than one. In amine form operation the selectivity coefficient directly relates to the ability of the ion exchange system to remove ionic contaminants, such as sodium. Table I summarizes the selectivity coefficients for many exchange processes. A comparison of the dissociation constants as functions of temperature for ammonia, morpholine and 2-amino-2-methyl-1-propanol (AMP) is shown in Figure 1 (EPRI NP-5594, 1988). This shows that to attain the same pH with morpholine as with ammonia, more base must be added. The opposite is true for AMP, but preliminary tests have shown it to be less effective than morpholine or ammonia for corrosion control (EPRI NP-5594, 1988) due to its high degradation rate.

Some fossil fuel electrical generating facilities and most pressurized water reactor (PWR) nuclear generating facilities use some form of pH control agent. The Electrical Power Research Institute (EPRI) recommends that feed water pH be maintained in the range of 9.3-9.6 in the absence of copper alloys and 8.8-9.2 when copper alloys are present (NP-5056 SR, 1987). This requires ion exchange systems to handle aminated water. This can be accomplished by MBIE in either the hydrogen cycle or with the cation resin in the amine form.

A model for MBIE operating in an amine cycle is of interest to electrical power generating facilities using some form of pH control additive. Current models for ammonia cycle exchange are of the

Table I  
Selectivity Coefficients

Coefficient	Value	Resin
Cation Resin		
$K_{H}^{Na}$	1.5	AMBERSEP 200
$K_{H}^{Ag}$	2.5	AMBERSEP 200
$K_{H}^{Ag}$	4.5	DOWEX 50 X 8
$K_{Na}^{Ag}$	1.7	AMBERSEP 200
$K_{Na}^{Ag}$	3.0	DOWEX 50 X 8
$K_{H}^{Am}$	2.5	AMBERSEP 200
$K_{Na}^{Am}$	1.7	AMBERSEP 200
$K_{Am}^{Na}$	0.8	AMBERSEP 252
$K_{Morph}^{Na}$	2.1	AMBERSEP 252
Anion Resin		
$K_{OH}^{Cl}$	15.0	AMBERSEP 900
$K_{Cl}^{NO_3}$	2.45	AMBERSEP 900

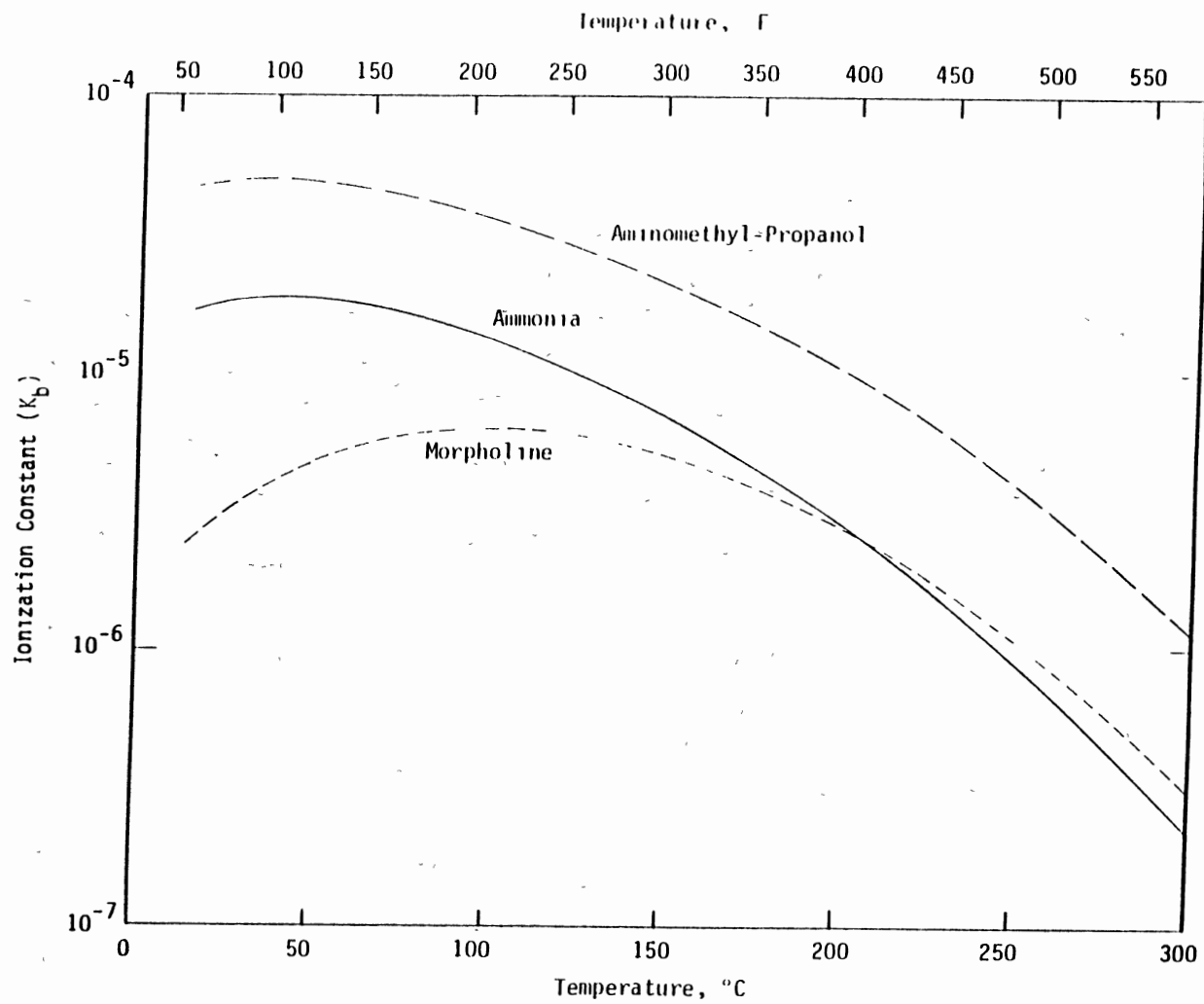


Figure 1 Variation in Ionization Constants ( $K_b$ ) of Ammonia, Morpholine and Aminomethyl-Propanol

mass-action equilibria type. The model developed by Bates and Johnson (1984) uses an empirical plate height method and equilibrium calculations to simulate an ammonia form MBIE unit. Models of this type are useful to industry because of their empirical basis, but they represent only limiting cases that may be improved on by more theoretical models. Consideration of low inlet concentrations ( $<10^{-4}$  M) requires that the diffusion controlled rate of exchange be examined. In these concentration ranges film diffusion is typically the rate controlling step. In film diffusion limited exchange, ions diffuse through a stagnant film which is assumed to exist around the particle. In order to model this situation, a description of the diffusion process and the film surrounding the particle is needed.

The objective of this work is to develop a model for amine cycle MBIE at low concentrations. This article presents the model development and evaluation as it applies to ammonium and morpholinium form cation exchange resins in a MBIE column.

#### Model Development

The model developed here addresses the inclusion of an amine into a typical MBIE system operating in the amine cycle. The ions that directly affect the exchange processes are  $\text{Na}^+$ ,  $\text{NH}_4^+$ ,  $\text{OH}^-$ , and  $\text{Cl}^-$ . The equations derived to describe the various conditions involved are presented, the details are included in Appendix A.

#### Assumptions

The number of assumptions involved with this development have been limited to produce as general a model as possible. MBIE has been

considered from a mass transfer limitation viewpoint. Using microscopic methods would be the most accurate approach, but modeling the variations in local concentrations, resin site strengths and their interactions is impossible. The overall approach is a macroscopic analysis with the goal of an experimentally verifiable model.

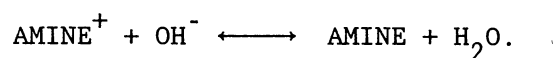
The major assumption is that the process is film diffusion controlled. Exchange resistance due to particle diffusion is not accounted for in the derived flux expressions. Also, the rates of reactions are assumed to be instantaneous compared to the rate of exchange. Other assumptions are; uniform bulk and resin phase compositions for a given particle, equilibrium at the particle film interface, bulk phase neutralization, negligible hydrogen ion concentration, activity coefficients equal to unity, pseudo-steady state mass transfer, isothermal operation, plug flow, and negligible axial dispersion. Table II lists all of the assumptions that have been applied to obtain a working model.

Simplifying assumptions have been employed only as necessary. The plug flow assumption has been used by Kataoka et al. (1972) and Haub and Foutch (1986a,b). Considering non-plug flow and non-uniform concentrations would more accurately represent the system. Unfortunately, the skills necessary to incorporate such considerations are beyond present capabilities. The negligible hydrogen ion concentration is a direct result of operation in the pH 9.0-9.8 range, since this gives hydrogen ion concentrations of  $10^{-9}$  -  $10^{-9.8}$  M. When this concentration level is compared with the concentrations of the other species, its contribution to the exchange process can be neglected.

Table II  
Model Assumptions

- 
- 1) Film diffusion control
  - 2) Pseudo steady state exchange ( variations of concentration with space are much more important than with time)
  - 3) No coion flux across the particle surface
  - 4) The Nernst-Planck equation incorporates all interactions between diffusing species
  - 5) All univalent exchange
  - 6) The static film model can be used to describe the film adhering to the particle surface
  - 7) Solid-film interface is maintained at equilibrium
  - 8) Reactions are instantaneous when compared with the rate of exchange
  - 9) Curvature of the film can be neglected
  - 10) No net coion flux within the film
  - 11) No net current flow
  - 12) Uniform bulk and resin compositions
  - 13) Activity coefficients are unity
  - 14) Negligible hydrogen ion concentration at high pH's
  - 15) Plug flow
  - 16) Isothermal, isobaric operation
  - 17) Negligible axial Dispersion
-

The dissociation of ammonia affects the bulk phase concentrations of the amine (dissociated and undissociated) and hydroxyl ions. The reaction between the dissociated amine and hydroxide has been restricted to the bulk phase to accommodate the release of these species from the cation and anion resins, respectively. The bulk phase concentrations of these ions are corrected based on the exchange process and the amount of undissociated amine present. The equilibrium reaction is given as:



The reaction consumes released amine and hydroxyl ions in order to maintain equilibrium. In turn, the bulk phase concentrations affect the exchange process by changing the concentration driving force across the film and the effective diffusivity of all species present. This shows the coupled nature of the exchange. The release or removal of various ions affects the bulk concentrations of the other constituents through the amine equilibrium relation. This equilibrium is expressed as:

$$K_B = \frac{(C_{\text{amine}^+}) * (C_{\text{OH}^-})}{C_{\text{NH}_3}} \quad (\text{eq. 2-2}).$$

### Flux Expressions

The flux expressions, and thereby the concentration of the bulk and resin phases, are derived using the Nernst-Planck equation. This expression incorporates the typical concentration driving force and includes an electrical potential effect due to differing ion mobilities. The flux is related using these equations by a diffusion

coefficient. The Nernst-Planck equation for ion (i) is

$$J_i = D_i \left[ \nabla C_i + \frac{Z_i F C_i}{RT} \nabla \phi \right] \quad (\text{eq. 2-3}).$$

This is used in conjunction with the static-film model. Using a different film model may be appropriate, but the static-film model has been shown to agree well with other models. The detailed derivation of the flux expressions that relate to this exchange with bulk phase neutralization are presented in Appendix A. The resulting expression for the flux of sodium through the film surrounding the cation resin is:

$$J_n = \frac{2 D_n D_x (C_x^o + C_n^o - C_x^* - C_n^*)}{(D_n - D_x) \delta} \quad (\text{eq.2-4}).$$

This combined with a similar expression for the flux of the chloride ion, for the anion resin, allows the application of the static film model to define the effective diffusivity for each species.

#### Particle Rates and Effective Diffusivities

The particle rate expression given by the static film model is:

$$\frac{\partial \langle C_i \rangle}{\partial t} = K'_i a_s (C_i^o - C_i^*) \quad (\text{eq. 2-5}).$$

Where the  $\langle C_i \rangle$  is the resin phase concentration of species i. This can be related to the flux across the film due to pseudo steady-state exchange as:

$$\frac{\partial \langle C_i \rangle}{\partial t} = -(J_i) a_s \quad (\text{eq. 2-6}).$$

This relation can be used to define the effective diffusivity for species i since the constant in the rate expression is:

$$K' = D_e / \delta \quad (\text{eq. 2-7}).$$



Where  $D_e$  is the effective diffusivity and  $\delta$  is the film thickness. The resulting expression for  $D_e$  is:

$$D_e = \frac{-\delta J_i}{(C_i^o - C_i^*)} \quad (\text{eq. 2-8}).$$

The expression derived earlier for the flux (eq. 2-4) can be used here and the result is an explicit expression for the effective diffusivity as:

$$D_e = \frac{2 D_x D_n (C_x^* + C_n^* - C_x^o - C_n^o)}{(D_n - D_x) (C_n^o - C_n^*)} \quad (\text{eq. 2-9})$$

It is more convenient to use fractional notation for the resin phase and liquid phase compositions. These fractions are defined as:

$$y_i = \langle C_i \rangle / Q ,$$

for the resin fraction and,

$$x_i = C_i / C_T ,$$

for the liquid phase concentration fraction. In these relations  $Q$  is the total resin capacity and  $C_T$  is the total counter ion (or coion) concentration. The selectivity coefficient can be used to eliminate the interfacial concentration in favor of the resin phase fraction when combined with the film concentration equation ( eq. A-3).

Fluid flow effects are incorporated depending on the particle Reynolds number using either Carberry's (1960) or Kataoka's (Kataoka et al., 1973) equations for the non-ionic mass transfer coefficients. These coefficients are included in the rate equation by the using the  $R_i$  factor.  $R_i$  is the ratio of electrolyte to non-electrolyte mass transfer coefficients:

$$R_i = \left( \frac{D_e}{D_i} \right)^{2/3} = K_i' / K_i \quad (\text{eq. 2-10}),$$

where  $K_i$  is the non-ionic mass transfer coefficient in the packed bed based on species  $i$ . It indicates the extent to which the differing mobilities of the ions effect the exchange process. The effective diffusivity is that derived earlier for the exchange process. Kataoka et al. (1973) showed that the two thirds power of the diffusivity ratio correlated very well with the value of what Pan and David's (1978) definition of  $R_i$ . Adding this relation to the previously defined particle rate yields:

$$\frac{\partial y_i}{\partial t} = K_i R_i a_s C_T (x_i^o - x_i^*) / Q \quad (\text{eq. 2-11}).$$

#### Material Balances

The overall material balances for the column are evaluated to determine the concentration profile within the column and its effluent concentration history. The column material balance is given from Appendix B as:

$$u \frac{\partial C}{\partial z} + \frac{\partial C}{\partial t} + \frac{(1-\epsilon)}{\epsilon} \frac{\partial q}{\partial t} = 0 \quad (\text{eq. D-1})$$

for one resin. The fact that the column is a mixed bed of cationic and anionic resins requires that the volume fraction of each resin be incorporated into the balances. This is accomplished by defining two system parameters FCR (cation resin volume fraction), and FCA (anion resin volume fraction). This allows for the inclusion of a third, inert resin, which is sometimes used as a separation aid. These allow both resins to be considered simultaneously. The form of the equations can be improved by a transformation to the dimensionless independent variables suggested by Kataoka et al. (1976). These new variables are:

$$\tau = \frac{K_i C_T^f}{d_p Q} \left( t - \frac{\epsilon z}{u_s} \right) \quad (\text{eq. D-2}), \text{ and}$$

$$\xi = \frac{K_i (1-\epsilon)}{u_s} \frac{z}{d_p} \quad (\text{eq. D-3}).$$

The resulting material balance equations are derived in Appendix D as:

$$\frac{\partial x_i}{\partial \xi} + FC_j \frac{\partial y_i}{\partial \tau} = 0 \quad (\text{eq. D-5}).$$

Where  $FC_j$  is the volume fraction of the resin that the balance is conducted over. A basis for the new variables must be selected, the case here has been based on the parameter values for sodium. This requires the chloride material balance equation to use sodium based independent variables which changes the form of the equation slightly. The particle rate equations must be transformed to the new independent variables. This is given from Appendix D as:

$$\frac{\partial y_n}{\partial \tau} = 6 R_n (x_n^o - x_n^*) \quad (\text{eq. D-11}), \text{ and}$$

$$\frac{\partial y_c}{\partial \tau} = \frac{K_c d_{pc} Q_c}{K_n d_{pa} Q_a} (x_c^o - x_c^*) \quad (\text{eq. D-12}).$$

Hence, the material balance equation can be written in the form:

$$\frac{\partial x_i}{\partial \xi} = - \frac{\partial y_i}{\partial \tau} = \text{Rate}_i \quad (\text{eq. 2-12}),$$

where the rate equation is given by the particle rate expression.

This resultant system of equations can be solved by the method of characteristics. The numerical technique evaluates these equations along curves of constant  $\tau$  and  $\xi$ . This requires the ability to solve a system of ordinary differential equations. Their solution is accomplished by using the Adams-Bashforth (fourth order) explicit

method in  $\tau$  and Adams-Bashforth-Moulton (fourth order) in  $\xi$ . A detailed description of this technique is in Appendix E.

#### Temperature Effects

There are a number of model parameters that are temperature dependent properties. Divekar et al. (1987) modified the model developed by Haub and Foutch to account for temperature effects. The equations developed there have been supplemented with the additional ones required for this work. Those that can be incorporated for different temperatures have been fit in the typical zone of operation (20 °C to 90 °C). Table III summarizes the properties that have been considered as temperature dependent and the equations used to evaluate them. The diffusion coefficients use the limiting ionic mobilities given by Robinson and Stokes (1959). The dissociation constants were fitted to the curves presented in Figure 1 (EPRI NP-5594, 1988).

The necessary equations and parameters have been determined for the MBIE column under consideration. These can now be evaluated and compared with existing data to evaluate the model's ability to describe amine cycle ion exchange.

#### Discussion

The necessary model parameters are summarized in Table IV. These are system or species dependent properties that can be obtained from manufacturers data or the literature. This is the major advantage of a theoretical model, existing parameters can be used to compare with experimental results and examine hypothetical situations.

Table III  
Temperature Dependent Values

---

Ionic Diffusion Coefficients

$$\text{Na}^+ \quad D_n = (RT/F^2) (23.00498 + 1.06416 T + 0.0033196 T^2) \quad *$$

$$\text{H}^+ \quad D_h = (RT/F^2) (221.7134 + 5.52964 T - 0.014445 T^2) \quad *$$

$$\text{NH}_4^+ \quad D_x = (RT/F^2) (1.40549 T + 39.1537)$$

$$\text{K}^+ \quad D_x = (RT/F^2) (1.40549 T + 39.1537)$$

$$\text{OH}^- \quad D_o = (RT/F^2) (104.74113 + 3.807544 T^2)$$

$$\text{Cl}^- \quad D_c = (RT/F^2) (39.6493 + 1.39176 T + 0.0033196 T^2) \quad *$$

Dissociation Constants

Species

$$\text{H}_2\text{O} \quad K_w = \exp(- (4470.99/T - 6.0875 + 0.01706T)) \quad *$$

$$\text{NH}_3 \quad K_B = 10^{**} (-(4.8601 + 6.31 \times 10^{-5} T - 5.98 \times 10^{-3} T^2))$$

$$\text{Morpholine} \quad K = 10^{**} (-(5.7461 + 8.095 \times 10^{-5} T - 0.013881 T^2))$$

Solution Properties

$$\text{Bulk Viscosity} \quad \mu = 1.5471 - 0.0317109 T + 2.3345 \times 10^{-4} T^2$$

---

\* Divekar et al. (1987)

Table IV  
Model Parameters

---

Bulk Phase

Viscosity ( $\mu$ )

Temperature (T)

Resins

Capacities ( $Q_c, Q_a$ )

Selectivity Coefficients

Particle Diameters ( $d_{pc}, d_{pa}$ )

Column Conditions

Flow rate

Column Diameter

Packed Height

Void fraction ( $\epsilon$ )

Cation resin volume fraction (FCR)

Anion Resin volume fraction (FCA)

Initial resin phase concentrations ( $y_i, t=0$ )

Inlet Conditions

Sodium and Chloride Concentrations

pH

Ionic Diffusion Coefficients (D 's)

---

## Rates of Exchange

The ratio of non-electrolyte to electrolyte mass transfer coefficients describes the effect that differing ionic mobilities have on the exchange process.  $R_1$  depends on the diffusivities of the exchanging species and the resin characteristics. Ammonium has a higher self diffusion coefficient than sodium so when ammonium is the exiting species from the resin the rate of exchange should be enhanced. This is shown in Figure 2. The lines for different pH's account for various bulk phase concentration ratios, and  $R_1$  is nearly linear with resin phase sodium loading. The effect of sodium bulk phase concentration at a fixed pH can be seen in Figure 3. The linearity seen in Figure 2 is again seen under these conditions. The observed behavior is due to the ratio of self diffusion coefficients of sodium and ammonium being nearly one. This coupled with the unfavorable and near unity value of the selectivity coefficient results in very limited sodium loadings for forward exchange. This is shown in Figure 4. Morpholine on the other hand has a lower diffusivity than sodium so the value of  $R_1$  will be less than one. This tends to retard the exchange process. The results of this are shown in Figure 5, where selectivity coefficients of 2.1 and 15 are compared for various pH's. The selectivity coefficient for sodium over morpholine is favorable for all cationic resins. The actual value of the selectivity coefficient varies greatly from resin to resin. The rate of exchange of sodium for morpholine for Ambersep 252 is shown in Figure 6 ( $K_{Mo}^{Na} = 2.1$ ). This rate is positive over a larger loading range than for ammonia due to the favorable selectivity

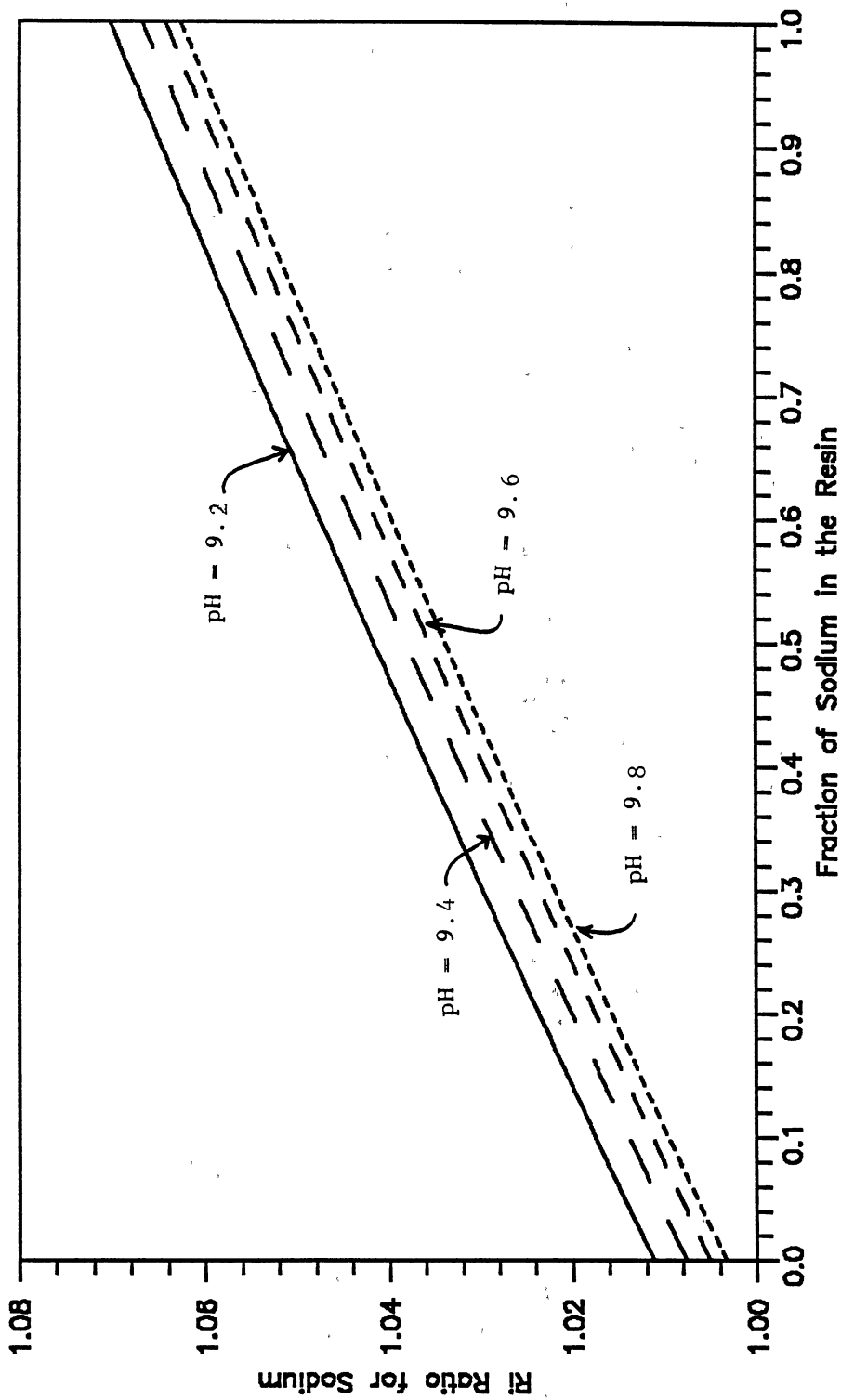


Figure 2. Ratio of Electrolyte to Non-Electrolyte Mass Transfer Coefficients For Sodium-Ammonium Exchange at various pH's



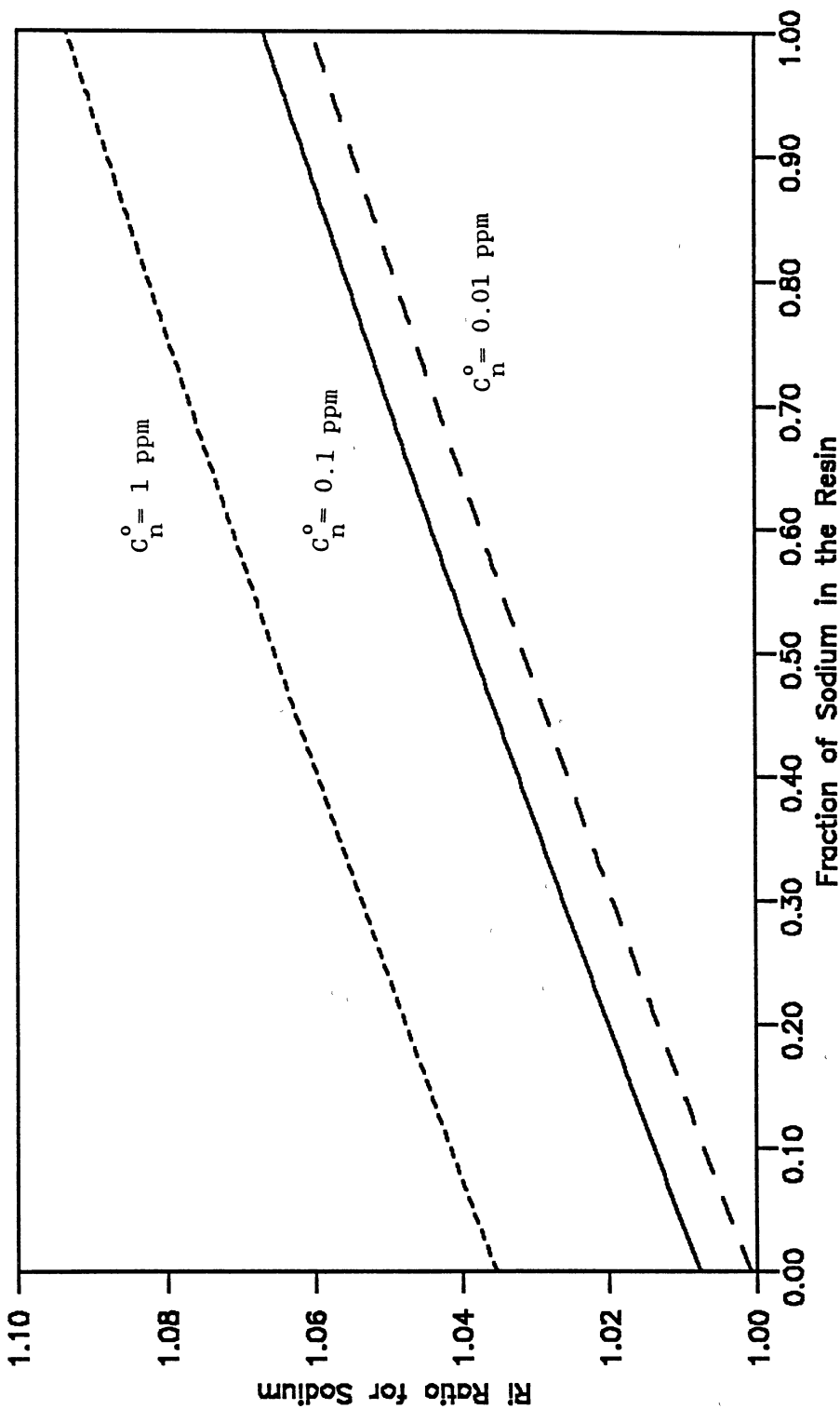


Figure 3. Ratio of Electrolyte to Non-Electrolyte Mass Transfer Coefficients for Sodium-Ammonium Exchange at pH = 9.4

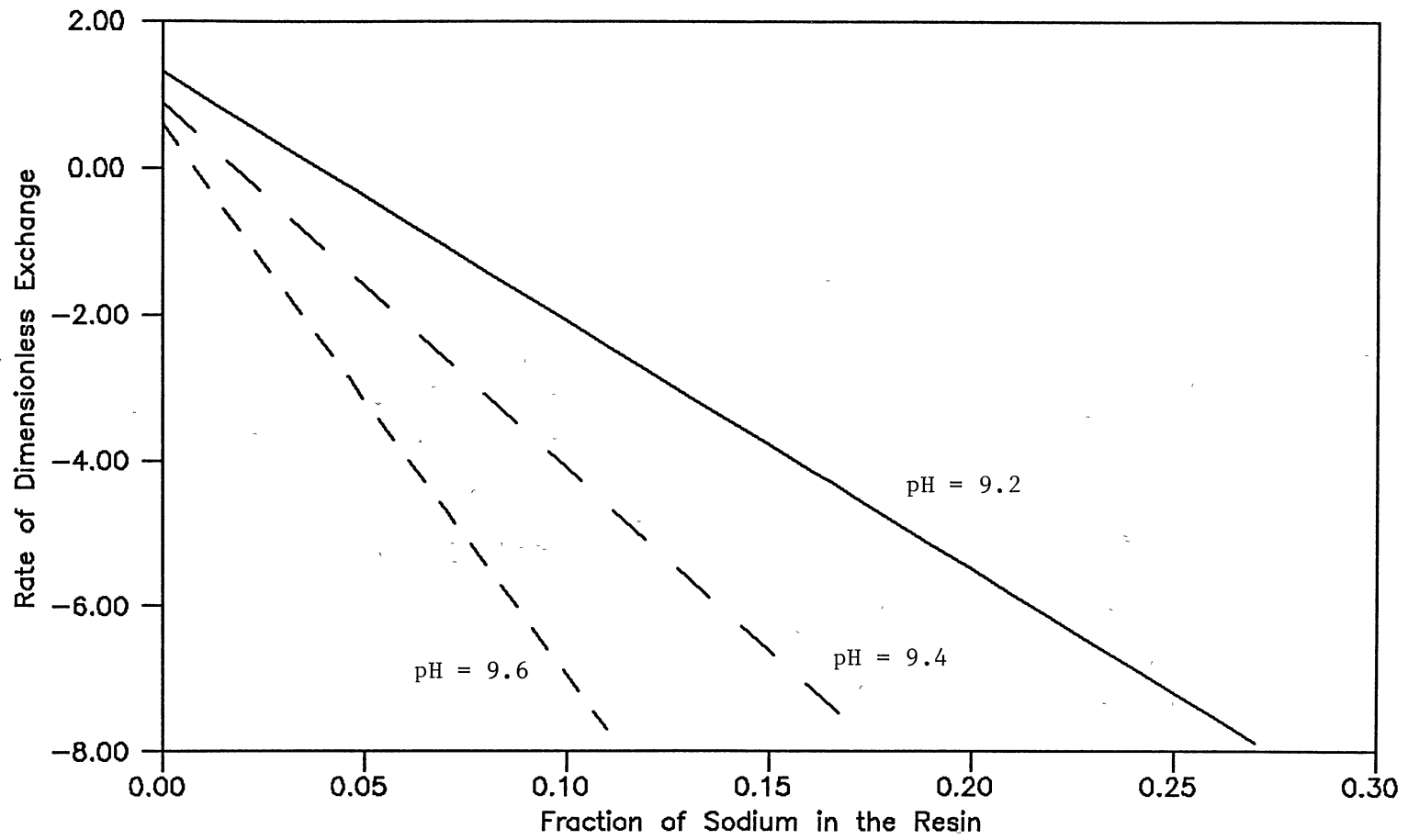


Figure 4. Rate of Dimensionless Exchange of Sodium for Ammonium at Various pH's

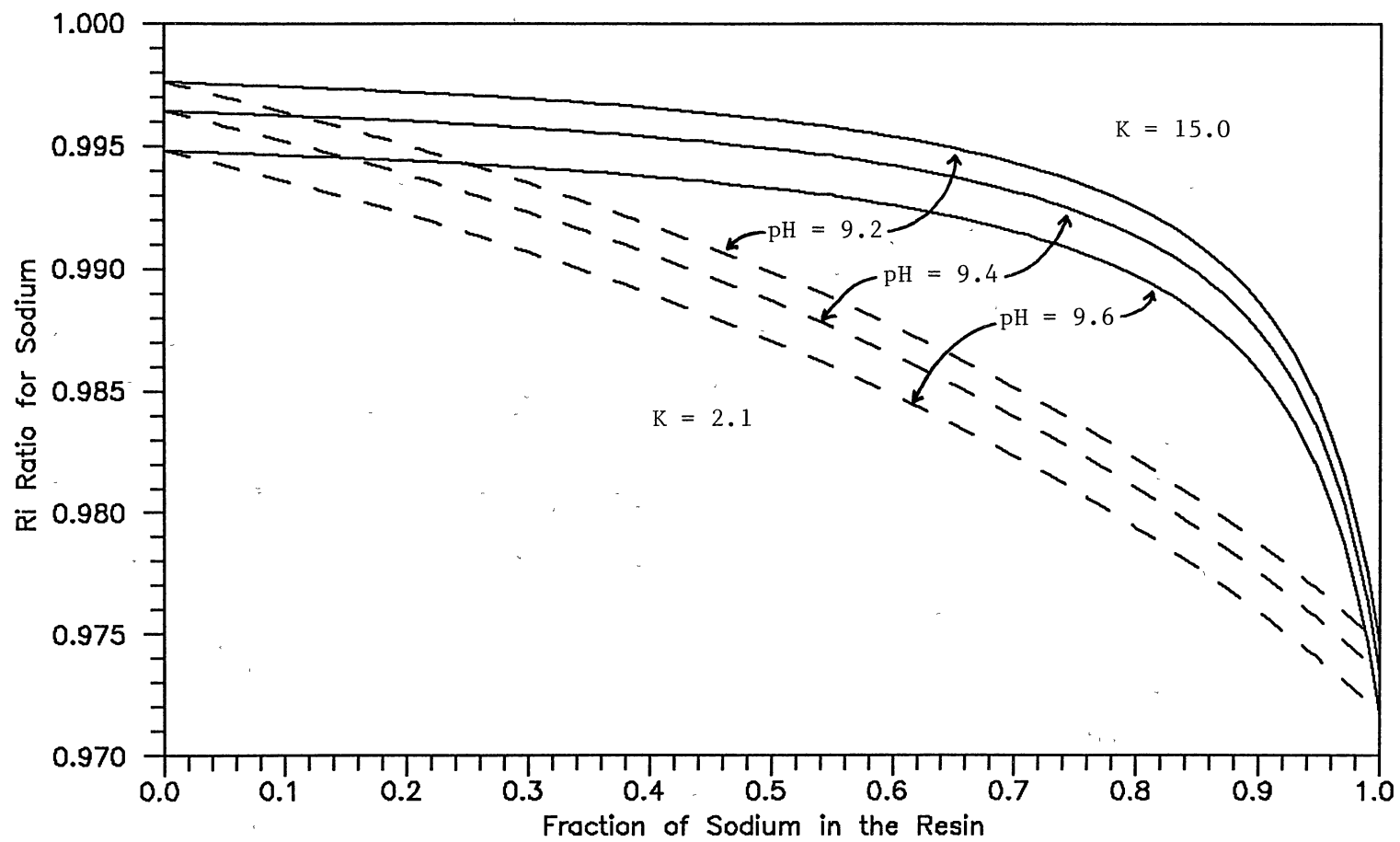


Figure 5. Ratio of Electrolyte to Non-Electrolyte Mass Transfer Coefficients for Sodium-Morpholine Exchange, various pH's, and Two Selectivities

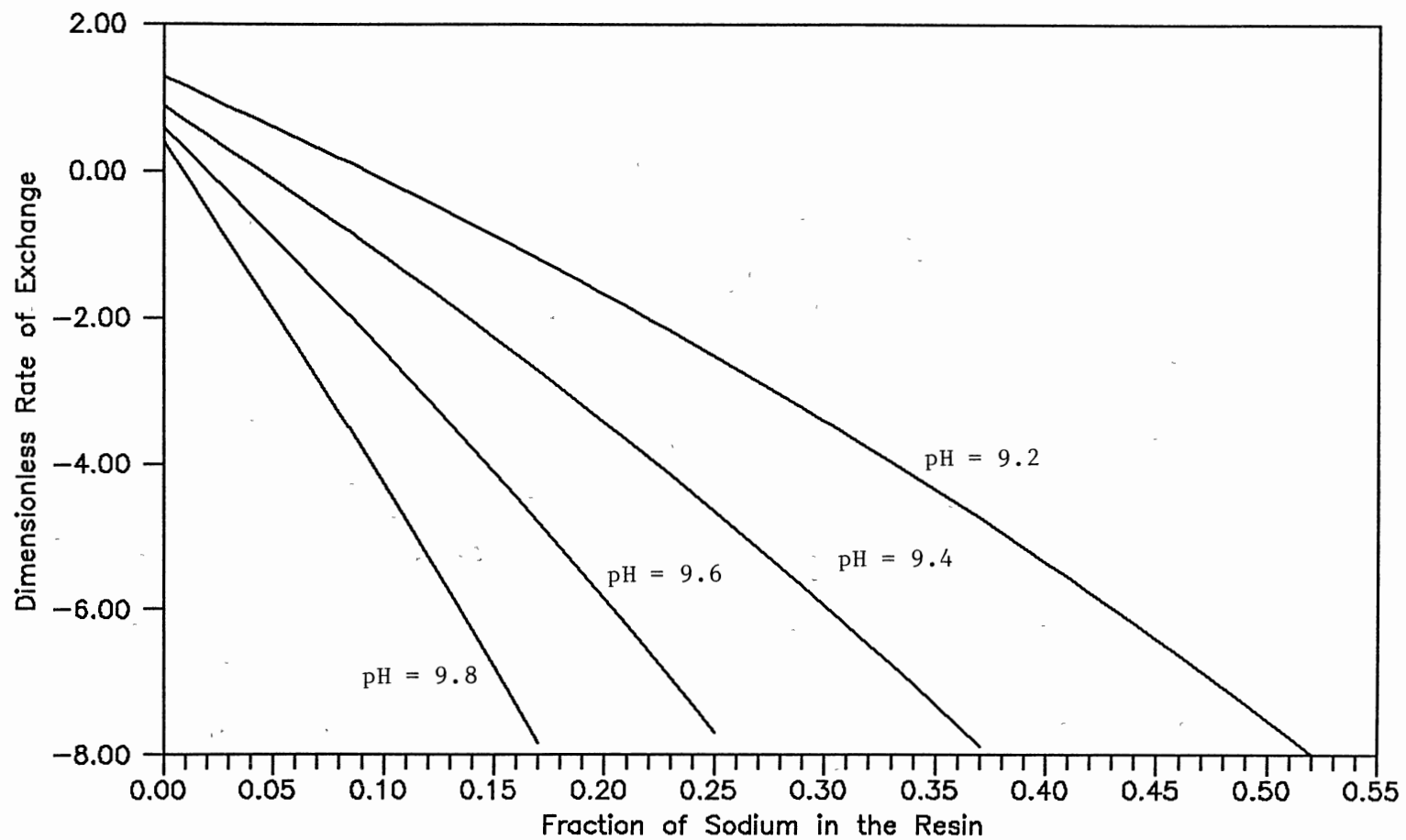


Figure 6. Dimensionless Rate of Exchange of Sodium for Morpholine at Various pH's on Ambersep 252 (  $K = 2.1$  )

coefficient. Ambersep 200 has a significantly higher selectivity coefficient for sodium over morpholine. This can be seen in Figure 7, the range of positive rates has increased considerably when compared with Ambersep 252. The selectivity coefficient in this case is 15. The rate remains positive for a wider range of sodium loadings and then drops off sharply as the equilibrium loading is exceeded. This implies that morpholine, although detrimental to  $R_i$ , has a significantly greater capability for sodium exchange. If the residence time within the bed is sufficient, morpholine will have more favorable exchange characteristics than ammonia.

#### Column Simulations

Column conditions equivalent to those used by Bates and Johnson (1984) have been adopted so that the results of the AMMLEAK model can be compared with the one developed here. The pH conditions vary from 9.2 to 9.8 for ammonia cycle exchange and inlet sodium concentrations have been evaluated from 10  $\mu\text{g}/\text{Kg}$  to 1  $\text{mg}/\text{Kg}$ . This gives a wide range of conditions for model evaluation.

Bates and Johnson (1984) conducted one experimental run on a one meter tall column at  $\text{pH} = 9.4$  to compare model predictions with actual data. The AMMLEAK model over predicts the time for breakthrough based on an intermittent condenser leak of 1  $\text{mg}/\text{Kg}$ . The model developed here is compared with their experimental data in Figure 8. The predicted curve breaks through earlier than the experimental data, which is a preferable situation when compared to over predicting break through times.

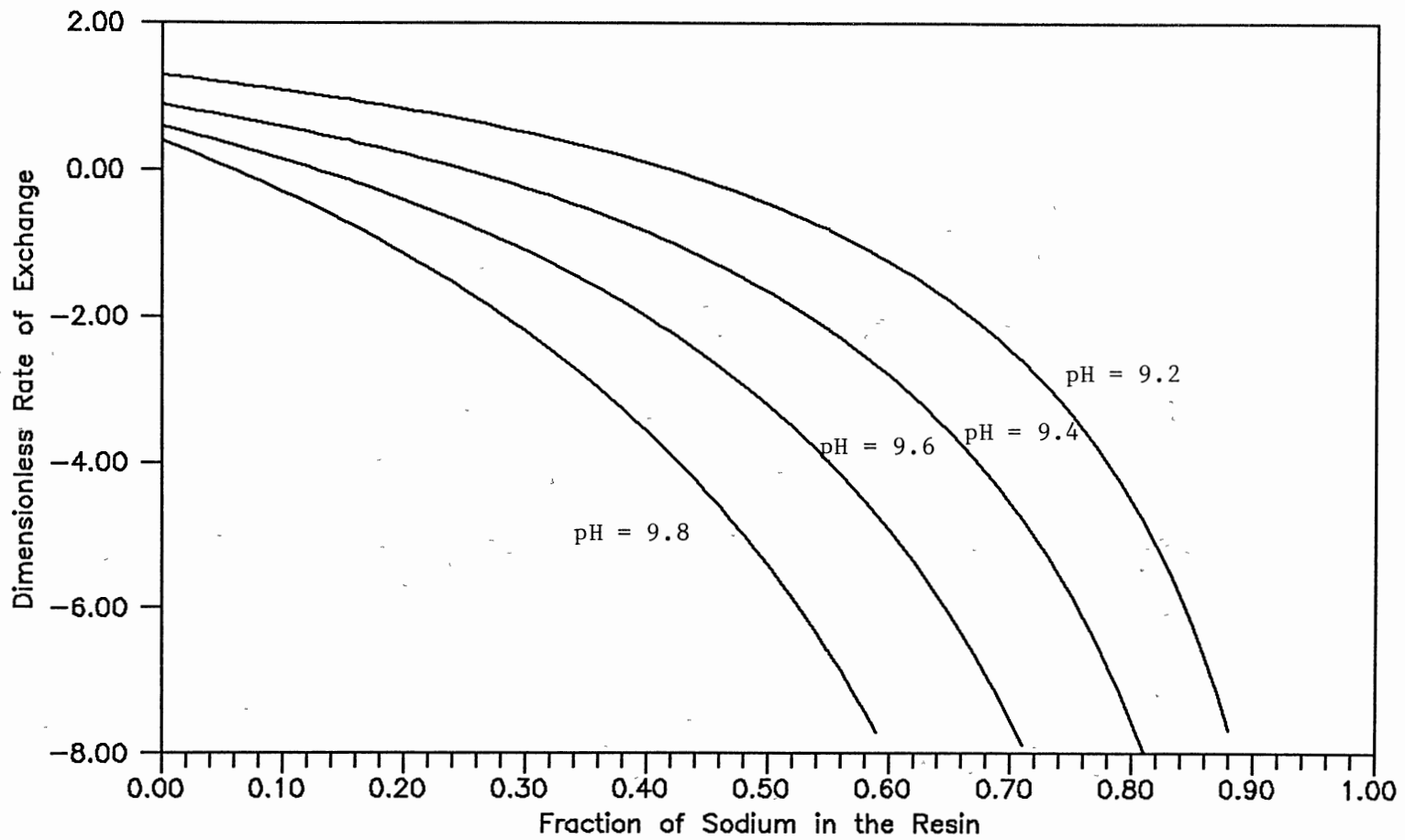


Figure 7. Dimensionless Rate of Exchange of Sodium for Morpholine at Various pH's on Ambersep 200 (  $K = 15.0$  )

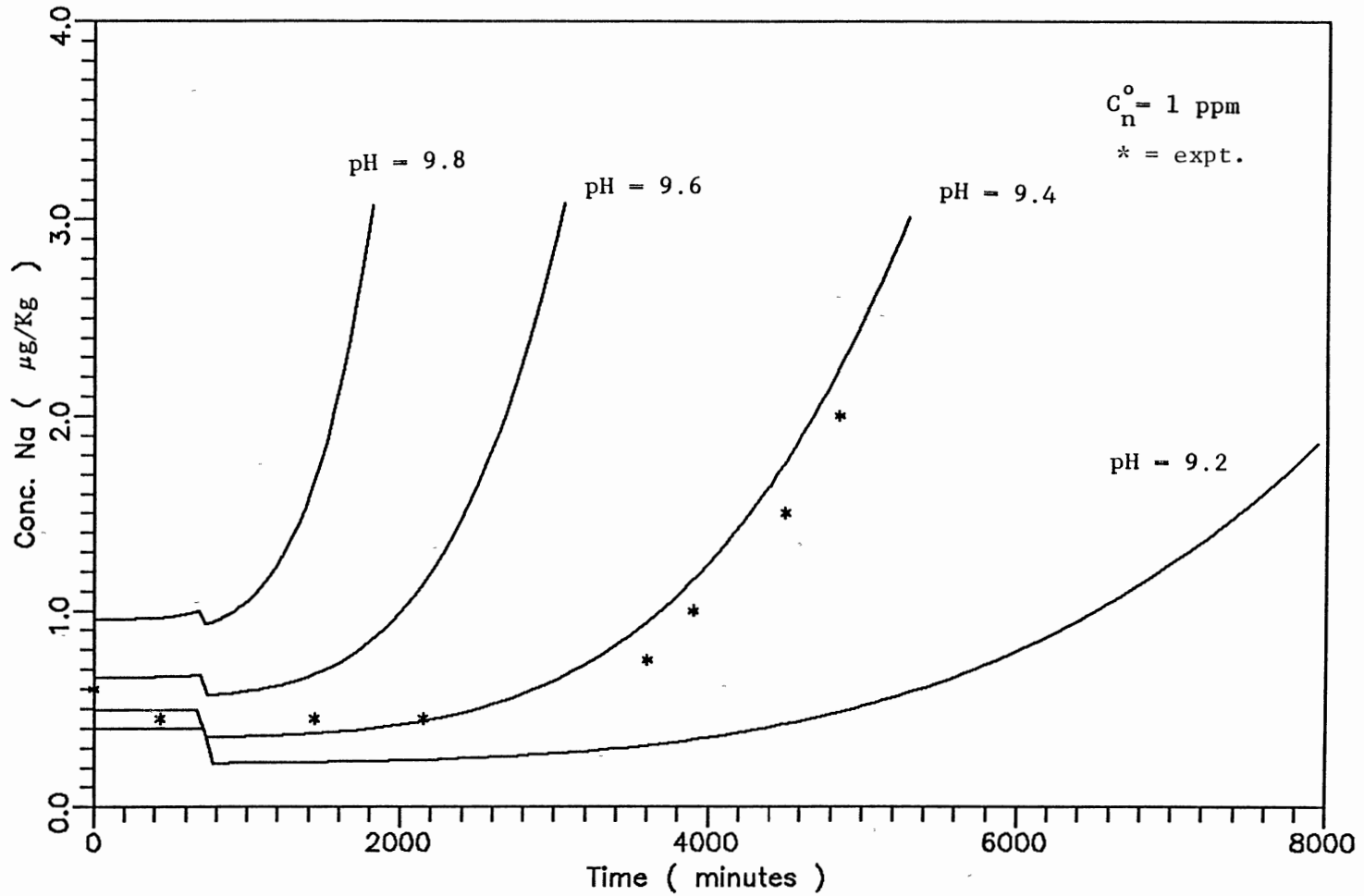


Figure 8. Predicted Sodium Break through for Ammonia Cycle Exchange with a Step Change in Inlet Concentration Compared to Bates and Johnson (1984), Experimental

A comparison of AMMLEAK predicted times to 2  $\mu\text{g}/\text{Kg}$  break through, for constant sodium inlet concentrations, and the present models predictions are given in Figure 9. The current model under predicts the time at each inlet concentration for  $\text{pH} = 9.4$ . This is again favorable from a predictive stand point since the model would require the removal of the bed from service before any excessive sodium leakage occurred. The break through curves for the  $\text{pH} 9.4$  and constant feed sodium concentration are shown in Figure 10. The AMMLEAK model predicts break through times reasonably well for ammonia cycle exchange due to the small impact of  $R_1$ , as shown by Figure 2. The models failings will become more evident when the possibility of hydrogen cycle exchange is considered.

The effect of cation-to-anion resin ratio on ammonia cycle exchange is shown in Figure 11. The net effect of an increase in the cation resin volume fraction is to increase the bed capacity for sodium. The increase in break through times for sodium is evident from this figure. The possible breakthrough of chloride only becomes important at very high cation resin fractions since the selectivity coefficient for chloride on the anionic resin is 16.5. This fact will change when considering the morpholine cycle.

The current model seems to compare favorably with the limited amount of experimental data available. Its under prediction of break through times increases the usefulness in ammonia cycle exchange evaluations.

Break through curves for 25  $^{\circ}\text{C}$ , 40  $^{\circ}\text{C}$  and 60  $^{\circ}\text{C}$  are shown for total ammonia concentration equivalent to  $\text{pH} 9.6$  at 25  $^{\circ}\text{C}$ , in Figure 12. The net effect of increased operation temperature is to increase



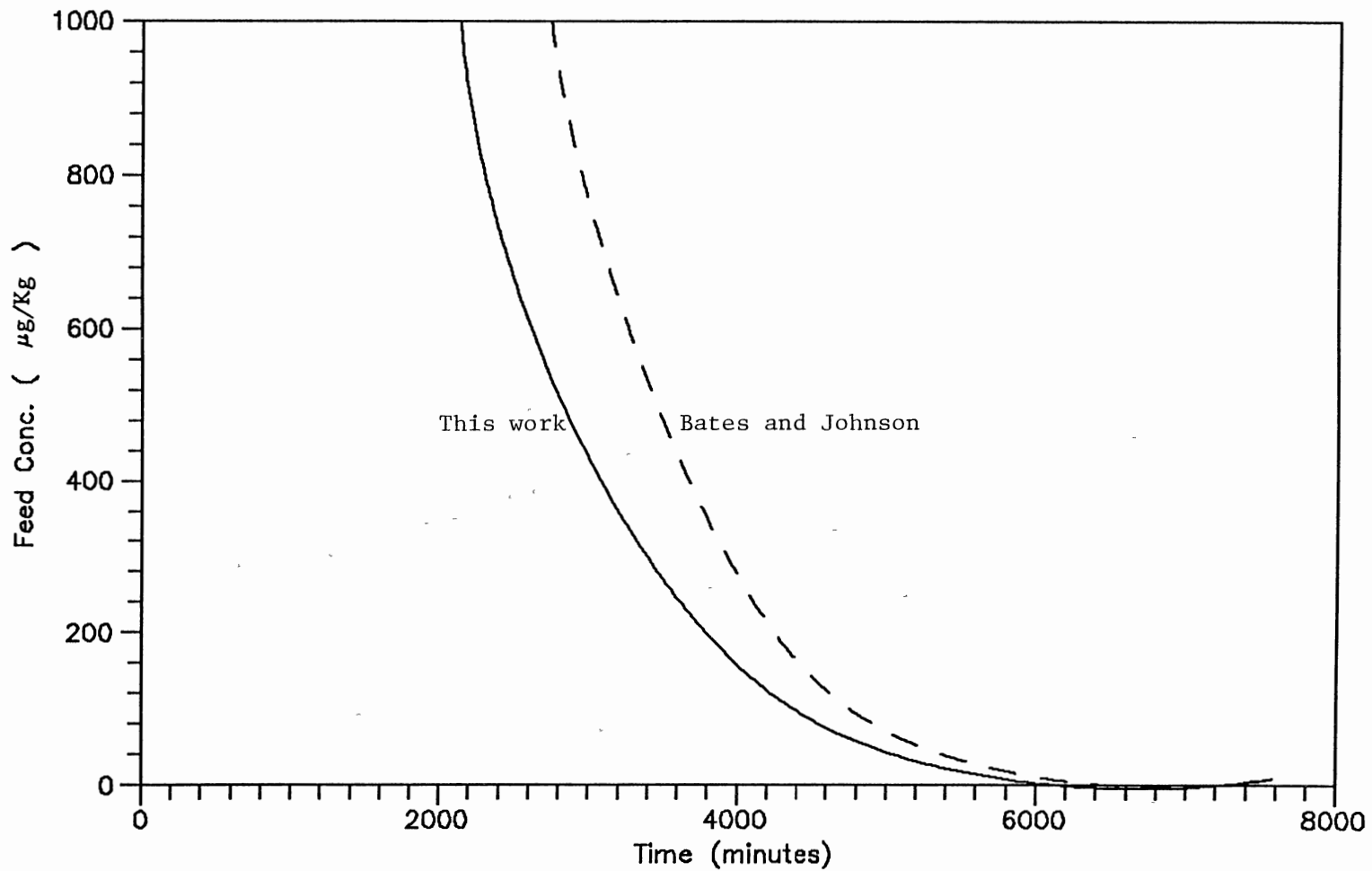


Figure 9. Comparison of time for 2 mg/ml Breakthrough Between This Work and Bates and Johnson (1984)

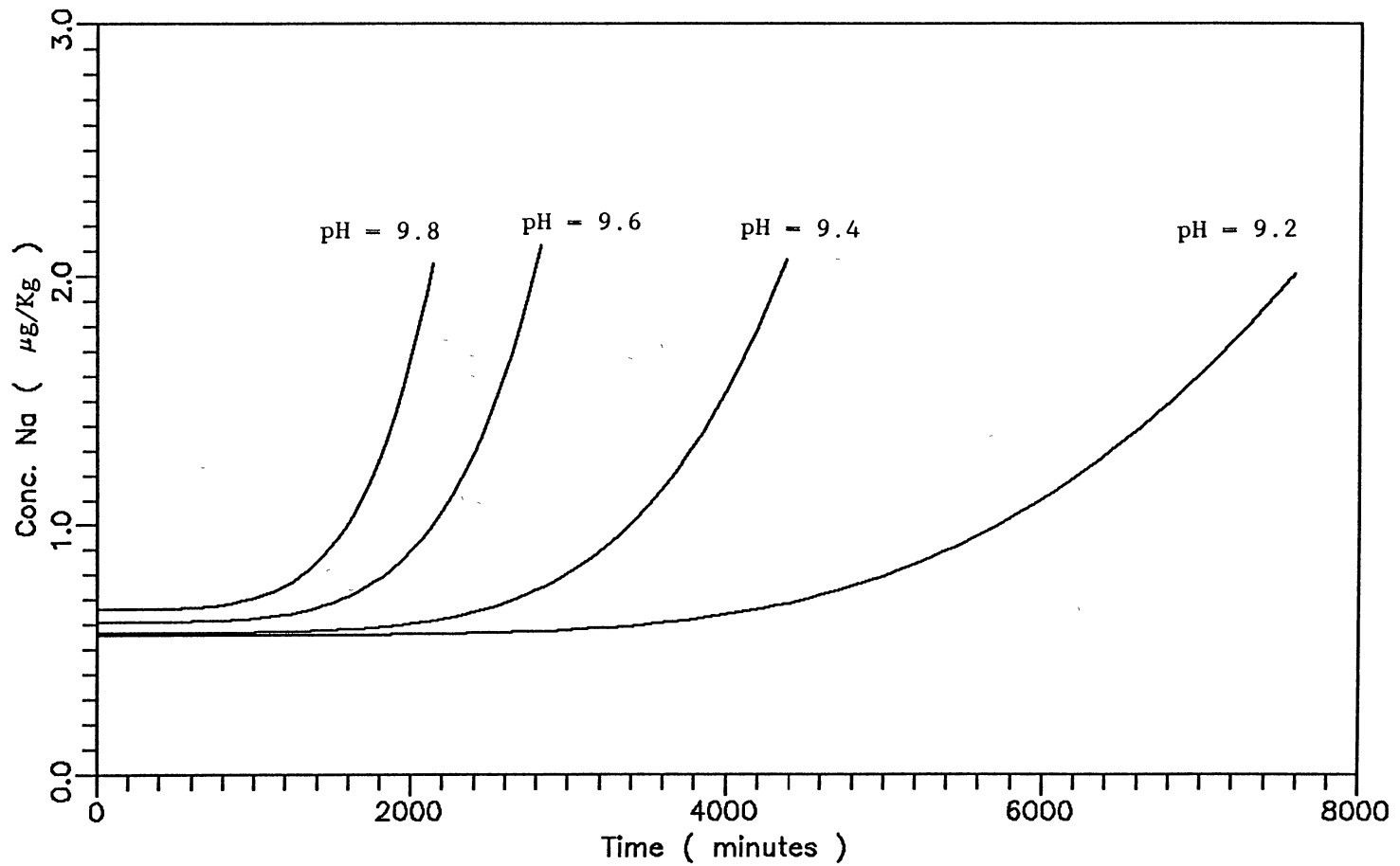


Figure 10. Sodium Break Through Curves for Constant Feed Concentration, Ammonia Cycle Exchange at several pH's

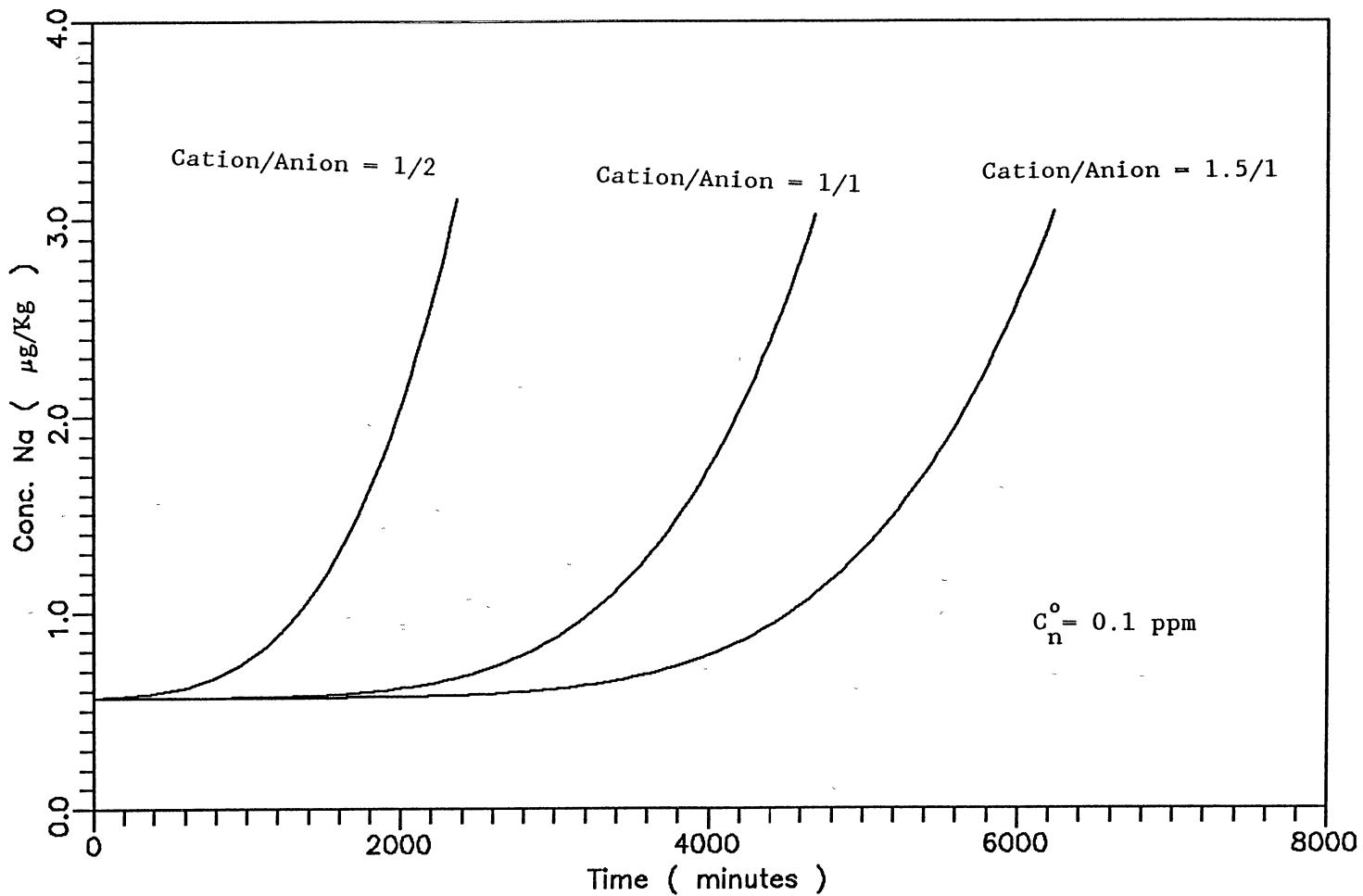


Figure 11. Predicted Sodium Break through for Ammonia Cycle Exchange at Various Cation-to-Anion Resin Ratios for pH 9.6

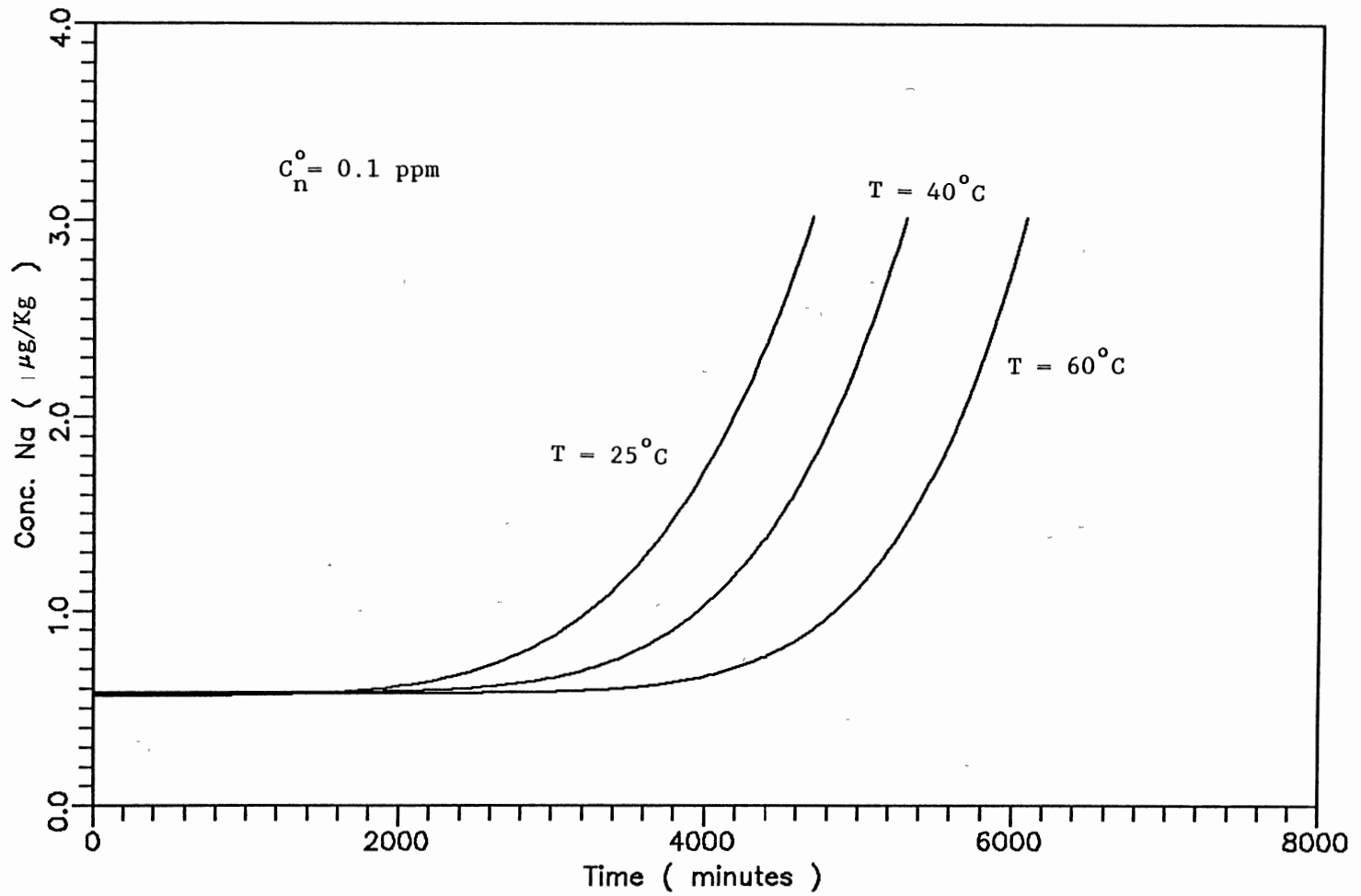


Figure 12. Predicted Sodium Break through for Ammonia Cycle Exchange at 25, 40 and 60°C for Temperature Independent Selectivity

the break through time for sodium. This does not consider the resin selectivity coefficient as temperature dependent. The lack of information in this area required this assumption. Industrial scale ion exchange units are typically run at temperatures in the range of 40 - 60 °C.

The addition of morpholine instead of ammonia for pH control has a major drawback. The dissociation constant for morpholine is nearly an order of magnitude lower than that for ammonia. This requires a nearly order of magnitude increase in the bulk phase concentration of morpholine to attain the same pH. This results in increased cost of operation due to the required increase in morpholine concentration. The favorable selectivity for sodium over ammonium and the reduced corrosion rates may, in the long run, outweigh the increased cost.

The same conditions used to evaluate the ammonia cycle have been applied for the morpholine cycle. The selectivity coefficient for Ambersep 252 (2.1) was used in these model evaluations. This allows the comparison of both cycles on essentially equal ground. The breakthrough characteristics equivalent to those in Figure 8 are shown for morpholine in Figure 13. The predicted time for breakthrough has increased because the column is sufficiently large to overcome the unfavorable diffusivity affect. The condition of constant sodium inlet concentration is compared with the break through times to a 2  $\mu\text{g}/\text{Kg}$  limit for ammonia and morpholine in Figure 14. This figure implies that morpholine has the potential for longer MBIE unit service times than ammonia under the same process conditions.

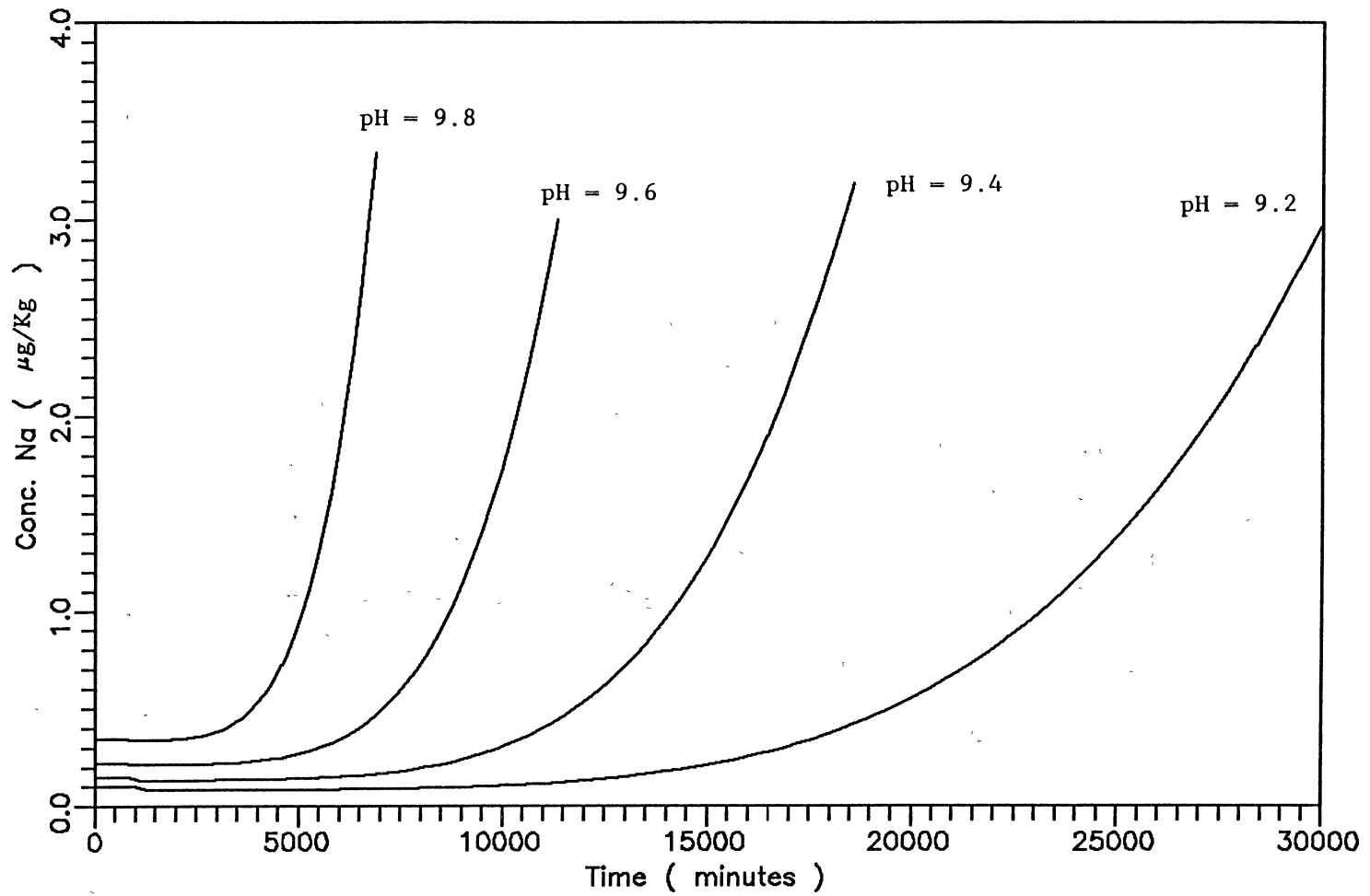


Figure 13. Predicted Sodium Break Through Curves for Morpholine Cycle Exchange at Various pH's and Conditions Equivalent to Figure 8

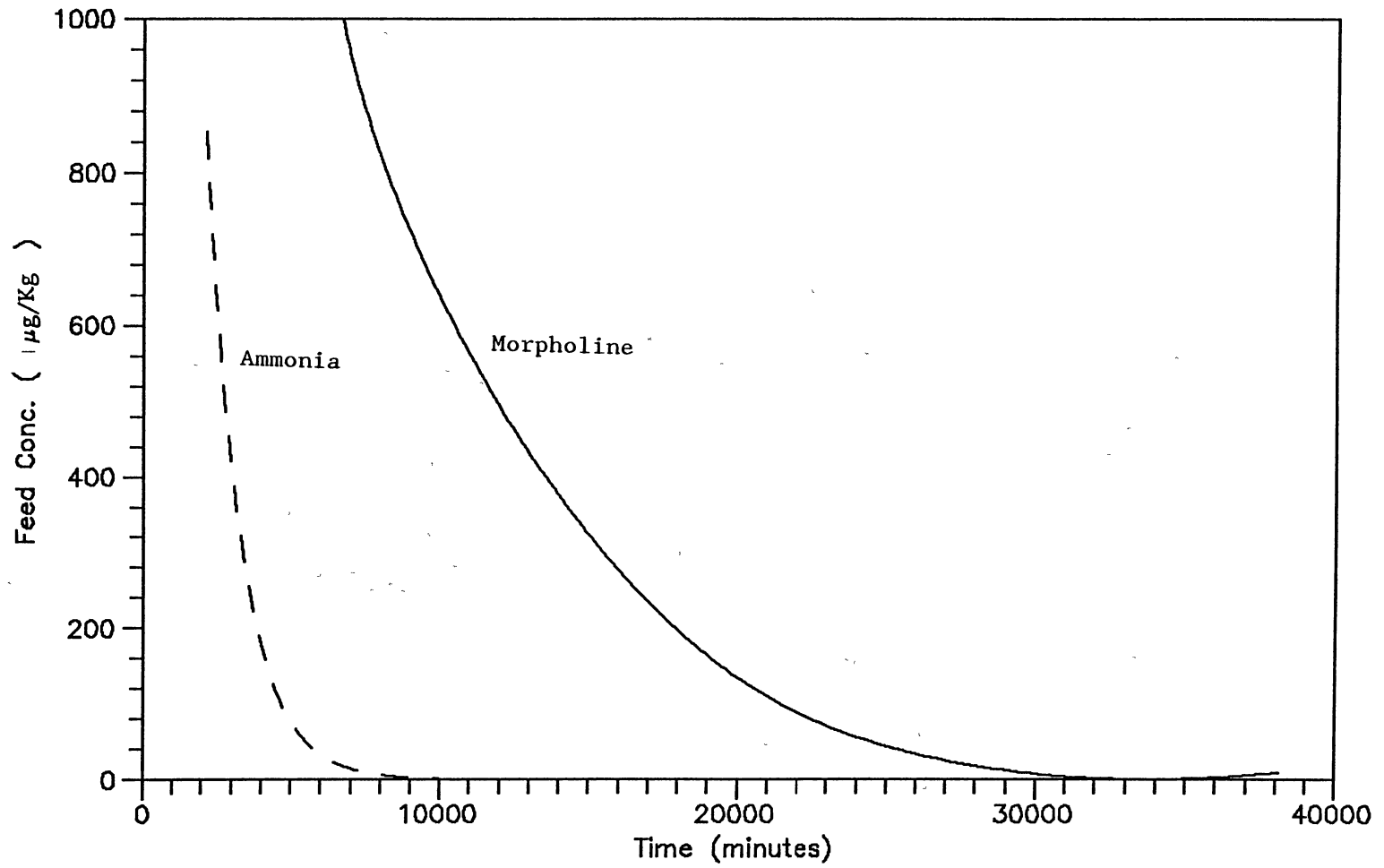


Figure 14. Comparison of time for 2 mg/ml Breakthrough for Ammonia Cycle and Morpholine Cycle Operation

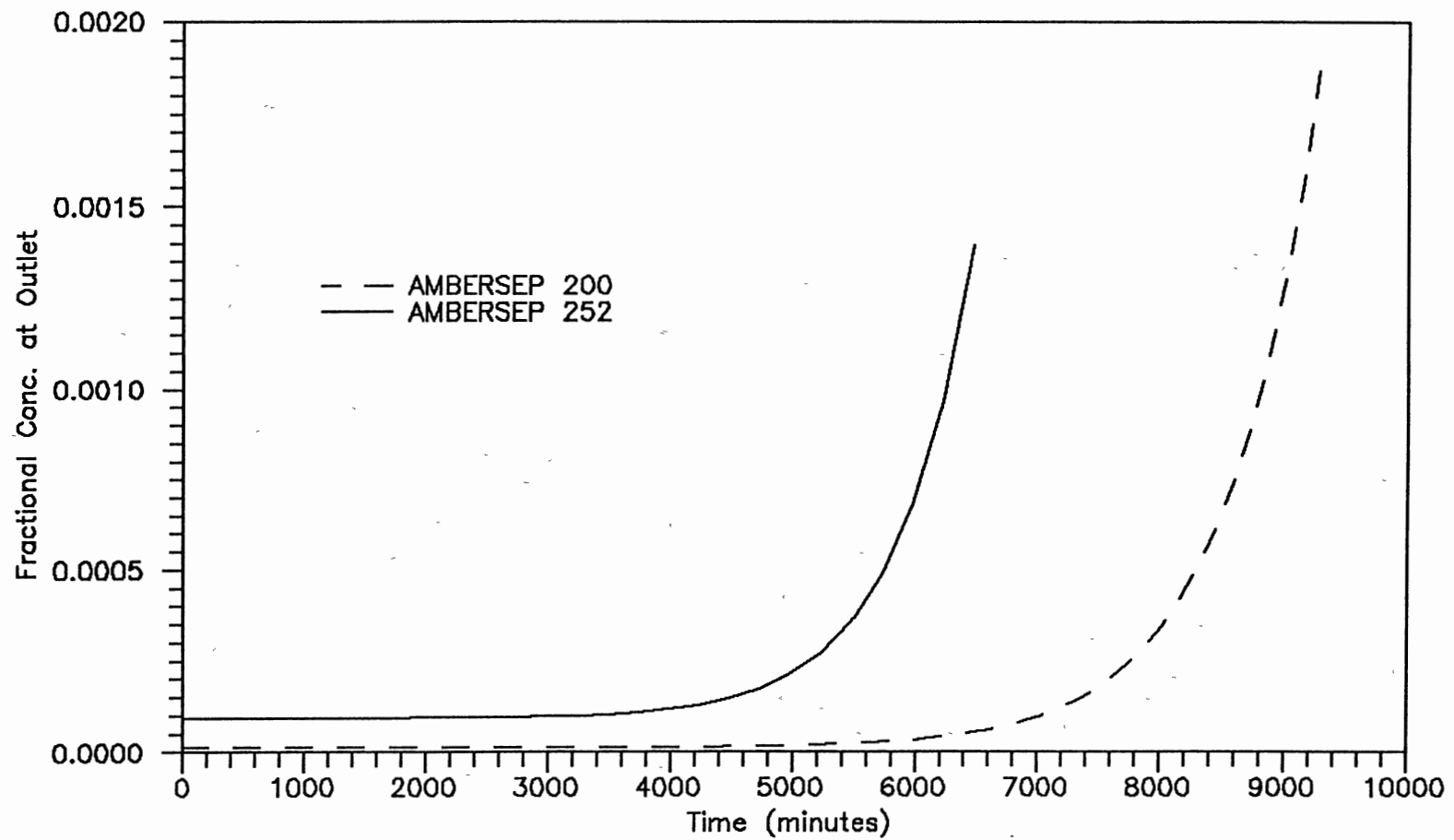


Figure 15. Comparison of Sodium Breakthrough in the Morpholine Cycle for AMBERSEP 200 and AMBERSEP 252



A comparison between using Ambersep 252 and 200 is shown in Figure 15. The increased selectivity coefficient greatly increases the time for break through, as one would expect. In the case of Ambersep 200 the break through of chloride must also be considered since the anionic resins have typically 60% of the exchange capacity of the cation resins. This operational scheme is when the model can be used to select the optimum cation-to-anion resin ratio. The possibility of chloride break through prior to sodium is shown in Figure 16. Here the chloride has reached the inlet concentration level before the sodium break through has fully developed. The level of contamination that is acceptable influences which species must be tracked. The sodium concentration rises sooner than the chloride, but when break through occurs the chloride concentration rises rapidly. The detrimental affect of using Ambersep 200 in these cycles is that it is extremely difficult to regenerate. The favorable selectivity coefficient coupled with the low degree of dissociation make converting the cation resin into the amine form extremely difficult.

#### Conclusions and Recommendations

The model presented here compares favorably with the existing experimental data and the mass action equilibria model of Bates and Johnson (1984). The major advantage of the model is the ability to make these predictions based on available literature parameters. Additionally, the model can be modified to evaluate other alternative amines effects on ion exchange by using experimental values for the system properties. The Wilke-Chang equation (1955) can be used to

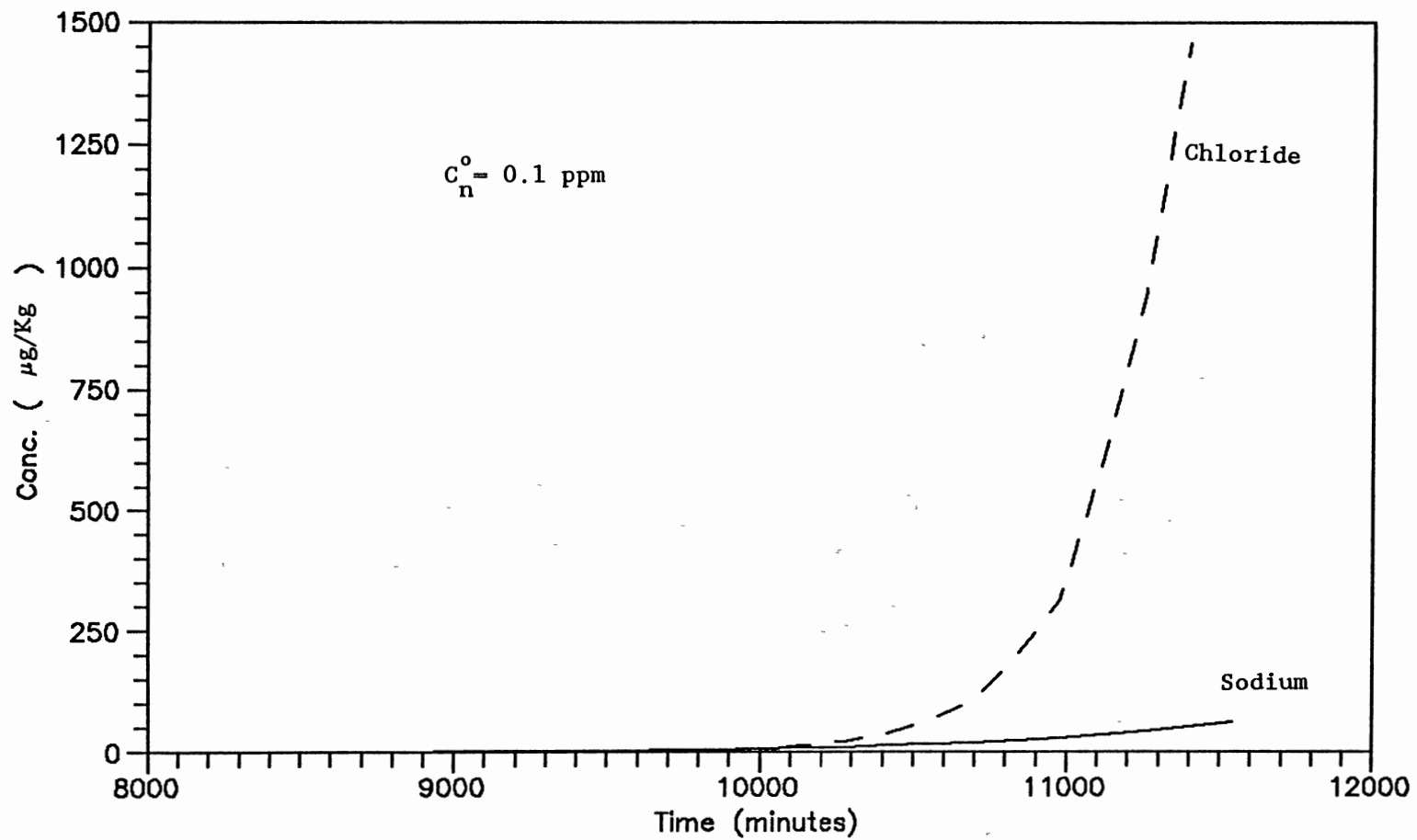


Figure 16. Break Through Curves For Sodium and Chloride in the Morpholine Cycle at pH 9.6 for Ambersep 200 Cation Resin

estimate self diffusion coefficients for species that are not readily available within the literature.

The comparisons between ammonia and morpholine as pH control agents show morpholine, operating in the morpholine cycle, to be a viable alternative to ammonia. The major drawback of morpholine is its degradation within the steam cycle and the effects that its breakdown products have on the corrosion process.

The model is limited by the accuracy of the available data. Most of the parameters used within the model are accurate to two significant digits. This combined with the tremendous effect an error in a parameter such as the capacity of the resin can have suggests that more reliable values are needed for these system parameters.

Additional considerations need to be incorporated within the model. The extension of the above model to handle hydrogen cycle exchange in the presence of amines and other multiple ion systems needs to be addressed. Also, a detailed sensitivity analysis of the model to various parameters will yield those that have the greatest effect on the exchange process and the overall columns operation.

## References

- Bates, J.C. and Johnson, T.D., Society of Chem. Ind., Int. Conf. on Ion Exchange, Cambridge, GB, 1984.
- Carberry, J.R., A.I.Ch.E. J., 4, 460, 1960.
- Darvill, M.R., Bates, A.J., Bates, J.C., Ellis, G.W., Gardner, D.J., and Sadler, M.A., CEGB report SWR/SSD/0842/N/86, 1986.
- Divekar, S.V., Foutch, G.L., and Haub, C.E., Ind. Eng. Chem. Res., 26, 1906, 1987.
- EPRI Report, NP-5056, 1987.
- EPRI Report, NP-5594, 1988.
- Haub, C.E., M.S. Thesis, Oklahoma State University, 1984.
- Haub, C.E. and Foutch, G.L., Ind. Eng. Chem. Fund., 25, 373, 1986a.
- Haub, C.E. and Foutch, G.L., Ind. Eng. Chem. Fund., 25, 381, 1986b.
- Kataoka, T, Yoshida, H., and Yamada, T., J. Chem Eng. Jpn., 5, 132, 1972.
- Kataoka, T, Yoshida, H., and Yamada, T., J. Chem Eng. Jpn., 6, 172, 1973.
- McNulty, J.T., Personal Communication, 1990.
- Pan, S.H., and David, M.M., A.I.Ch.E. Symp. Ser., 74, 74, 1978.
- Robinson, R.A., and Stokes, R.H., Electrolyte Solutions, Butterworths: England, 1959.
- Sawochka, S.G., Power, 67, April, 1988.

## CHAPTER III

### MULTI-COMPONENT UNI-VALENT MIXED-BED ION EXCHANGE MODELING IN NEAR NEUTRAL SYSTEMS

#### Abstract

A model for multi-component mixed-bed ion exchange is developed based on film diffusion limited mass transfer.. The model predictions compare favorably with the existing ternary data for the limiting case of no anion resin exchange only. The model is then extended to handle six component exchange (three cations and three anions) for uni-valent systems with bulk phase neutralization.

#### Introduction

Binary ion exchange systems have been thoroughly investigated by many researchers. However, the area of ternary, and larger component systems have been addressed only in a limited fashion. The development of a model that can predict column effluent concentration profiles for ternary systems will extended the ability of engineers to design and evaluate more complex systems. The approach for multi-component systems has followed the same route as that for binary exchange. The development of binary exchange models is based on equilibrium calculations, followed by single particle investigations of transport properties. This approach represents the state of

multi-component ion exchange theory at the present, with two notable exceptions.

There are many possible applications of a multi-component mixed bed ion exchange (MBIE) model. These include; power plant secondary cycles, micro-chip processing, waste water cleanup and ion chromatography. Those industries that are required to meet stringent guidelines, either government or self imposed, need the ability to improve process evaluation to optimize regeneration times. This has been met by equilibrium models, or by fixed regeneration cycles to determine when a mixed bed should be removed from service. A model that can predict accurately the fate of multiple components will allow the regeneration schedules to be improved upon and thereby decrease operating costs.

Consideration of multi-component exchange in single resin systems began with Dranoff and Lapidus (1958). They approximated the rate of exchange with a reaction kinetic model. This required the rate constants for the exchange process as well as the equilibrium constants for the resin to be experimentally determined. The advantages of this model are that the model will accurately predict shallow-bed operation for a wide range of process conditions. The major disadvantages are, the need to determine rate constants each time process modifications are made, and the inability of a kinetic model to describe the diffusion limited nature of the exchange process. Dranoff and Lapidus (1961), evaluated the approach, they found that it could only handle shallow-bed systems. The method also determined equilibrium constants for the resin that differed substantially from the published resin characteristics.

Helfferich (1967), developed a multi-component equilibrium model that could handle as many exchanging species as were present. This model predicts the intermediate plateaus that other investigators have since observed. The plateau regions bring out a further drawback of the model of Dranoff and Lapidus (1958), the inability to predict the intermediate plateaus with the kinetic model limited their development to shallow beds. Wagner and Dranoff (1967) considered film diffusion limited ternary exchange for cationic resins. They relied on a strong base solution that consumed the exiting hydrogen ion at the cation resin surface. In essence, this limited the exchange process to binary exchange with a slightly modified interfacial boundary condition.

Bajpai et al. (1974), conducted particle studies of ternary cation exchange. These studies were limited to the particle diffusion regime of ion exchange. This was the first investigation that considered the diffusional limitations that were first discovered by Boyd et al. (1947). The Nernst-Planck equation was used to determine the species fluxes within the resin framework, with the resulting equations solved numerically. This was the first step in the development of ion exchange models for multi-component diffusional rate limited exchange.

Particle diffusion in multi-component systems has been further developed by Hwang and Helfferich (1987) and Yoshida and Kataoka (1987). Hwang and Helfferich developed a model for general exchange accompanied by fast reversible reactions within the particle. The Nernst-Planck equation is combined with a reaction coefficient matrix to determine concentrations within the particle. This method has not

been extended to consider film diffusion or to evaluate column performance. The work of Yoshida and Kataoka was restricted to ternary cation systems exchanging on DOWEX 50 X 8. The mean resin phase concentration was compared between the numerical model and the experimental data that they collected. Their model considered only particle diffusion for single resin beads.

The first detailed consideration of multi-component film diffusion controlled ion exchange was presented by Omatete et al. (1980a,b). The first article was a theoretical consideration of the process generalized to compare the Nernst-Planck equation with Fick's law. The method was not restricted to film diffusion and also considered the possibility of concentration dependent diffusion coefficients. This development supports the work conducted by Yoon (1990) where the Haub and Foutch (1986a,b) model was found to be inadequate based on the diffusion coefficients. Omatete et al. (1980b) addressed experimental evaluation of column performance for ternary exchange. Unfortunately, the manner in which the diffusion coefficients and mass transfer coefficients were defined restricted their development to experimentally determined overall mass transfer coefficients. They considered only one set of ternary data in the evaluation. This set of data had an interesting characteristic, the intermediate plateaus predicted by Helfferich (1967) were fully developed.

The most recent consideration of ternary, film diffusion controlled ion exchange was conducted by Wildhagen et al. (1985). They considered the selection of the appropriate effective diffusivity. The Nernst-Planck equation and the static film model were used to



develop a new basis for effective diffusivity expressions. The study was limited to the evaluation of one ternary case, for a fluidized-bed liquid-phase reactor. They failed to address the effects of external reactions and was limited to single resin studies. The work presented is well thought out but the data presented by Omatete et al. (1980b) was not considered, and systems where intermediate plateaus exist were ignored.

The currently accepted design methods for ion exchange systems are summarized by Gottlieb (1990). These require the determination of the resin phase that limits the exchange process. The method does have several distinct advantages. It is straightforward and fairly simple to use and also can handle multi-valent exchange processes. The design technique is primarily based on graphical representations of mixed bed unit combined with equilibrium calculations. Combining the multi-valent capabilities of this technique with a general uni-valent model should be able to describe most ion exchange systems. The graphical method is an excellent approach for preliminary design considerations, but should be extended to include general systems where the limiting resin is not known. This type of operation was Yoon's (1990) major conclusion. The species that breaks through first is dependent on many parameters and is directly affected by the defined breakthrough limits. The defined breakthrough limits are the allowable contaminant concentrations at the bed outlet. Assuming that sodium (for instance) will exceed the outlet criteria first, is dependent on the inlet concentrations, pH and cation-to-anion resin ratio. Equilibrium calculations will sometimes cause false conclusions for MBIE unit operations.

The model developed in this article addresses uni-valent multi-component (three cations and three anions) exchange in a mixed-bed unit. The initial resins are assumed to be in the hydrogen and hydroxide form and the only reaction occurring is the water dissociation reaction. The process is considered from a film diffusion limited exchange viewpoint and is compared with the limited existing data for ternary cation exchange.

### Model Development

The model developed here is for film diffusion limited MBIE. The method follows closely that presented in an earlier article (this Dissertation Chapter 2). The film diffusion fluxes are described using the Nernst-Planck model combined with the continuity equation for the film. This application shows that some of the assumptions made in earlier developments are really derived properties of the system. Column effluent concentrations are determined by using the material balance equations which are solved numerically.

### Assumptions

The assumptions in the development have been limited to as few as possible to develop a generalized uni-valent theoretically based model. The assumptions presented in earlier work (this Dissertation Chapter 2) are modified to reflect the process under consideration. Table I summarizes the previous assumptions and the additional assumptions used in this model. Those that are actually derived conditions are presented at the bottom of the table in a new category.

Table I  
Model Assumptions

- 
- 1) Film diffusion control
  - 2) Pseudo steady state exchange ( variations of concentration with space are much more important than with time)
  - 3) No coion flux across the particle surface
  - 4) The Nernst-Planck equation incorporates all interactions between diffusing species
  - 5) All univalent exchange
  - 6) The static film model can be used to describe the film adhering to the particle surface
  - 7) Solid-film interface is maintained at equilibrium
  - 8) Reactions are instantaneous when compared with the rate of exchange
  - 9) Curvature of the film can be neglected
  - 10) Uniform bulk and resin compositions
  - 11) Activity coefficients are unity
  - 12) Plug flow
  - 13) Isothermal, isobaric operation
  - 14) Negligible axial Dispersion

Derived Conditions

No net coion flux within the film

No net current flow

---

The major assumptions involved are; film diffusion limited rates, uni-valent exchange, bulk phase reactions (for three counter ions), and that binary selectivity coefficients can be used to describe the ternary exchange process. Kataoka and Yoshida (1980) showed that ternary interactions for the selectivity coefficients can be important. Unfortunately, the new constants must be determined experimentally for the system under consideration. These observations were made at high concentrations when compared with the conditions considered in this article. At significantly lower concentrations where the ionic activity coefficients are essentially unity, the impact of the ternary exchanges should be lessened.

#### Flux Expressions

The flux expressions used to determine the effective diffusivity are based on the Nernst-Planck model which has been used extensively in ion exchange processes. The case of binary exchange on one resin has been discussed earlier and the extended model developed by Haub and Foutch (1986a) can be used in these near neutral systems. The film reaction model is limited to the case of binary exchange based on the need to determine the flux of hydrogen (or hydroxide) in terms of the other diffusing counter ion. It also requires that the concentration of the species be fixed at the reaction plane. This cannot be done in pH adjusted waters.

The binary flux expressions have been developed for hydroxide-chloride exchange in Appendix A. These same equations apply to binary exchange on the cationic resin when hydroxide and chloride are replaced with hydrogen and sodium, respectively.

The ternary flux expressions are derived in Appendix B. A method similar to that proposed by Wildhagen et al. (1985) is used. The conditions that are not truly assumptions but derived expressions are presented in Appendix B as well. The method used considers all of the coions together, rather than individually, as has been done before. Consequently a pseudo single coion (p) is defined to be the sum of all the coion concentrations within the film:

$$C_p = \sum_j C_j, \text{ where } j = \text{coions} \quad (\text{eq. 3-1}).$$

This allows the elimination of the assumption that each individual coion flux within the film is zero, and makes use only of the assumption that there is no net coion flux. This pseudo component is used to eliminate the electrical potential as:

$$\frac{d\phi}{dr} = \frac{RT}{F} \left( \frac{1}{C_p} \frac{dC_p}{dr} \right) \quad (\text{eq. 3-2}).$$

The necessary restriction to homo-valent exchange must now be applied, in order to eliminate the electrical potential term. The model has been limited to uni-valent exchange because the ions typically of interest in MBIE are uni-valent as opposed to di or tri-valent. The pseudo steady state nature of the exchange can be used to derive the fact that the flux of each counter ion within the film is a constant.

The major conclusion of Appendix B is the determination of the flux expression for ternary exchange. This expression for component i (any counter ion) is:

$$J_i = \frac{2_i D (C_p^* - C_p^o)}{\delta} \left( \frac{C_p^* Y_i^* - C_p^o Y_i^o}{C_p^{*2} - C_p^{o2}} \right) \quad (\text{eq. 3-3}).$$

This equation can be combined with the static film model to determine

the effective diffusivity for the exchange process. An effective diffusivity must be obtained because the static film model does not yield an explicit means of determining the film thickness,  $\delta$ . The effective diffusivity combines the previous expression for the flux and the overall mass transfer coefficient, giving a means to evaluate the exchange process.

#### Particle Rates

The particle rate expressions can now be derived based on the same technique that has been applied earlier (Haub and Foutch, 1986a and this Dissertation Chapter 2). The particle rate expressions derived in Appendix C apply equally as well to ternary exchange as to binary exchange. The difference appears in the equation derived to relate bulk phase and interfacial concentrations. The resulting expression arises from the exact differential that can be expressed in terms of the concentrations of the diffusing species. For ternary exchange, the relation is obtained from Appendix C as:

$$\begin{aligned} (C_A^* + C_B^* + C_C^*)(D_A C_A^* + D_B C_B^* + D_C C_C^*) = \\ (C_A^o + C_B^o + C_C^o)(D_A C_A^o + D_B C_B^o + D_C C_C^o) = \text{RHS} \quad (\text{eq. C-7}), \end{aligned}$$

where A, B and C are the three exchanging species and,  $^o$ , denotes bulk phase while,  $^*$ , denotes interfacial concentrations. The interfacial concentrations can be solved for in terms of the resin phase fractions, selectivity coefficients and the bulk phase concentrations as:

$$C_A^* = y_A \left[ \text{RHS} / \left( (1-K_C^A)y_A + (K_B^A - K_C^A)y_C + K_C^A \right) \right. \\ \left. \left( (D_A - D_C K_C^A)y_A + (D_B K_B^A - D_C K_C^A)y_B + D_C K_C^A \right) \right]^{1/2}$$

This has assumed that the binary selectivity coefficients can be used to describe the ternary exchange process. Since the charge balance must be everywhere satisfied, the pseudo coion concentration is equivalent to the sum of the counter ion concentrations. This allows the effective diffusivity to be calculated and  $R_i$  determined. The resultant rate expression is:

$$\frac{\partial y_i}{\partial \tau} = R_i K_i \frac{a}{Q} (C_i^o - C_i^*) \quad (\text{eq. C - 6}).$$

Where  $R_i$  is defined as:

$$R_i = \left( \frac{D_{ei}}{D_i} \right)^{2/3} = K_i' / K_i,$$

$K_i'$  is the overall mass transfer coefficient and  $K_i$  is the packed bed non-ionic mass transfer coefficient for species  $i$ . This is used in conjunction with the ternary system as it was for the binary system because of the approximation of the process as a series of binary exchanges. This is a direct result of assuming that the binary selectivities can be used for ternary exchange.

#### Material Balances

The form of the material balance equations does not change from those used earlier. The solution process must be extended to incorporate an additional component in each resin phase balance. That is the major difference between ternary and binary exchange. The

effluent concentration history of the bed is determined from the solution of these equations and the evaluation at the column exit.

The numerical techniques employed to solve the resultant system of equations is the method of characteristics. The resin and bulk phase fraction equations are then solved using fourth order Adams-Bashforth in  $\tau$  and fourth order Adams-Bashforth-Moulton in  $\xi$ . The method is briefly described in Appendix E.

With these necessary equations and conditions, the determination of effluent-concentration profiles of some MBIE units in ternary systems is possible. The model will first be compared with the limiting case of ternary cation exchange with a single coion.

## Discussion

### Ternary Data

The model developed in this article for multi-component ion exchange, can be compared for the limiting case of ternary cation exchange, with the experimental data of Omatete et al. (1980b). The three components are  $\text{Na}^+$ ,  $\text{Ag}^+$  and  $\text{H}^+$ . The single coion is  $\text{NO}_3^-$  since silver chloride is essentially insoluble. The effluent-concentration history for a 55.6 cm tall column was determined for specific inlet conditions on DOWEX 50 X 8 resin. The model compares reasonably well with the experimental data as shown in Figure 1. The break zones, where there is a drastic change in concentration in a short period of time, are extremely sharp for the model predictions. The most likely cause of this is the assumption that activity coefficients are unity, which is not the case in this concentration range (0.05 M). An



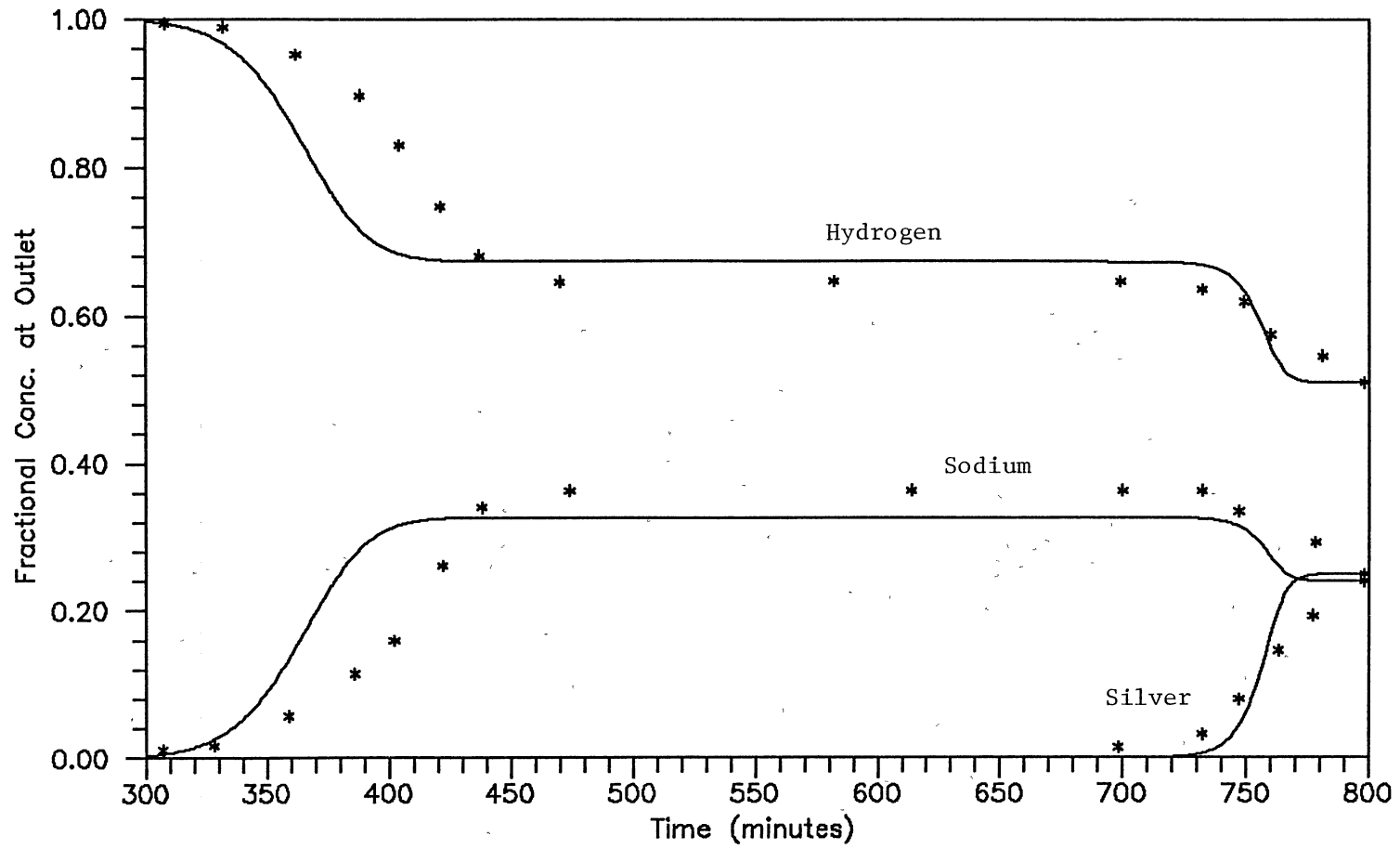


Figure 1. Comparison of Ternary Model Predictions with Omatete, et. al. (1980) Experimental

activity coefficient model could be used to adjust the impact of the selectivity coefficients, and more accurately represent the data. Modifying the selectivity coefficient tends to flatten the breakthrough curve. The general trend and location of transition zones between the model and the experimental results are very good. These comparisons imply that the model should provide a good qualitative method for determining effluent concentration profiles.

Figure 2 compares a model predicted curve with data presented by Dranoff and Lapidus (1961), for a shallow bed of DOWEX 50 X 8 cation resin 2.46 cm tall. The feed was a 0.0995 M solution of nearly one to one silver and sodium nitrates. The model significantly under predicts the time for each major response in the data. Considering activity coefficient non-ideality should improve the results. The height of the transient zone is over predicted by the model, and the original leakage level is under predicted. The combination of these two observations with the shallow bed nature and relatively high flow rate of the experiment leads to the conclusion that kinetic leakage may well be present under these conditions.

Comparing Figure 1 and 2, the greater than feed concentration zone in the sodium fraction is noticed. In Figure 2 the plateau zone is not fully developed but transient. The shallow column and possible presence of kinetic leakage, causes this transient behavior. The column height for Figure 1 is roughly twenty times greater than that for Figure 2. The greater height allows for the development of distinct regions within the bed that operate in essentially binary exchange. The first binary exchange area is between silver and sodium after the hydrogen has been displaced, the second zone is

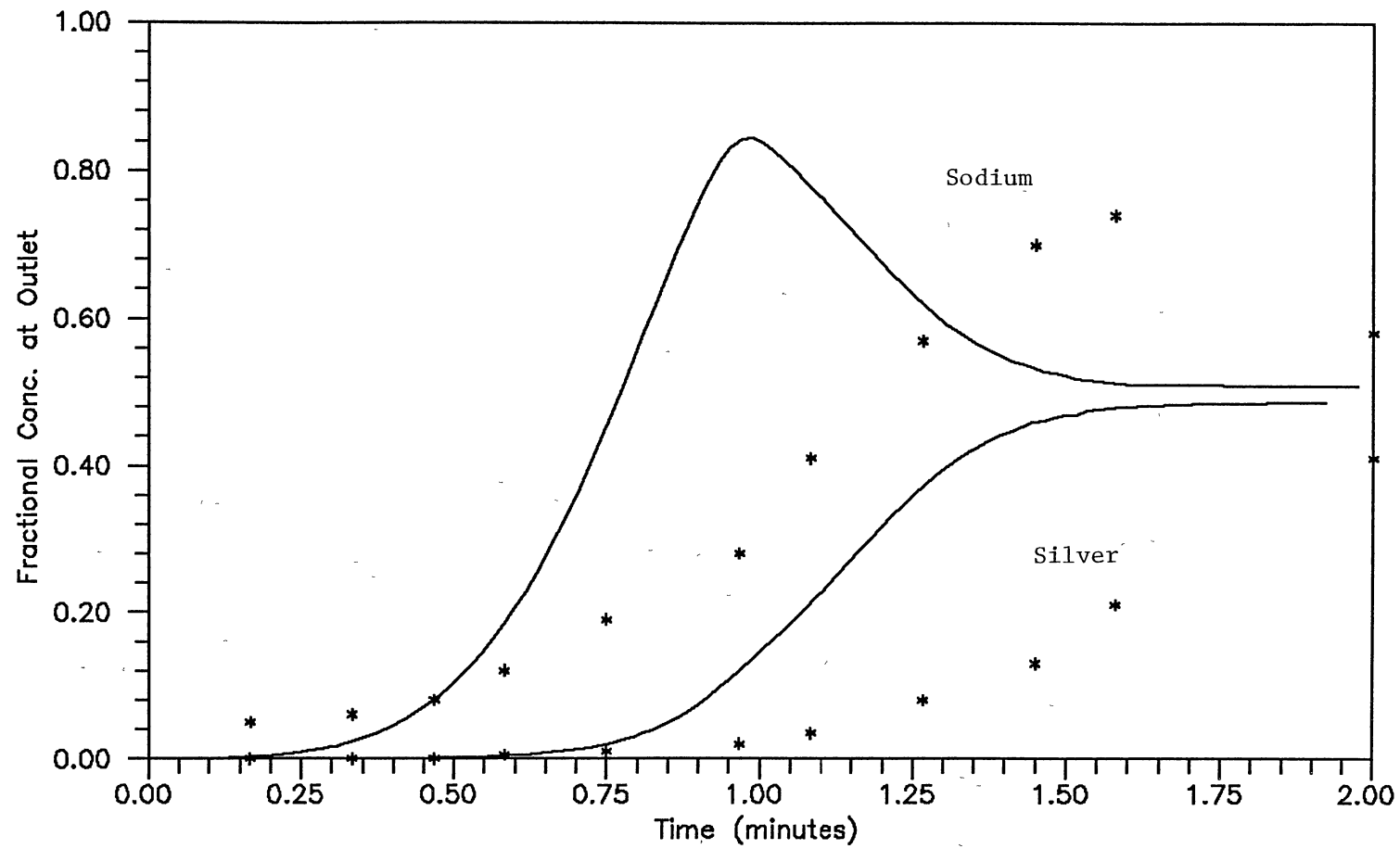


Figure 2. Comparison of Ternary Model Predictions with Dranoff and Lapidus (1961), Experimental (Hydrogen Omitted for Clarity)

sodium-hydrogen exchange, and the third region is unreacted hydrogen form resin. As the process progresses, the silver zone expands thereby displacing the sodium zone, which is also expanding. When the sodium concentration has leveled off in Figure 1, the sodium exchange zone has displaced all of the unreacted hydrogen form resin. This causes a constant sodium outlet concentration. Once the bed is entirely at equilibrium with silver, the silver begins to break through. This results in the final achievement of equilibrium and the constant outlet concentrations for all species. The existence of the transient and fully developed plateau zones is qualitatively predicted by the model.

#### Exchange Rates

The effect on the exchange rate in a ternary system is significantly more complex than in a binary system.  $R_i$  and the rate must be determined for two species, since there are three ions involved in the exchange process. The overall result is a three dimensional surface for  $R_i$  and the rate, with two of the resin phase fractions as independent variables, for each bulk phase composition. Figure 3 shows  $R_i$  for sodium under specific bulk phase concentrations at various resin loadings. The same conditions and their effect on  $R_i$  for potassium is shown in Figure 4. The  $R_i$  for sodium is enhanced significantly, with a discontinuity in the region of reverse exchange. The effect of potassium is to reduce the slope in the low sodium regions. As the equilibrium zone is approached, the value of  $R_i$  approaches an asymptote. This asymptote is where the bulk phase and interfacial concentrations are equal. Hence, there is no driving

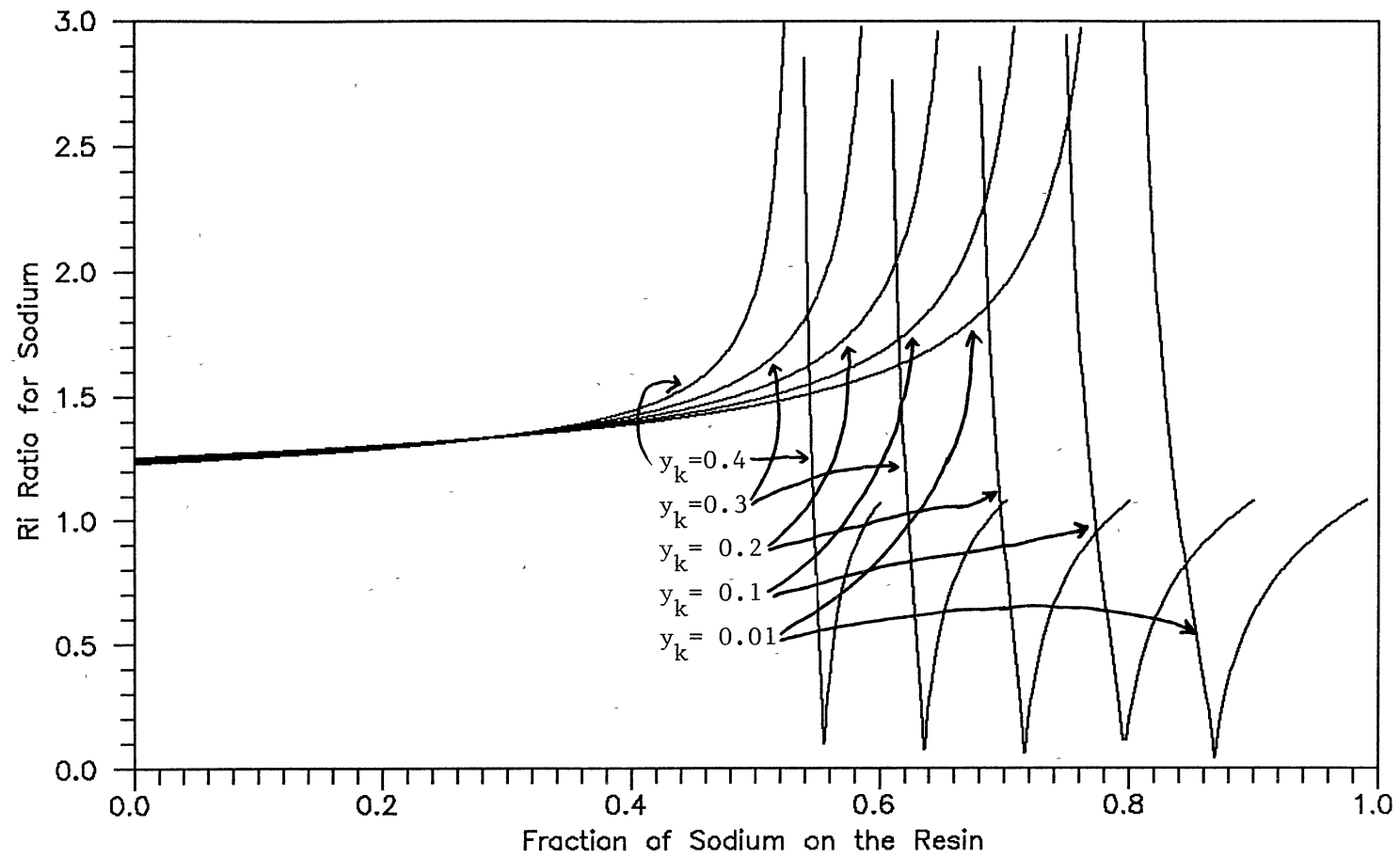


Figure 3.  $R_i$  Ratio for Sodium in the Ternary System: Sodium, Potassium, Hydrogen, at Various Potassium Resin Phase Loadings

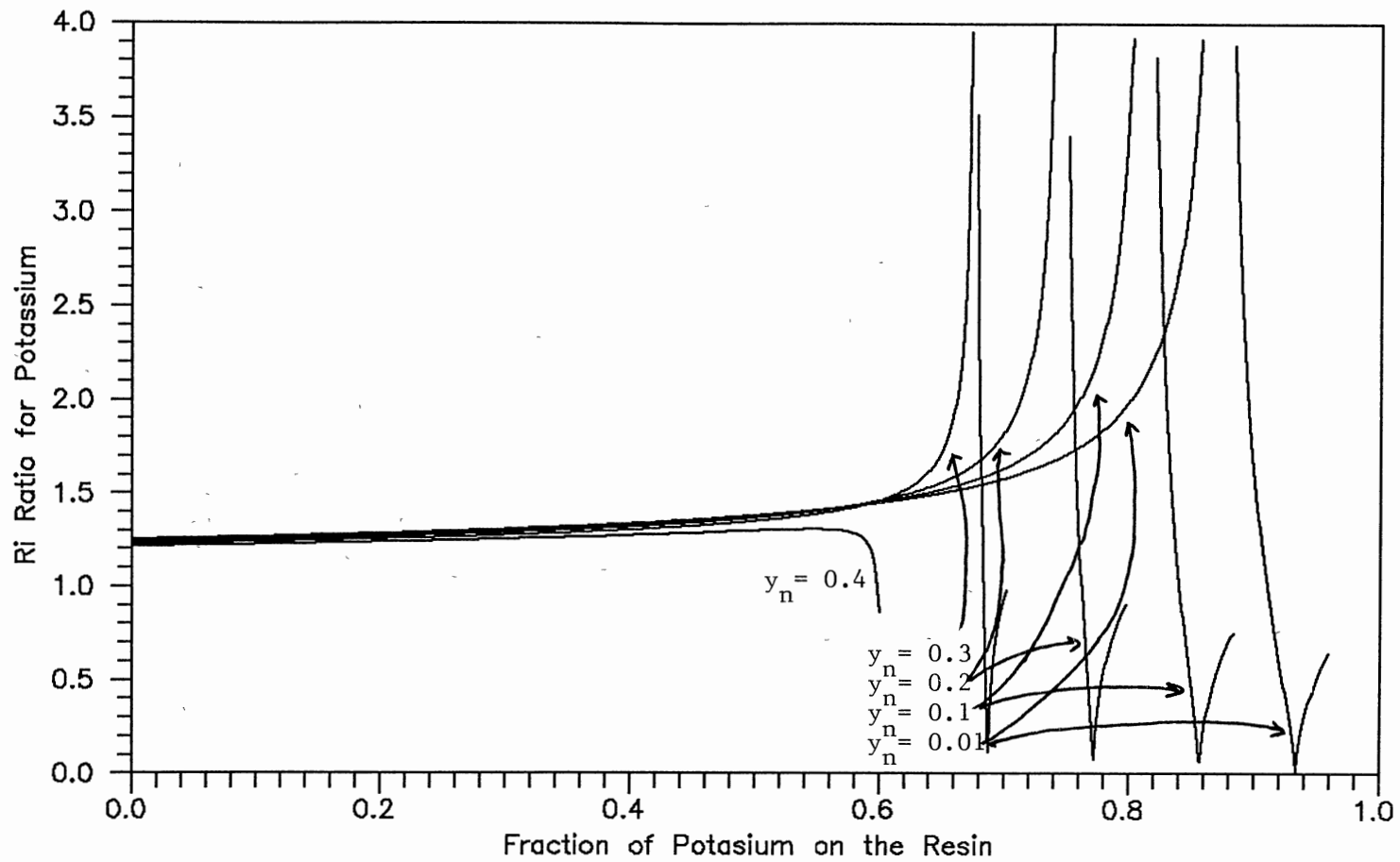


Figure 4.  $R_i$  Ratio for Potassium in the Ternary System: Sodium, Potassium Hydrogen, for various Sodium Resin Phase Loadings

force for exchange and the value of the effective diffusivity is irrelevant. This discontinuity arises because of the effective diffusivity being defined in terms of the driving force. The effect of increasing potassium resin phase loading is to decrease the value of  $R_i$  from what it would be for sodium-hydrogen exchange only. Increasing sodium resin phase loading decreases the value of  $R_i$  for potassium from what it would be for binary exchange only. This is the same effect that was noticed in earlier work (this Dissertation Chapter 2), where the morpholine diffusion coefficient was lower than the sodium diffusion coefficient. This effect is most noticeable for the sodium resin phase loading of 0.4. The decrease in  $R_i$  arises since the less mobile of the two species is on the resin. In addition to this, there is a significant change in the nature of  $R_i$  for potassium. The curve changes direction from increasing to decreasing because of the combined effect of the diffusion coefficients and the previously mentioned discontinuity at equal bulk and interface concentrations. Lower potassium loadings, and sodium loadings, cause a significant portion of the exchange to be between potassium and hydrogen. The exchange between  $K^+$  and  $H^+$  has a positive effect on  $R_i$ . As the fraction of the available exchange species becomes predominantly sodium, the unfavorable diffusivity ratio between  $K^+$  and  $Na^+$  causes  $R_i$  to cross over the discontinuity and be less than one. The observations of the effects of exchange on  $R_i$  agree well with the one set of conditions presented by Wildhagen et al. (1985) within the data ranges they presented. This comparison is limited to the effective diffusivity variation with interfacial concentration, when the interfacial concentration is considered as dependent on the resin

phase compositions. In addition, the regions where the discontinuities occur was not considered by Wildhagen et al. or any other researcher.

The effect of resin phase loadings on the rate of exchange for the same conditions as  $R_1$  is shown in Figures 5 and 6, for sodium and potassium respectively. The decrease in the selectivity coefficient for  $K^+ - Na^+$  exchange and the decrease in the diffusivity ratio leads to the change in exchange rate that can be seen in Figures 5 and 6. The change in rate is similar to, and a direct result of, the change in the value of  $R_1$ . Additionally, the rate experiences a second peak as the equilibrium conditions for  $K^+ - H^+$  exchange are exceeded, but  $Na^+ - H^+$  is not. This significant change in slope is caused by the drastically lower rate of exchange of  $Na^+ - K^+$  from the exchange of each species with hydrogen. The ternary nature of the exchange causes a shift in the rates based on the concentrations of all three species present. Trying to describe the process in terms of binary exchange behavior is misleading. At the point where the equilibrium becomes unfavorable for  $K^+ - H^+$  exchange, the presence of a significant portion of sodium on the resin allows for a finite (positive) rate of exchange between  $K^+$  and  $Na^+$ . The rate of potassium exchange shown in Figure 6 does not show the second peak for a sodium resin phase loading of 0.4. The lack of a second peak is caused by a significant portion of the exchange process occurring between potassium and sodium. The second near equilibrium resin phase loading does not occur because of the high sodium loading. Thus, the positive effect that the  $Na^+ - K^+$  exchange has on the rate is continuous, hence the change in rate results in a curve with an intermediate peak which is expected from



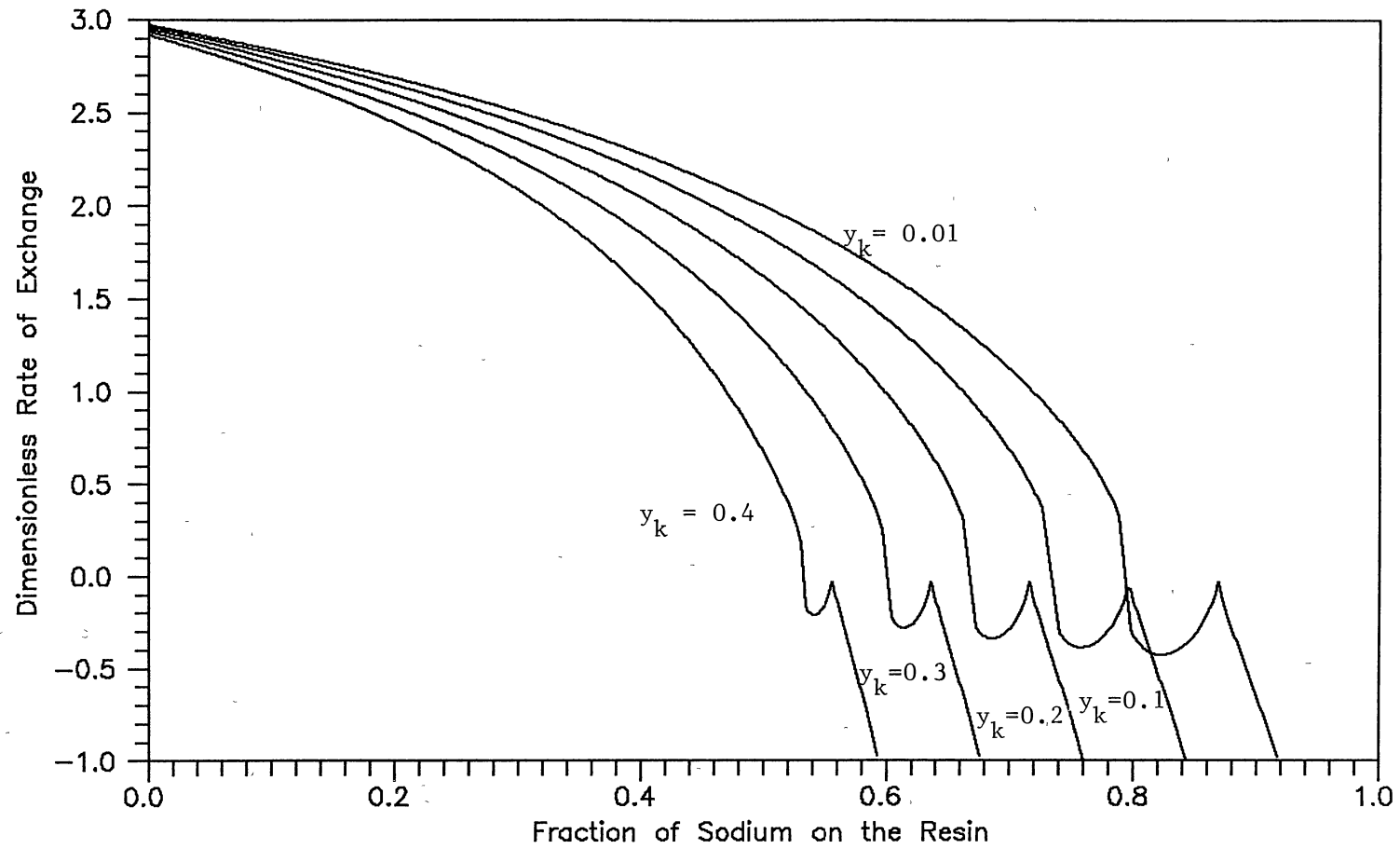


Figure 5. Dimensionless Rate of Exchange for Sodium in the Ternary System: Sodium, Potassium and Hydrogen

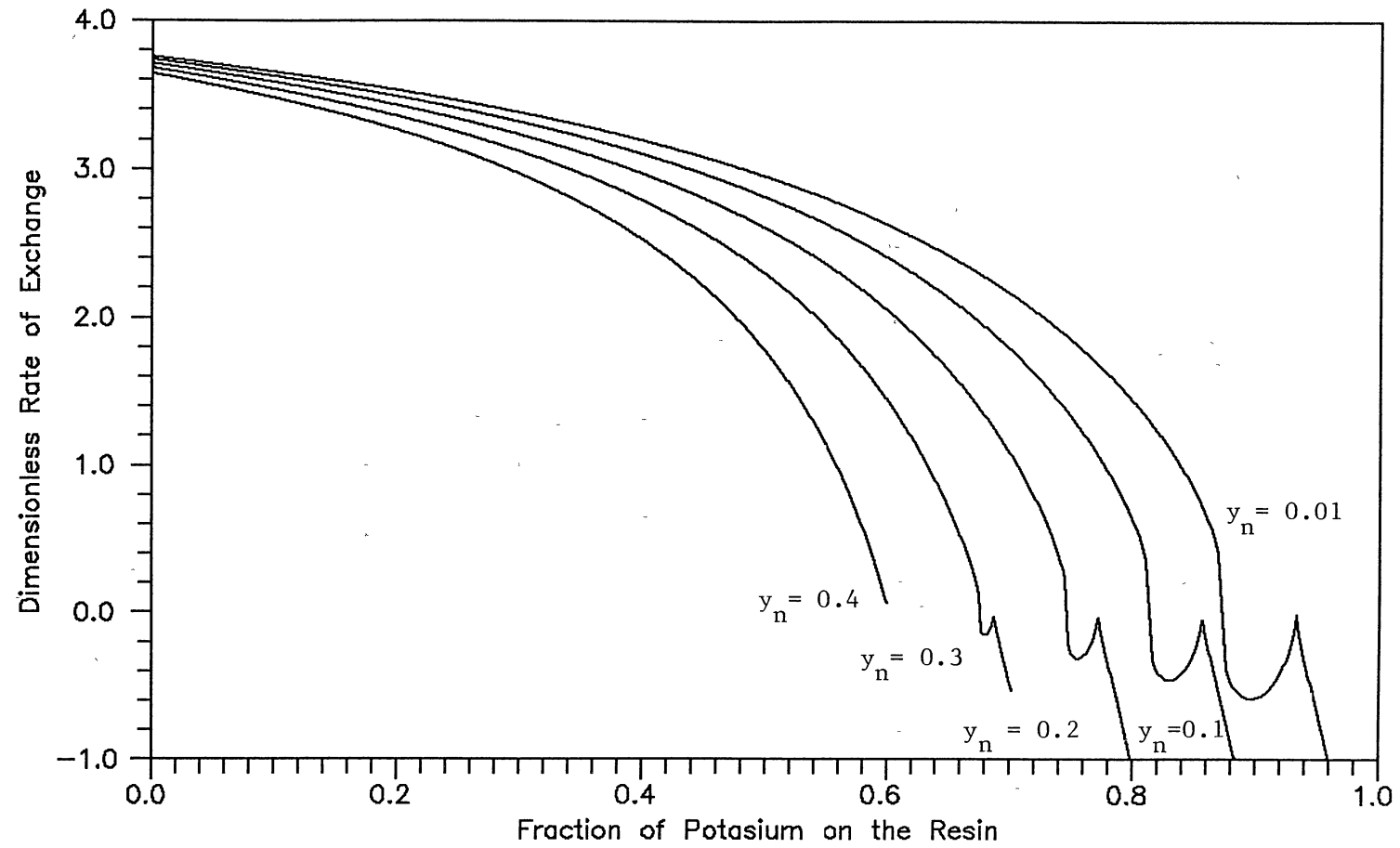


Figure 6. Dimensionless Rate of Exchange for Potassium in the Ternary System: Sodium, Potassium and Hydrogen

the three component nature of the process, except as discussed for high sodium loadings.

#### Column Evaluations

Column operation effluent-concentration profiles were determined for a five and six component MBIE unit. The three cations considered were;  $\text{Na}^+$ ,  $\text{K}^+$  and  $\text{H}^+$ . The three anions considered were;  $\text{OH}^-$ ,  $\text{Cl}^-$  and  $\text{NO}_3^-$ . The system parameters were determined from literature values and resin manufacturers information. The column conditions are similar to those used experimentally by Yoon (1990). The effect of cation-to-anion resin ratio and varying feed inlet concentration ratio was accomplished by modifying the initial conditions for the bed.

The three cation two anion ( $\text{Cl}^-$ ,  $\text{OH}^-$ ) results are shown in Figure 7 for a cation-to-anion resin ratio of one. The transient bump noticed in Figure 2 is again observed. The transient nature is due to a fairly shallow bed (5 cm) at a moderate flow rate (1 ml/sec). The bulk-film neutralization method developed by Haub (1984) can be used in the case of binary anion exchange. The ternary exchange on the cation resin can not use this method because an actual value for the distance to the reaction plane is necessary to solve the resulting flux expressions. The static film model does not allow for the reaction plane location to be explicitly defined. Figure 8 shows a cation-to-anion resin ratio of 1/1.5 for the same conditions as in Figure 7. Figures 7 and 8 can be compared with Figure 9 where the cation-to-anion resin ratio was set at 1.5/1. The three figures show that the cation-to-anion resin ratio can be used to adjust the time to

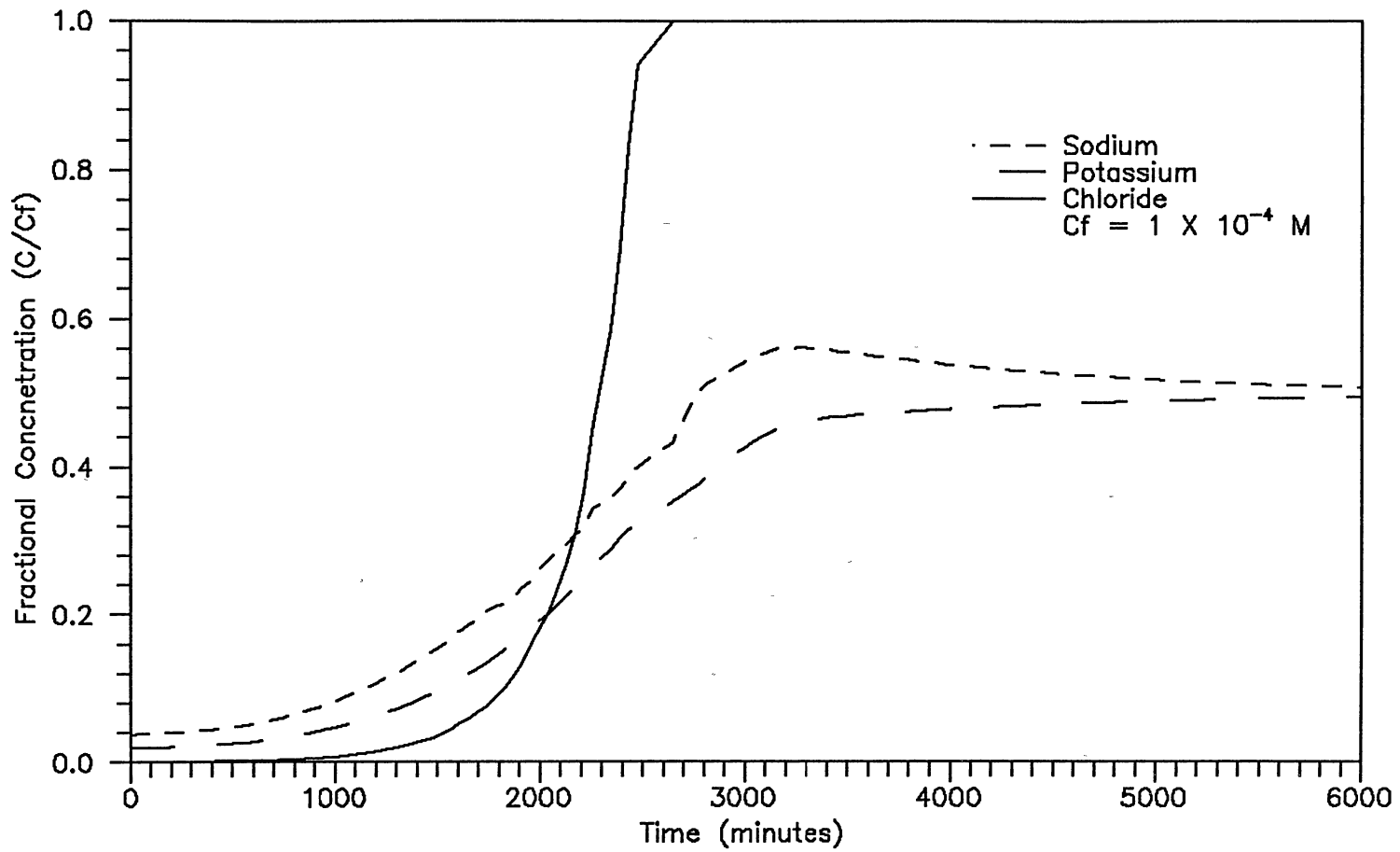


Figure 7. Five Component Break Through Curves for Sodium, Potassium and Chloride at a Catio-to-Anion Resin Ratio of 1/1

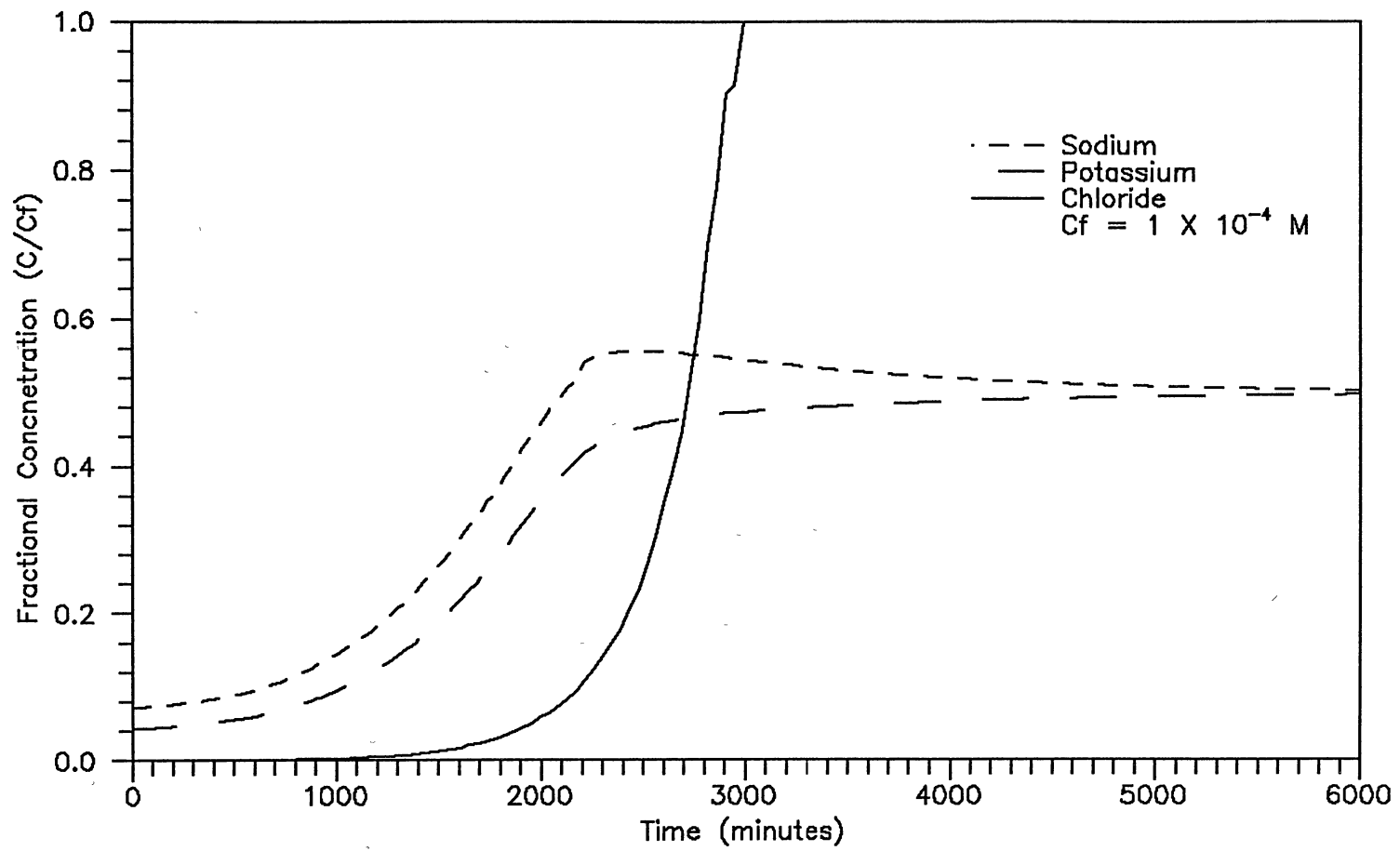


Figure 8. Five Component Break Through Curves for Sodium, Potassium and Chloride at a Catio-to-Anion Resin Ratio of 1/1.5

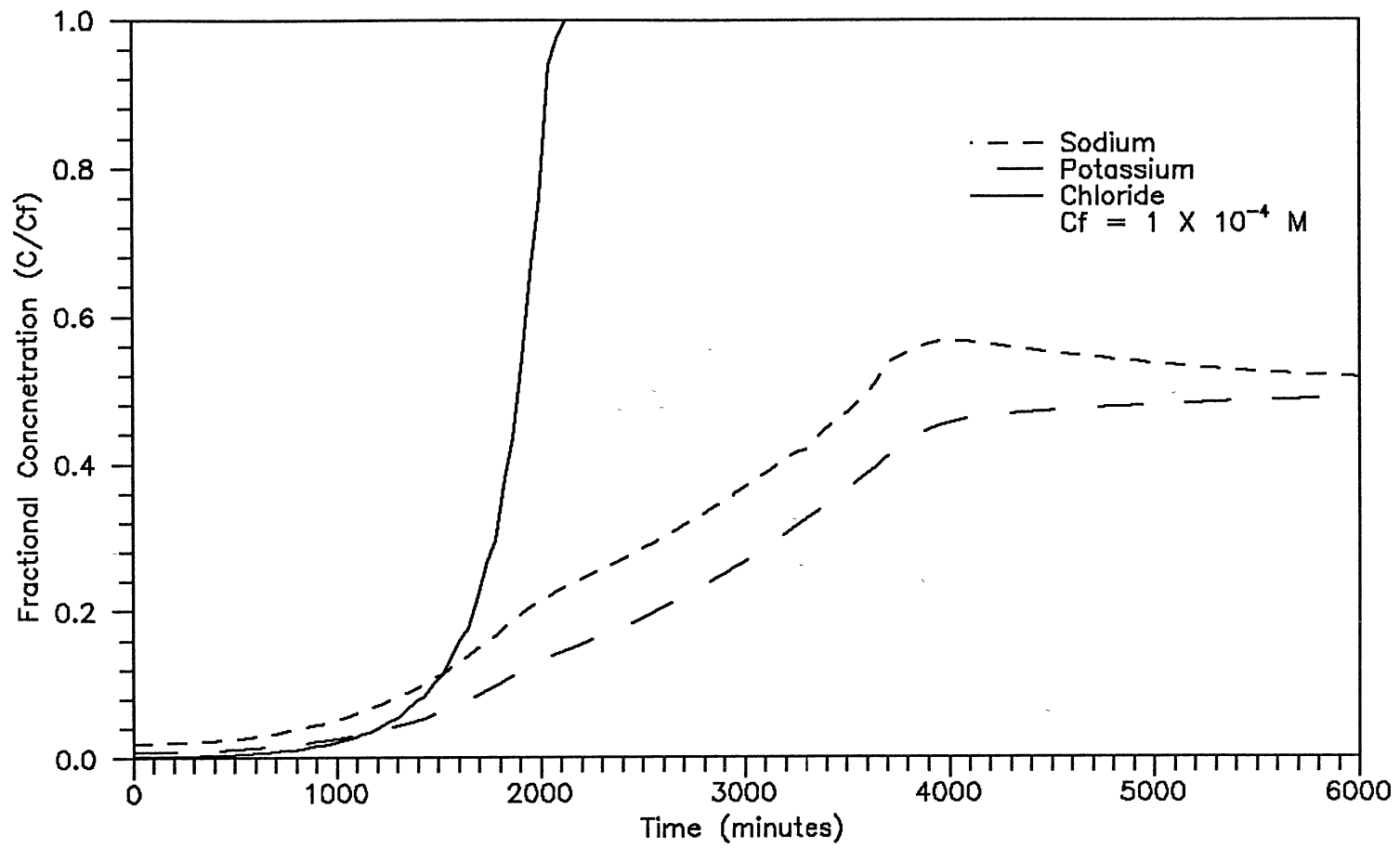


Figure 9. Five Component Break Through Curves for Sodium, Potassium and Chloride at a Catio-to-Anion Resin Ratio of 1.5/1.0

a significant breakthrough or to adjust initial resin leakages. The resin ratio of 1.5/1 results in lower initial leakage of the cations which is off set by an earlier chloride breakthrough. Depending on the zone of desired operation, this parameter can be adjusted to improve both parameters. Figure 10 shows a cation-to-anion resin ratio of 1/1 for an order of magnitude lower inlet concentration than Figures 7,8 and 9. The net effect of the lower inlet concentration is to extend the breakthrough for each species in time. The initial resin phase leakages are nearly the same because the surface concentration effects the exchange process significantly more than the bulk phase concentrations, and the outlet conditions are equilibrium values for the resin phase loadings. All of these factors can be combined with an allowable effluent concentration to determine the optimum cation-to-anion resin ratio for a given exchange process.

The case of six component uni-valent exchange is shown in Figures 11 through 15, for various cation-to-anion resin ratios, inlet concentrations and anionic resin types. Figure 11 shows the effect of a Type I anion exchange resin on the exchange process. The selectivity coefficient for  $\text{Cl}^-$  on this type of resin is roughly 16.5. The  $\text{NO}_3^-$  selectivity coefficient is even greater, roughly 40. When these are compared with the cation resin selectivities of 2.4 for  $\text{K}^+$  over  $\text{H}^+$  and 1.5 for  $\text{Na}^+$  over  $\text{H}^+$ , a significant change in the exchange process results. The type I resin results in very low anion resin leakages because of the extremely high selectivity coefficients for chloride and nitrate. The transient hump discussed with Figure 2 appears again for both the chloride and sodium concentrations, although it is significantly more pronounced for chloride. The

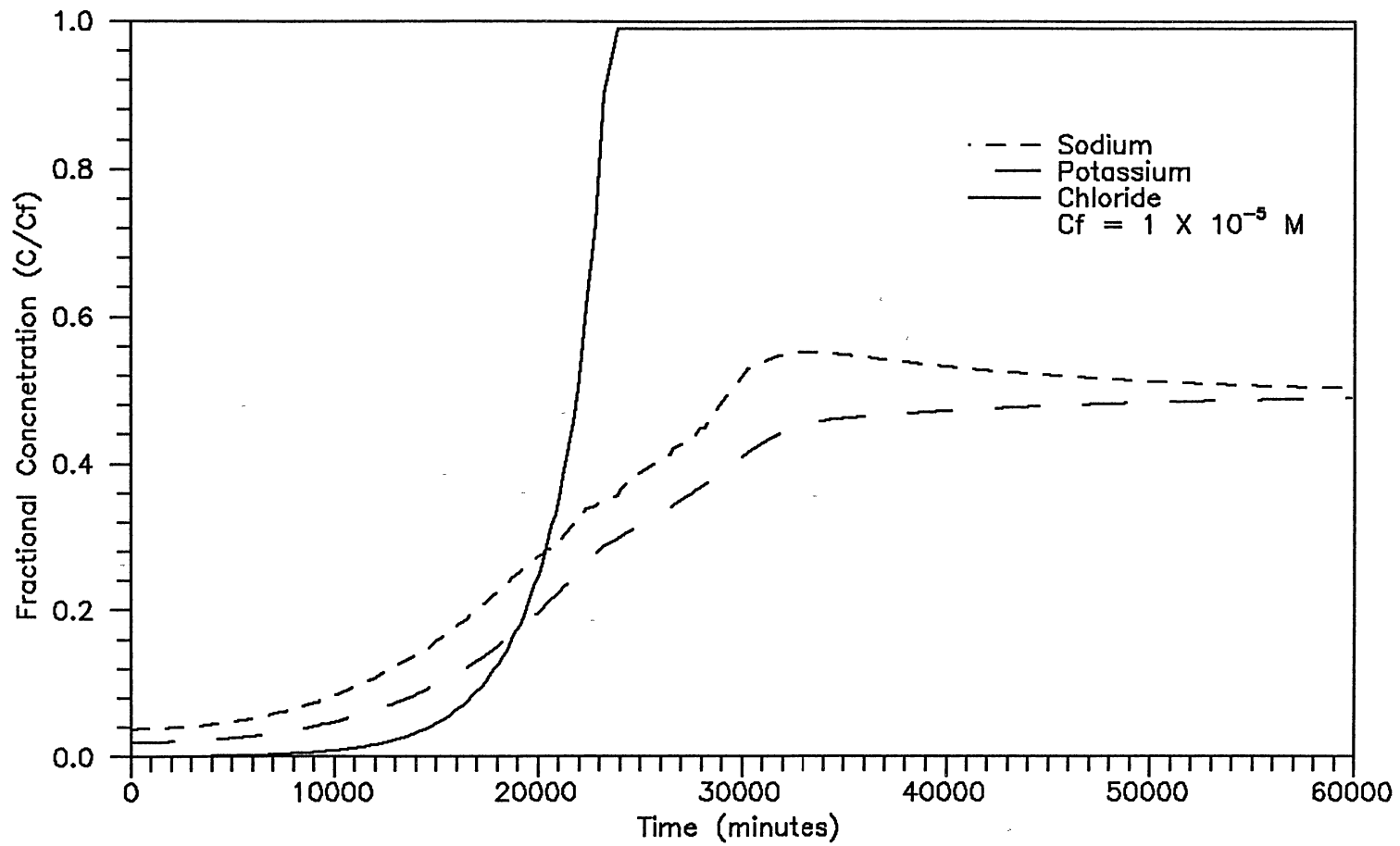


Figure 10. Five Component Break Through Curves for Sodium, Potassium and Chloride at a Catio-to-Anion Resin Ratio of 1/1



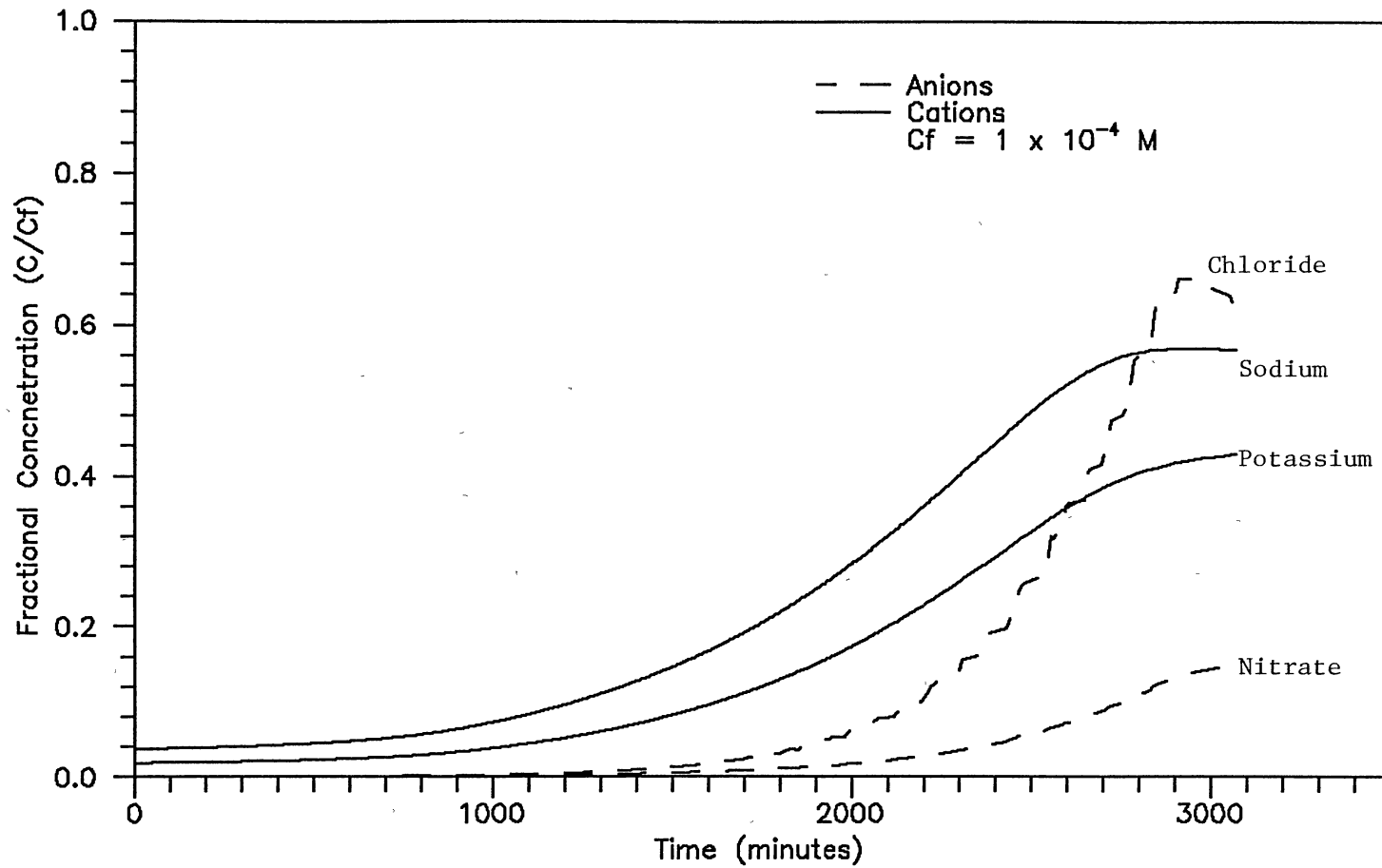


Figure 11. Six Component Break Through Curves for Sodium, Potassium, Chloride and Nitrate on a Type I Anion Exchange Resin

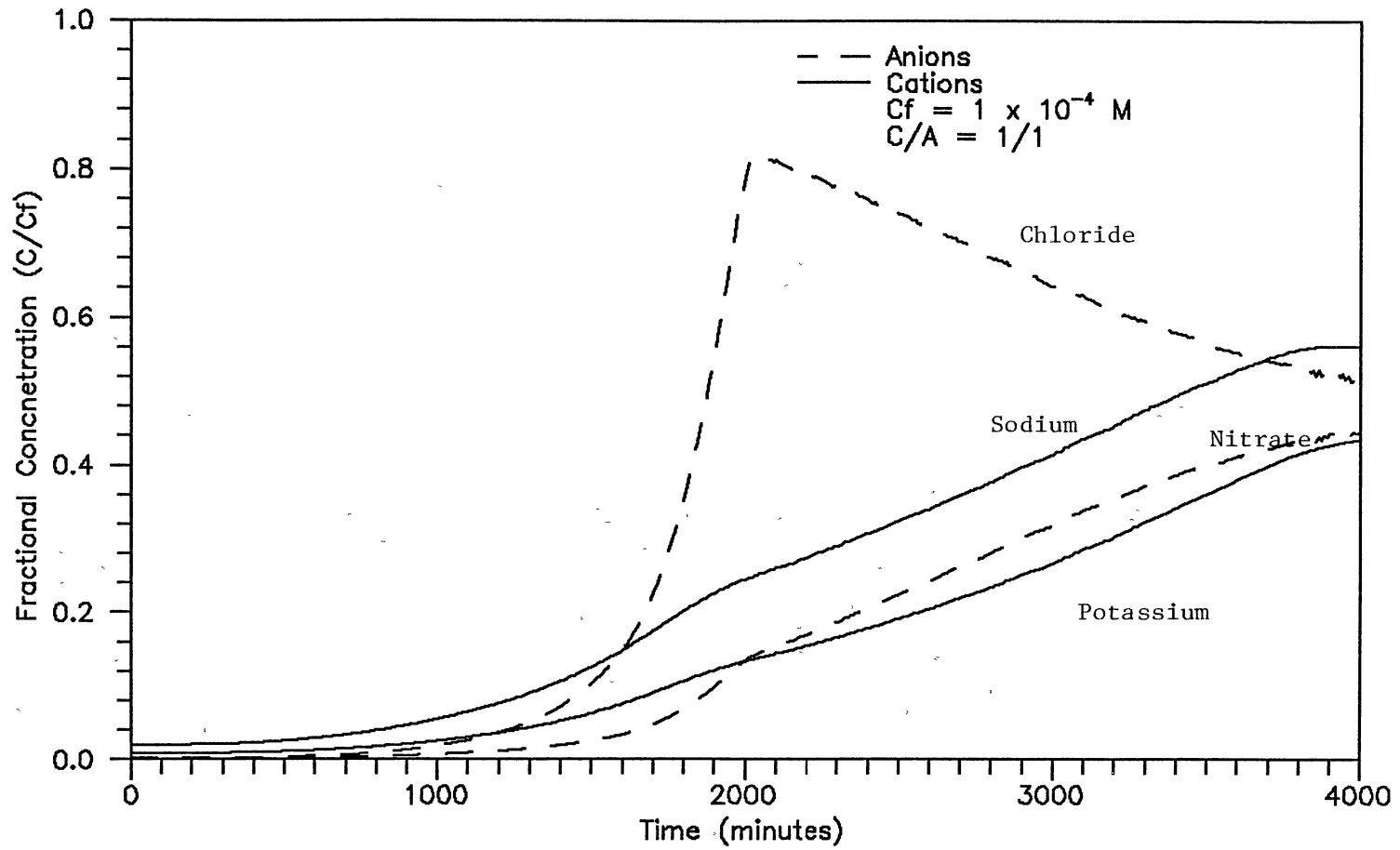


Figure 12. Six Component Break Through Curves for Sodium, Potassium, Chloride and Nitrate on a Type II Anion Exchange Resin

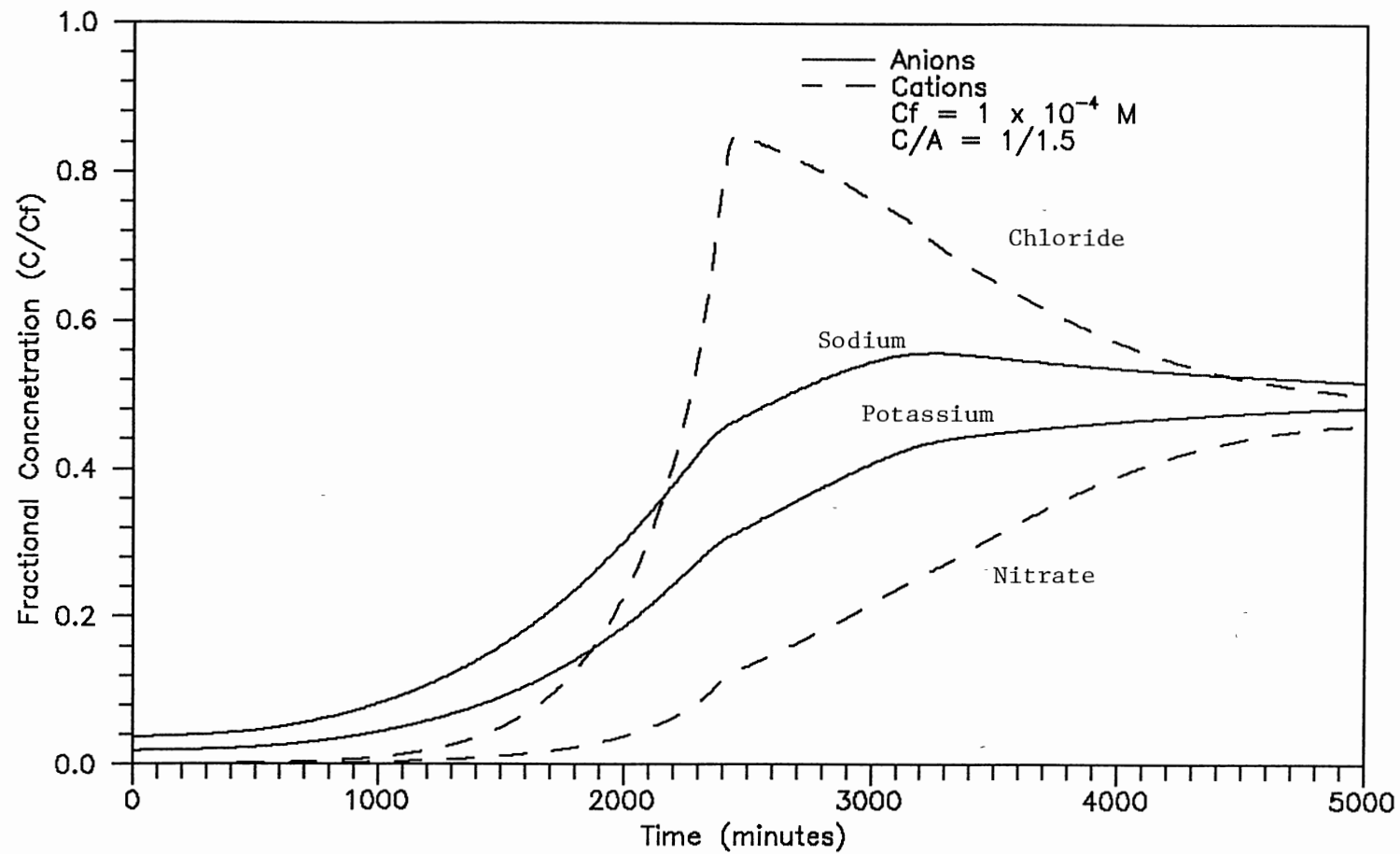


Figure 13. Six Component Break Through Curves for Sodium, Potassium, Chloride and Nitrate on a Type II Anion Exchange Resin

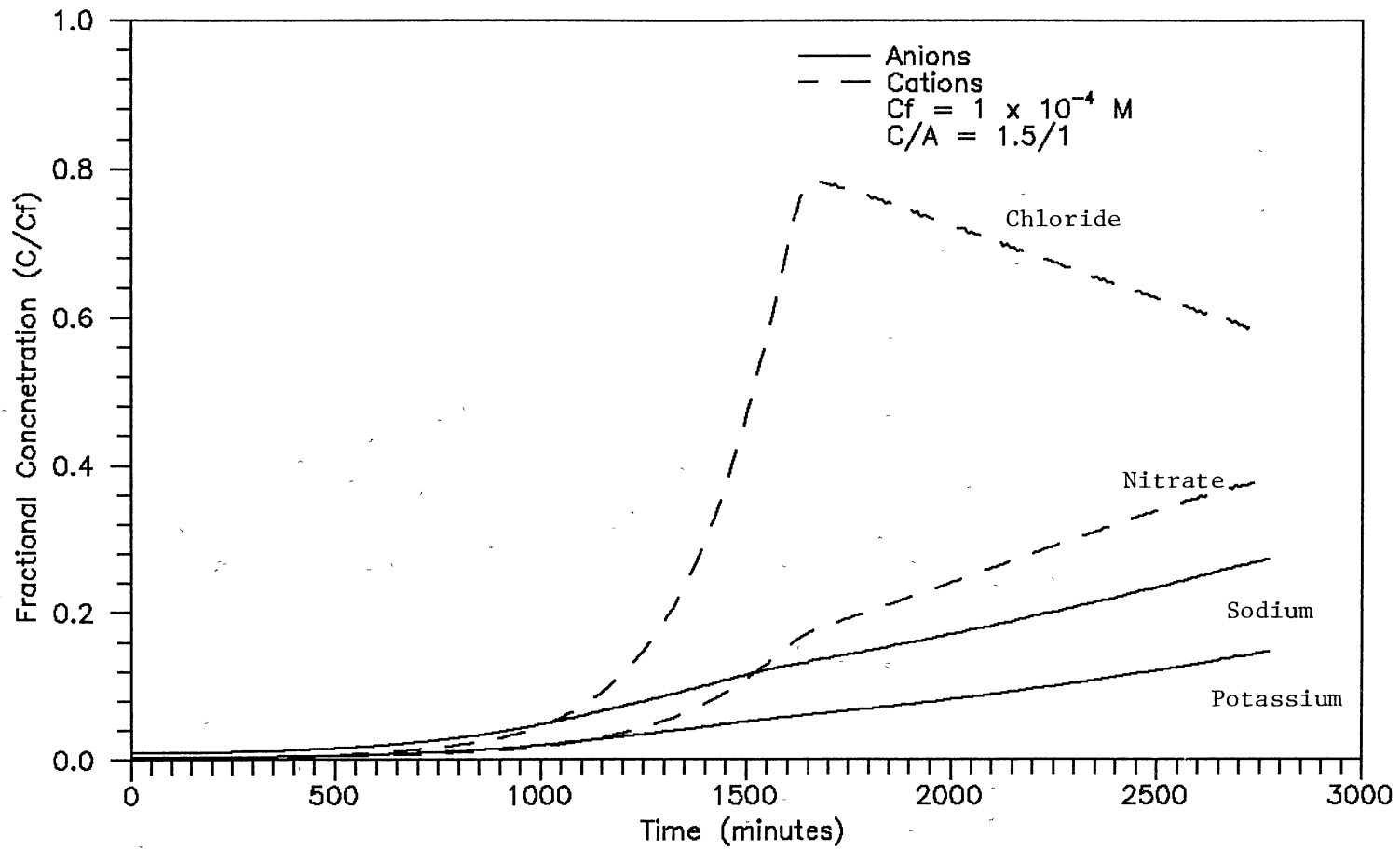


Figure 14. Six Component Break Through Curves for Sodium, Potassium, Chloride and Nitrate on a Type II Anion Exchange Resin

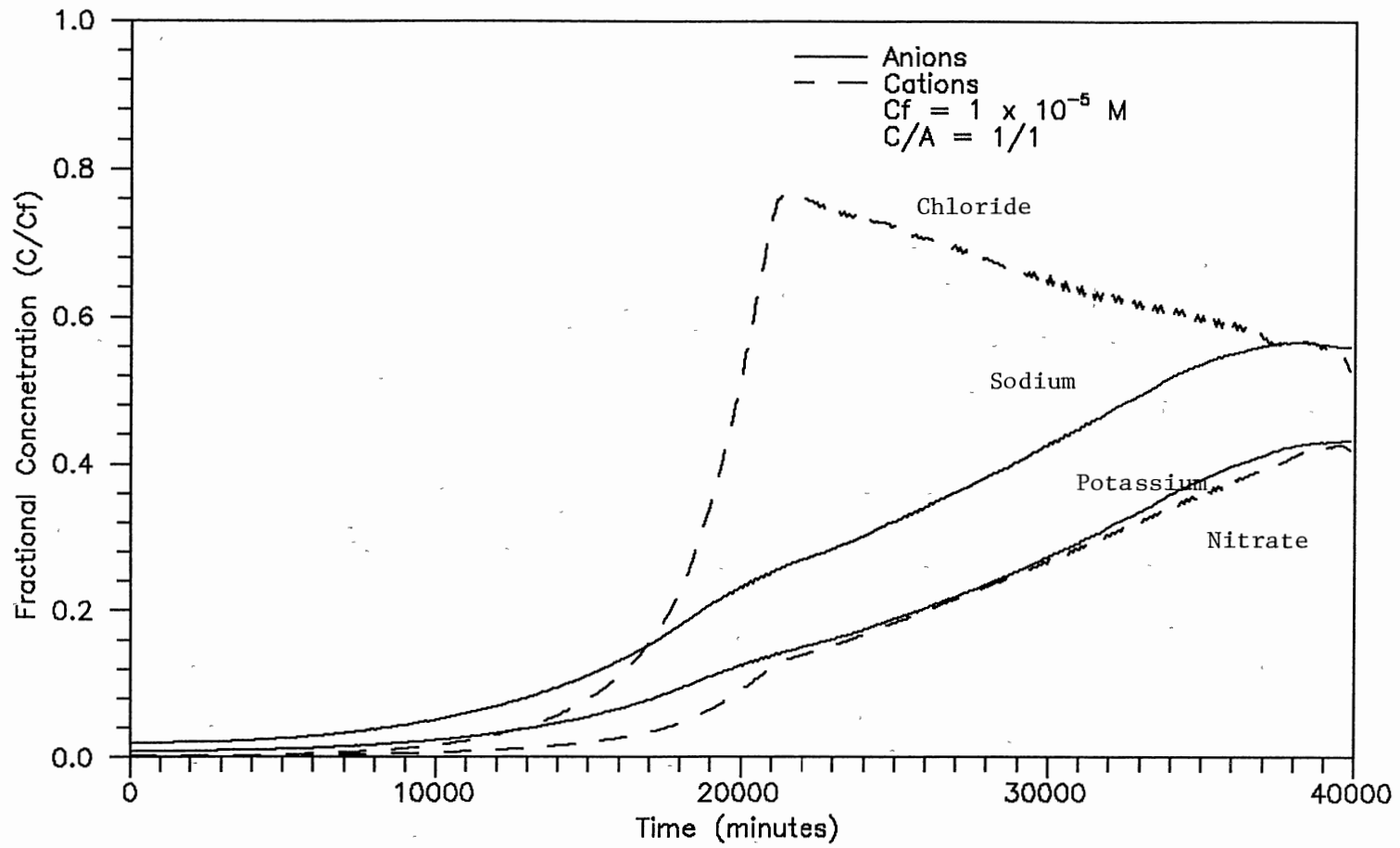


Figure 15. Six Component Break Through Curves for Sodium, Potassium, Chloride and Nitrate on a Type II Anion Exchange Resin

extremely high selectivity coefficients have a side effect on the calculation procedure, any small error in the concentrations becomes magnified by these large values. The instability combined with the relatively long breakthrough times suggested that a Type II anion exchange resin may be a more interesting case to examine.

Figures 12, 13 and 14 compare Type II anion exchange resins for the same three cation-to-anion resin ratios used for five component exchange. Changing the resin ratio results in shifting the breakthrough curves along the time axis. The same effect on initial leakages and overall effects as seen in five component exchange still exists. The major difference is the shape of the chloride peak after the initial breakthrough. The "shark fin" type shape is caused by the nearly equal diffusion coefficients of chloride and nitrate combined with a lower selectivity coefficient for this exchange. The shape arises from the diffusion process becoming mostly a convective driving force. This corresponds nearly to the case of  $D_A = D_B$  considered in many binary studies. Figure 15 shows the breakthrough curves for an order of magnitude inlet concentration. Again, the same type of observations made for five component exchange apply to this six component system. One, difference between Figures 12 and 15 is the height of the chloride peak. This is a direct result of the lower inlet concentration yielding a lower driving force for the displacement of chloride by nitrate.

A second effect of changing the cation-to-anion resin ratio is on the local bulk phase pH. The bulk phase pH deviates from neutrality as expected due to the differing exchange rates for anions and cations. The net effect is to gradually increase the bulk phase

pH as the anion resin capacity is consumed. After the anion resin is saturated with  $\text{Cl}^-$  and  $\text{NO}_3^-$ , the still exchanging cation resin gradually decreases the bulk phase pH. This pH change improves the cation exchange rate as long as all of the exiting hydrogen ions are consumed in the neutralization reaction. As the anion resin becomes saturated, the decrease in bulk phase pH causes an unfavorable effect on the cation exchange. Fortunately, in most applications, the maximum allowable effluent concentration of ionic species would already have been exceeded and the MBIE unit would have been taken out of service. The increase in bulk phase pH, while favorable for cation exchange is unfavorable for anion exchange. Thus, an optimum operating cation-to-anion resin ratio that maintains a near neutral bulk phase is desirable. The effluent concentrations in this case would result in near simultaneous cation and anion breakthrough.

#### CONCLUSIONS AND RECOMMENDATIONS

The model can predict multi-component exchange processes in the film diffusion controlled regime for bulk-phase neutralization and uni-valent exchange. The qualitative agreement between model predictions and the existing ternary exchange data is shown in Figures 1 and 2. The model's inability to quantitatively describe the experimental results of Omatete (1980b) and Dranoff and Lapidus (1961) could be due to three factors. The concentration ranges under consideration for the exchange process are nearing the region where particle diffusion can become important, the model does not account for particle diffusion limitations. The same concentrations that cause particle diffusion to be a factor also require that the

non-ideality of the exchange process be accounted for by using activity coefficients. The inclusion of an activity coefficient model such as the Extended Debye-Hückle equation should improve the models qualitative agreement with the experimental data. Yoon's (1990) observations that the diffusion coefficients that were necessary to match his experimental data in ultra-low concentration systems differ by almost an order of magnitude from the literature values. The determination of more appropriate diffusion coefficients or non-ionic mass transfer coefficients for low concentration ranges should improve the quantitative abilities of the model. Dranoff and Lapidus's data also appears to imply that kinetic leakage (or by-pass) may be important, in most low concentration MBIE units this is not the case.

The lack of any experimental data for multi-component systems in the ultra-low concentration ranges eliminates the possibility of evaluating the models quantitative abilities. The trends that were observed and the rates calculated in these low concentration ranges agree conceptually with what would be expected. The total lack of information on the temperature dependence of the selectivity coefficients limits the model evaluations to 25°C. Ternary interactions and their consequences on the exchange process, as described by Kataoka and Yoshida (1980), need to be determined experimentally.

The model developed here is the only one capable of handling multi-component uni-valent MBIE in the film diffusion control regime. Previous models and ternary studies have only considered relatively high concentrations and no neutralization reactions. The major



conclusion that can be drawn is that there is a tremendous need for experimental data in the ultra-low concentration ranges for multi-component systems in order to evaluate and improve the existing models.

## References

- Bajpai, R.K., Gupta, A.K., and Rao, M.G., A.I.Ch.E. J., 20, 989, 1974.
- Boyd, G.E., Adamson, A.W., and Myers, L.S., Jr., J. Am. Chem. Soc., 69, 2836, 1947.
- Dranoff, J.S. and Lapidus, L., Ind. Eng. Chem. Fund., 50, 1648, 1958.
- Dranoff, J.S. and Lapidus, L., Ind. Eng. Chem., 53, 71, 1961.
- Gottlieb, M.C., Ultra Pure Water, 61, March, 1990.
- Haub, C.E., M.S. Thesis, Oklahoma State University, 1984.
- Haub, C.E. and Foutch, G.L., Ind. Eng. Chem. Fund., 25, 373, 1986a.
- Haub, C.E. and Foutch, G.L., Ind. Eng. Chem. Fund., 25, 381, 1986b.
- Helfferich, F.G., Ind. Eng. Chem. Fund., 6, 352, 1967.
- Hwang, Y-L., and Helfferich, F.G., Reactive Polymers, 5, 237, 1987.
- Kataoka, T., and Yoshida, H., J. Chem Eng. Jpn., 13, 328, 1980.
- Kataoka, T., and Yoshida, H., A.I.Ch.E. J., 21, 1020, 1988.
- Omatete, O.O., Clazie, R.N., and Vermeulen, T., Chem. Eng. J., 19, 229, 1980a.
- Omatete, O.O., Clazie, R.N., and Vermeulen, T., Chem. Eng. J., 19, 241, 1980b.
- Wagner, J.D., and Dranoff, J.S., J. of Phys. Chem., 71, 4551, 1967.
- Wildhagen, G.R.S., Qassim, R.Y., Rajagopal, K., and Rahman, K., Ind. Eng. Chem. Fund., 24, 423, 1985.
- Yoon, T.Y., Ph.D. Dissertation, Oklahoma State University, 1990.
- Yoshida, H., and Kataoka, T., Ind. Eng. Chem. Res., 26, 1179, 1987.

## CHAPTER IV

### MULTI-COMPONENT MIXED-BED ION EXCHANGE MODELING IN AMINATED WATERS

#### Abstract

A model for multi-component mixed-bed ion exchange in pH adjusted water is developed. The model specifically addresses water with a weak base added for pH adjustment. Film diffusion controlled mass transfer is combined with bulk-phase reaction to determine the effluent-concentration profile of the mixed bed. The cationic resin is initially in the hydrogen form operating in the hydrogen cycle. As the exchange process progresses, the hydrogen cycle is replaced by the amine cycle. Operation past the ammonia break produces a characteristic of ammonia form operation, sodium throw. The model predicts the transient sodium outlet concentration surge and switches automatically to ammonia cycle operation.

#### Introduction

Nuclear power facilities using pressurized water reactors (PWR) and some fossil fired power plants operate with a pH adjusted secondary water cycle. Operating at a pH in excess of 9.0 results in reduced corrosion rates and longer process equipment lives. A detailed discussion of motivations and system parameters can be found in an earlier article (this dissertation, Chapter 2). Addition of a

weak base into the secondary cycle water improves process conditions, but creates problems in the removal of dissolved salts. The dissolved salts are typically sodium chloride and sodium sulfate, which cause corrosion problems. The weak base is added mainly to control iron transport, not to reduce the corrosion properties of sodium and chloride, however, removal of the dissolved salts is required in addition to the pH adjustment. The salt removal is accomplished by ion exchange.

The ion exchange processes are an intricate part of the overall water purification system. The exchange can be accomplished by two different operational schemes. The first is to use a cationic exchange column followed by an anionic exchange column. Using two beds in series does not, typically, achieve the purity levels that are required for power plant waters. The second method uses a mixed-bed ion exchange (MBIE) unit. The mixed bed offers certain properties that are highly beneficial to water purification. The release of hydrogen from the cationic resin and hydroxide from the anionic resin allow for the water neutralization reaction to aid the exchange process. Using a MBIE unit combined with pH adjusted water can result in improved iron transport properties and low levels of dissolved salts.

There are two possible methods to implement MBIE in conjunction with pH adjustment. The first method is to convert the cationic resin to the weak base form and regenerate the bed as needed. Operation with an amine form cation resin was addressed in an earlier article (this dissertation, Chapter 2). The second possible manner for addressing MBIE in the presence of a weak base is to operate in

the hydrogen cycle. Hydrogen cycle operation involves using the cationic resin initially in the hydrogen form. The hydrogen form resin removes both the sodium contaminant as well as the dissociated base. The water neutralization reaction, which aids the exchange process, is detrimental to the overall scheme of operation. The base neutralized by the water equilibrium and cation resin must be replaced. Typically, the outlet water must be redosed with additional amine to achieve the desired operating pH. Redosing the water leads to increased operating expenses due to additional chemicals and man power. Some of the detrimental aspects of operating in the hydrogen cycle can be overcome by allowing the unit to continue past the amine break. The amine break occurs when the cationic resin becomes saturated with the incoming sodium and dissociated base. Operating past this point transfers the bed from the hydrogen cycle to the amine cycle.

The amine cycle operation has been addressed earlier (this dissertation Chapter 2), and can be incorporated into a model which describes the system up until the amine break occurs. The methods developed in an other article (this dissertation, Chapter 3) can be utilized to describe the exchange process up to and past the amine break.

A model that can address operation in either the amine form or the hydrogen cycle with pH control will allow for the improvement of water purification systems currently in use. Since any given facility has its own individual characteristics, a model that can be modified to reflect the operating conditions will be valuable. This value should result in improved operation and lower costs.

## Model Development

The model developed in this article is designed to handle MBIE systems that are using the hydrogen cycle combined with pH control. The pH control is typically a weak base. The weak bases that are being used industrially are; ammonia, and morpholine. Each of these bases has its own influences on the cycle performance. The major impact of these will be in the selectivity coefficients and the dissociation constants. Operating with a weak base present in the water system will require the determination of a multiple reaction equilibrium. This will be satisfied by using bulk-phase neutralization incorporating the correction of the appropriate bulk phase concentrations.

### Assumptions

The major assumptions involved in developing the model are the same as those used in earlier work (this dissertation, Chapter 3). The assumptions are listed in Table I so that they are readily available. The most important of the assumptions is that the reactions occur in the bulk phase. Allowing the reactions to take place within the film surrounding the cationic resin would be a more accurate representation of the exchange process. Unfortunately, the information required to account for this can not be obtained for the systems under consideration. The film neutralization model developed by Haub (1984) is limited to binary exchange with the water equilibrium occurring at a reaction plane within the film. This requires that concentrations be specified at the reaction plane, as

Table I  
Model Assumptions

- 
- 1) Film diffusion control
  - 2) Pseudo steady state exchange ( variations of concentration with space are much more important than with time)
  - 3) No coion flux across the particle surface
  - 4) The Nernst-Planck equation incorporates all interactions between diffusing species
  - 5) All univalent exchange
  - 6) The static film model can be used to describe the film adhering to the particle surface
  - 7) Solid-film interface is maintained at equilibrium
  - 8) Reactions are instantaneous when compared with the rate of exchange
  - 9) Curvature of the film can be neglected
  - 10) Uniform bulk and resin compositions
  - 11) Activity coefficients are unity
  - 12) Plug flow
  - 13) Isothermal, isobaric, operation
  - 14) Negligible axial Dispersion

Derived Conditions

No net coion flux within the film

No net current flow

---

well as this plane having a known position for multi-component exchange. Using the static film model does not allow for this point to be specified. The static film model is not able to yield an actual value for the film thickness around the resin bead. Even so, the model is used because the actual film thickness need not be known to determine the effective diffusivities. Using a different film model may be appropriate for ion exchange systems, but the flux expressions will now be based on the finite film thickness that these other models predict. Either approach requires estimated values or assumptions that reduce the accuracy of the intended method. The advantage of the static film model is that for uni-valent bulk-phase neutralization, an analytical expression for the flux can be found. The analytical expression does not rely on a predicted film thickness that could be in error by a considerable amount, but does require that reactions be restricted to the bulk phase.

#### Flux Expressions

The description of the exchange process is accomplished by determining the flux of each of the exchanging species within the film surrounding the resin. Film diffusion control is assumed, and the Nernst-Planck equation is used to express the fluxes. The Nernst-Planck equation for component  $i$  is:

$$J_i = D_i \left( \frac{d C_i}{d r} + Z_i \frac{F C_i}{RT} \left( \frac{d \phi}{d r} \right) \right)$$

Solving each species flux equation in terms of concentrations allows for the effective diffusivity to be found. The development of the binary flux equations for the anionic resin and the amine cycle are



given in an earlier paper (this dissertation, Chapter 2) and Appendix A. The ternary uni-valent flux expressions were also derived in an earlier paper (this dissertation, Chapter 3) and in Appendix B. The same equations that the previous papers presented can be used in this model with minor changes. The goal of solving the flux expressions is to obtain  $J_i \delta$  as a function of species concentrations. After the appropriate expression for the product of the film thickness and the flux has been found, the static film model can be applied to determine the effective diffusivities. The ternary exchange on the cationic resin requires that two effective diffusivities be determined. The third component fractional concentration can be found by applying a simple material balance on the resin and the bulk phase. The binary effective diffusivity for chloride exchange on the anionic resin is:

$$D_e = \frac{2 D_o D_c}{(D_o - D_c)} \left( \frac{C_o^o + C_c^o - C_c^* - C_o^*}{(C_c^o - C_c^*)} \right)$$

The effective diffusivity for species  $i$  in the ternary exchange on the cationic resin is:

$$D_{ei} = \frac{2 D_i}{(C_c^o - C_c^*)} \left( \frac{1 - (C_p^*/C_p^o)(C_i^*/C_i^o)}{1 + (C_p^*/C_p^o)} \right)$$

The ternary effective diffusivity was determined by using a pseudo single coion within the cation film. The usage of a pseudo single coion was described in this dissertation Chapter 3. Once the effective diffusivities have been determined, they can be used in the rate expressions and the exchange process described.

## Rate Equations

The static film model can be used to determine the rate of exchange of a given species in terms of an overall mass-transfer coefficient. Kataoka et al. (1972) found that the two thirds power of the effective diffusivity correlated very well with the overall mass transfer coefficient when a packed bed mass transfer coefficient was used. The errors involved were on the order of a few percent for favorable exchange and less than ten percent for unfavorable exchange. Pan and David (1976) redefined the relation for the overall mass-transfer coefficient as:

$$R_i = \left( \frac{De}{D_i} \right)^{2/3} = K'_i / K_i,$$

where  $K_i$  is the packed bed mass transfer coefficient and  $K'_i$  the overall mass transfer coefficient. Recombining the value of  $R_i$  with the static film model gives the rate of exchange as:

$$\frac{\partial y_i}{\partial t} = K_i R_i \frac{a}{Q_s} (C_i^o - C_i^*)$$

The rate expressions are derived for multi-species exchange in general form in Appendix C. The rate of exchange can be used in combination with the material balance equations to determine the effluent-concentration profile for the MBIE unit in question.

## Material Balances

The material balance equations for any species  $i$  are developed in Appendix D. A change of variables is necessary so that the material balances lend themselves to an appropriate method of solution. The new variables are dimensionless and are represented as

$\xi$  and  $\tau$ , and are of the same general form as those proposed by Kataoka et al. (1976).  $\xi$  is a dimensionless distance variable while  $\tau$  is a combined distance time variable. The material balance equations for species  $i$  in terms of the new variables are:

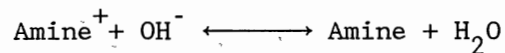
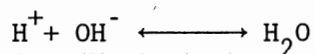
$$\frac{\partial X_i}{\partial \xi_x} + FC_j \frac{\partial y_i}{\partial \tau} = 0$$

$$\frac{\partial y_x}{\partial \tau} = 6 R_x (X_x^o - X_x^*)$$

These equations can be solved numerically by the method of characteristics. A brief discussion of the numerical techniques used for solving these equations is given in Appendix E.

#### Equilibrium Relations

In addition to the material balance equations, the complex equilibria of the bulk phase must also be considered. The two competing reactions are:



The reactions have been restricted to occur in the bulk phase, so the two equilibrium equations must be solved at each grid point. They are solved by accounting for the species released from the resin phases and then new bulk phase concentrations determined based on the equilibrium equations. This requires the solution of a non-linear system of algebraic equations. Newton's method was attempted but was unable to converge to the desired root. Hence, an iterative approach was the final method of choice. The roots are bounded since the

concentrations of any species cannot be negative, so the method was viable, although a bit slow.

The equations that describe the exchange process can now be applied to estimate column performance. The model is capable of handling multi-component uni-valent anion exchange in addition to the ternary cation exchange. This was demonstrated in an earlier paper (this dissertation, Chapter 3). Unfortunately, the second most important anion to consider is sulfate. Since sulfate is di-valent, an approach different than the one used for uni-valent exchange is required. At present, the only methods that can deal with this situation are the graphical techniques of Gottlieb (1990).

#### Discussion

The model developed in this chapter considers MBIE in the hydrogen cycle with the presence of a pH control agent. The goal of the model is to describe hydrogen cycle exchange through the amine break and then be able to describe amine cycle operation. This is accomplished by using the flux expressions, material balances and equilibrium relations discussed earlier. Previous chapters (2 and 3) have discussed the effect of resin phase loading on the rate of exchange and the ratio of electrolyte to non-electrolyte mass transfer coefficients. The same effects noted in those discussions apply to the model used here because the model is based on the relations developed in those chapters. For a discussion of  $R_i$  and the rates of exchange consult the appropriate chapter.

The model needs to consider very different pH control additives, ammonia and morpholine. In the past, ammonia was used as

the weak base for pH control, and is still used in most PWR's. The introduction of Morpholine in Great Britain around 1983 presented a viable alternative to ammonia with certain improved features. The distribution coefficient for morpholine results in a higher film pH than that for ammonia, which is highly desirable (Sawochka, 1988). Morpholine also has a selectivity coefficient less than one for sodium exchange, which means the resin prefers sodium, with all things equal. Morpholine does have some draw backs, degradation and a lower dissociation constant are two of these. Comparing MBIE performance between these two additives operating in the ammonia cycle should provide some insight into selection criteria.

#### Ammonia

Since ammonia is the historical pH additive, its performance in the hydrogen cycle will be considered first. Figure 1 shows a typical effluent-concentration profile for a hydrogen cycle MBIE unit with ammonia present. One feature of concentration profiles involving ammonia in the hydrogen cycle is the sodium "blip." The "blip" is a peak in the effluent concentration of sodium following shortly after the ammonia break (Emmett, 1983). This can be seen in Figure 1. The shape of the sodium curve agrees with that shown by Emmett (1983). The slow tail which approaches the inlet concentration agrees with observations of Salem (1969) and with the earlier model evaluations in Chapter 3. The fact that the sodium surge occurs after the ammonia break, even though ammonium is preferred by the resin, is related to the significantly higher bulk phase concentration of ammonium, and the presence of undissociated ammonia. Figure 1 also

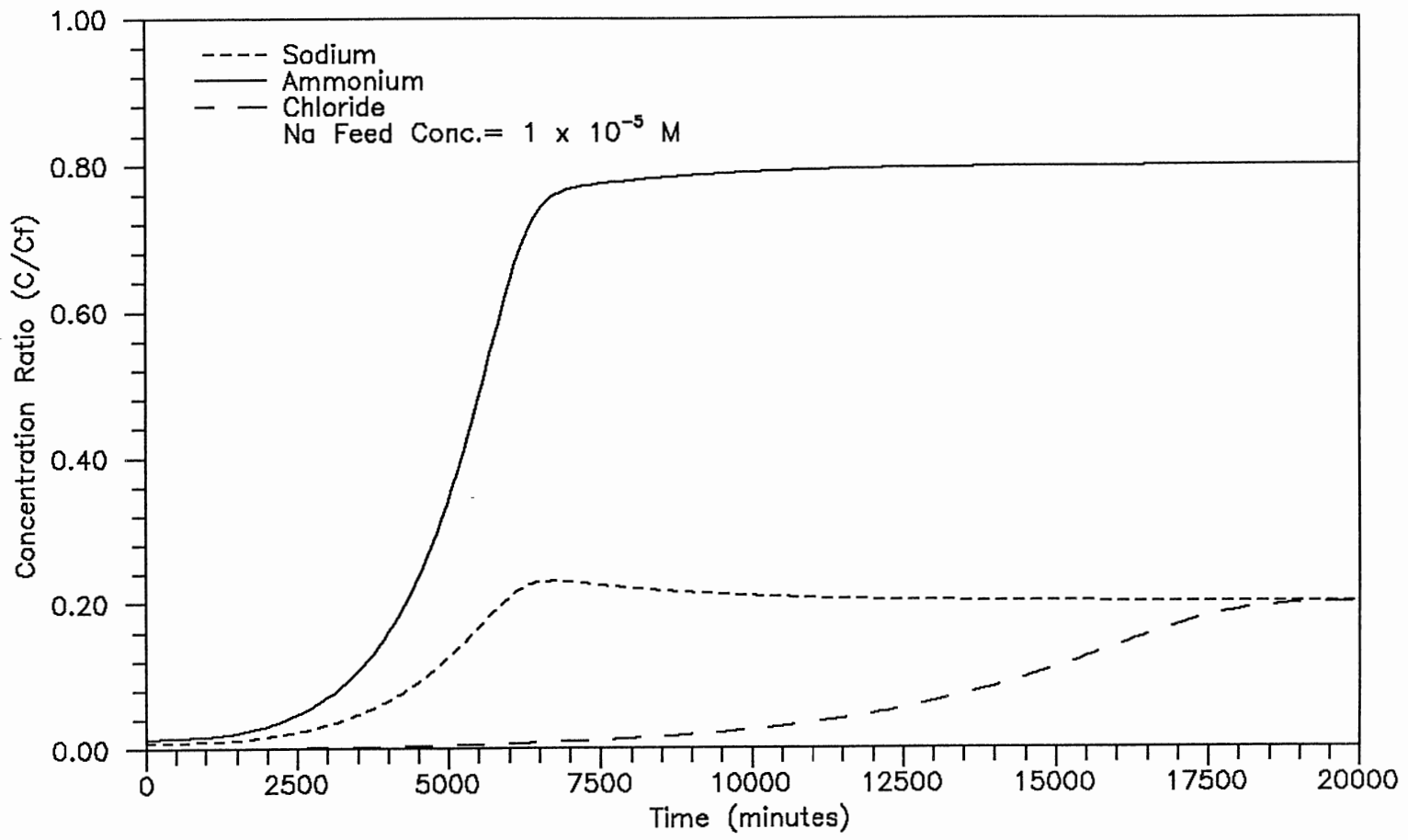


Figure 1. Ammonia Cycle Operation Past the Ammonia Break for pH 9.6 and Cation-to-Anion Resin Ratio of 1/1

demonstrates that for many cycle choices, the breakthrough of chloride is essentially negligible when compared with that of sodium. Figure 2 shows an exploded view of the sodium blip at an order of magnitude lower inlet concentration than in Figure 1. The lower inlet concentration does correspond to a longer time for sodium breakthrough, but not an order of magnitude. The earlier than expected breakthrough is a result of the ammonium acting as an elluant, much as a carrier does in gas chromatography. The ammonium is displacing the sodium down the bed. Since the pH is the same in this figure as in Figure 1, the ability of the ammonium to displace the sodium on the resin in less time was expected. One improvement of the lower concentration is a lower initial leakage off of the bed and a significantly lower outlet concentration. Typically, MBIE units experience high inlet concentrations only when a condenser leak occurs. If the inlet water is fairly pure than operation in the hydrogen cycle through the break may be warranted.

One drawback of operating in the hydrogen cycle is that the ammonia is removed from the water and the hydroxide present is neutralized to a great extent by the hydrogen released off of the cationic resin. The amount of hydrogen released by the sodium exchange is inconsequential when compared with the amount that is released due to ammonium exchange. This corresponds to a decrease in the water pH and ammonia concentration at the column outlet. Figure 3 shows the pH at the outlet of the bed that was considered in Figure 2. The pH is near neutral at the outlet, and is above neutral due to the release of hydroxide from the anionic resin and the presence of a small amount of undissociated ammonia. The pH gradually rises as the

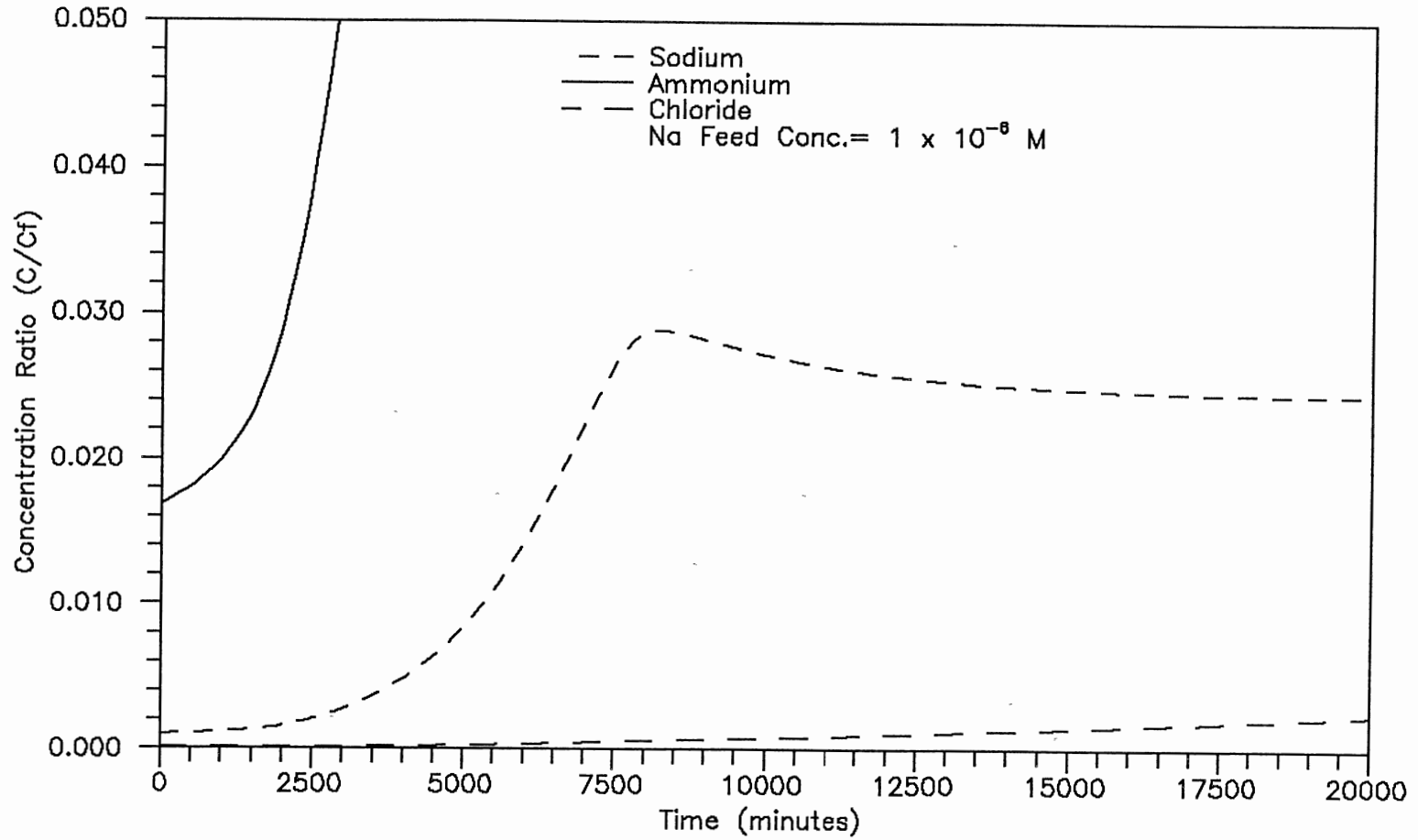


Figure 2. Ammonia Cycle Operation Past the Ammonia Break for pH 9.6 and Cation-to-Anion Resin Ratio of 1/1



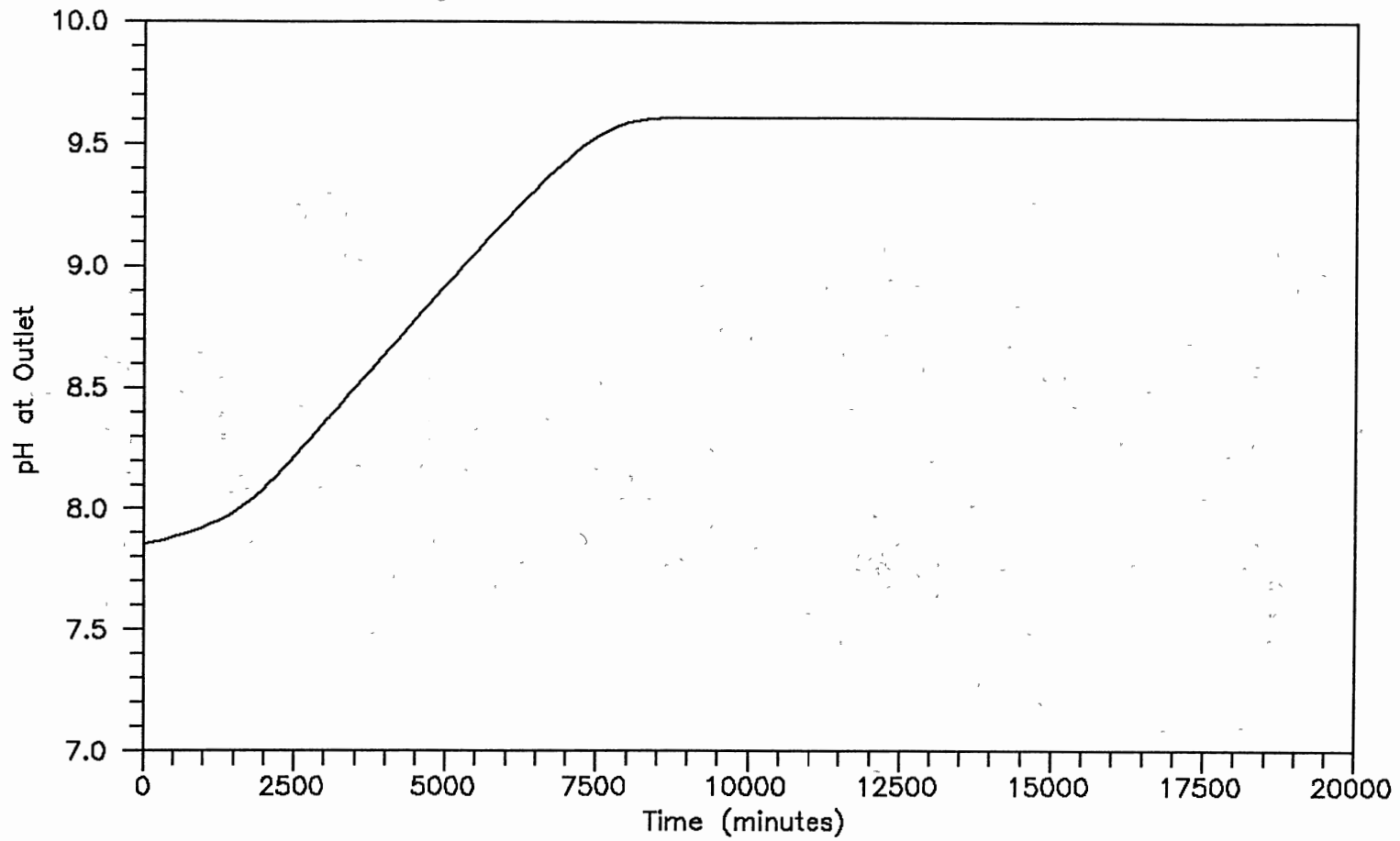


Figure 3. Outlet pH for Ammonia Cycle Operation Past the Ammonia Break for pH 9.6 and Cation-to-Anion Resin Ratio of 1/1

cationic acidic buffer capacity is consumed, and eventually reaches the inlet value once equilibrium has been established within the bed. Until this point is reached, the outlet water must be dosed with additional ammonia in order to maintain a secondary cycle pH of 9.6. The inlet pH in all of the figures is 9.6.

Since the chloride breakthrough trails behind the sodium breakthrough by a considerable margin, using a higher cation-to-anion resin ratio may result in longer run times. Figures 4 and 5 show runs with the same conditions as Figure 2 except for the cation-to-anion resin ratio. Figure 4 uses a ratio of 1.5/1. The initial leakage values are considerably lower than in Figure 2 and the time at which breakthrough occurs is further along. Figure 5 uses a cation-to-anion resin ratio of 2/1. Comparison with Figure 2 shows a further depressed initial leakage and an even greater time to breakthrough. One interesting feature of these curves is the height of the sodium "blip." As the cation-to-anion resin ratio is increased the transient sodium peak height also increases. This is caused by the more effective removal of sodium at the higher cation-to-anion resin ratios. The resin phase loadings of sodium are higher, and therefore the ammonium has a greater amount of sodium to displace. Increasing the cation-to-anion resin ratio leads to earlier leakage for chloride off of the bed. Even at a ratio of 2/1, the chloride leakage lags significantly behind the sodium leakage. Cation-to-anion resin ratios in the neighborhood of 1.5/1 and 2/1 are typical for industrial units.

The effect of extending the column height is seen in Figure 6. The height in this Figure is twice that of Figure 2. The time to breakthrough is increased for a column twice as tall, but not quite

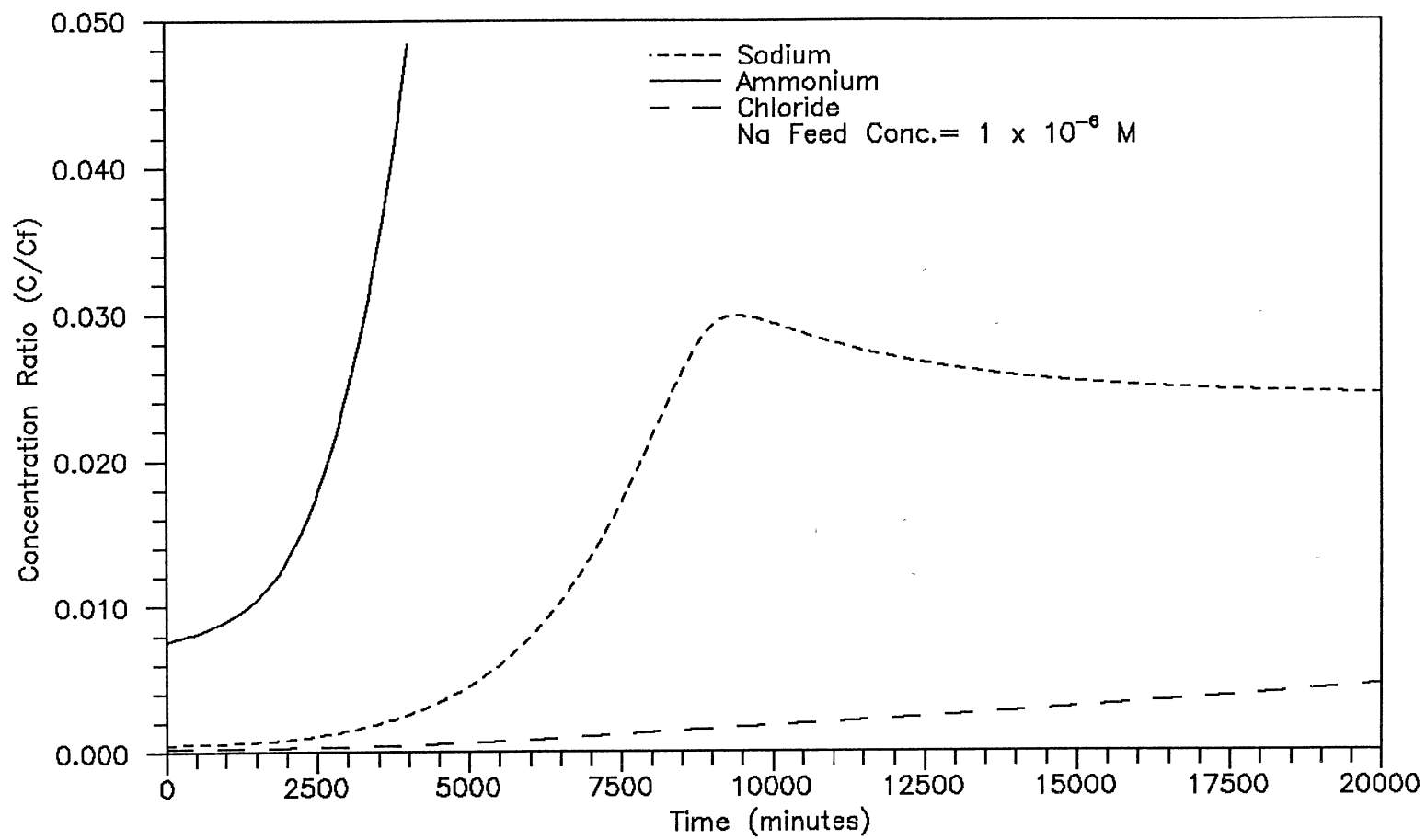


Figure 4. Ammonia Cycle Operation Past the Ammonia Break for pH 9.6 and Cation-to-Anion Resin Ratio of 1.5/1

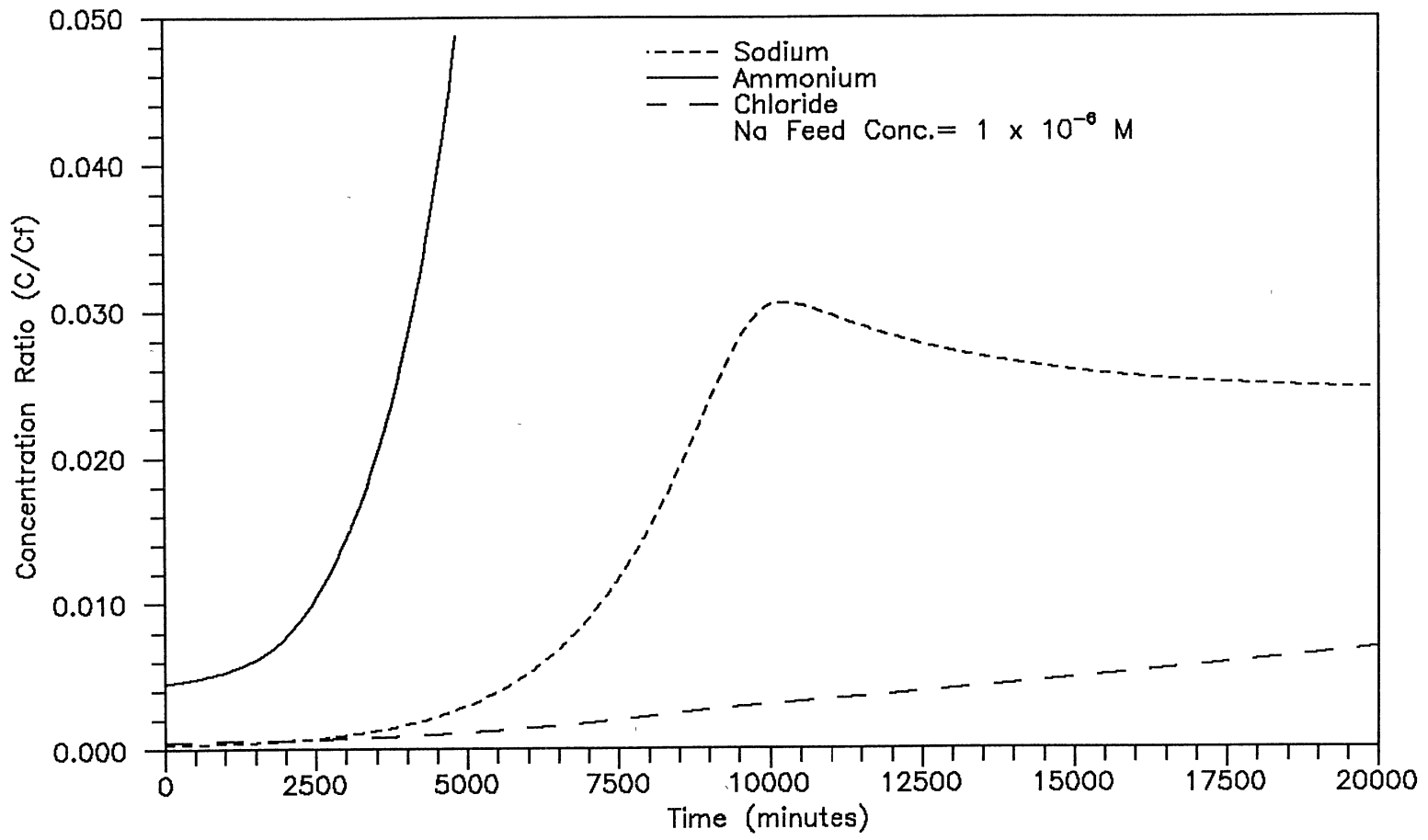


Figure 5. Ammonia Cycle Operation Past the Ammonia Break for pH 9.6 and Cation-to-Anion Resin Ratio of 2/1

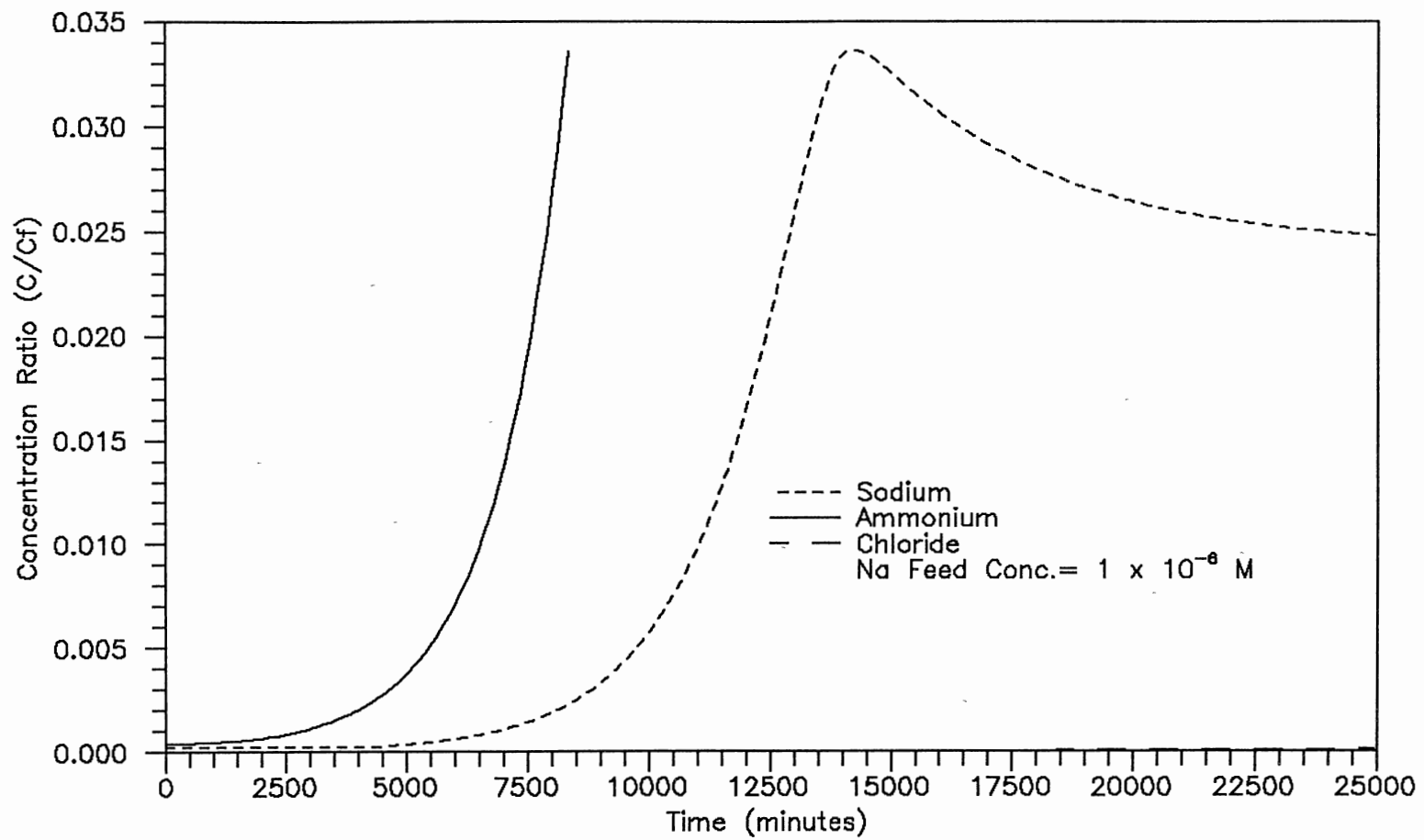


Figure 6. Ammonia Cycle Operation Past the Ammonia Break for pH 9.6, and Column Height of 10 cm, and a Cation-to-Anion Resin Ratio of 1/1

doubled due to the extremely high ammonium concentration pushing the sodium off of the bed, as witnessed with a higher cation-to-anion resin ratio. The sodium peak height is also increased due to the same factors that affected the peak height for a larger cation-to-anion resin ratio.

Considering how well the cycle contends with a simulated condenser leak is shown in Figure 7. The inlet concentration was stepped from  $1 \times 10^{-6}$  M to  $1 \times 10^{-5}$  M for a short time period. The square wave shape is what causes the two discontinuities present in the figure. The exaggerated peak height, followed by a decline to an outlet concentration higher than the original inlet concentration is caused by the intermittent leak. The same inlet and bed conditions are included on the figure for a situation with no condenser leak. The considerably lower response shows how the leak influences the outlet concentrations. The mixed bed is capable of reducing the outlet concentrations during a leakage. The bed's ability to handle leaks of this nature when operating in the amine cycle is extremely important.

#### Morpholine

The effect of using morpholine as a pH control agent on hydrogen cycle exchange is different than that seen for ammonia. The selectivity coefficient for morpholinium over hydrogen is slightly less than one. The exchange can be considered from the point of view of switching the values for ammonia and sodium. The selectivities and diffusion coefficient correspond nearly to those for ammonium-sodium exchange if the identities of the two species were interchanged. The

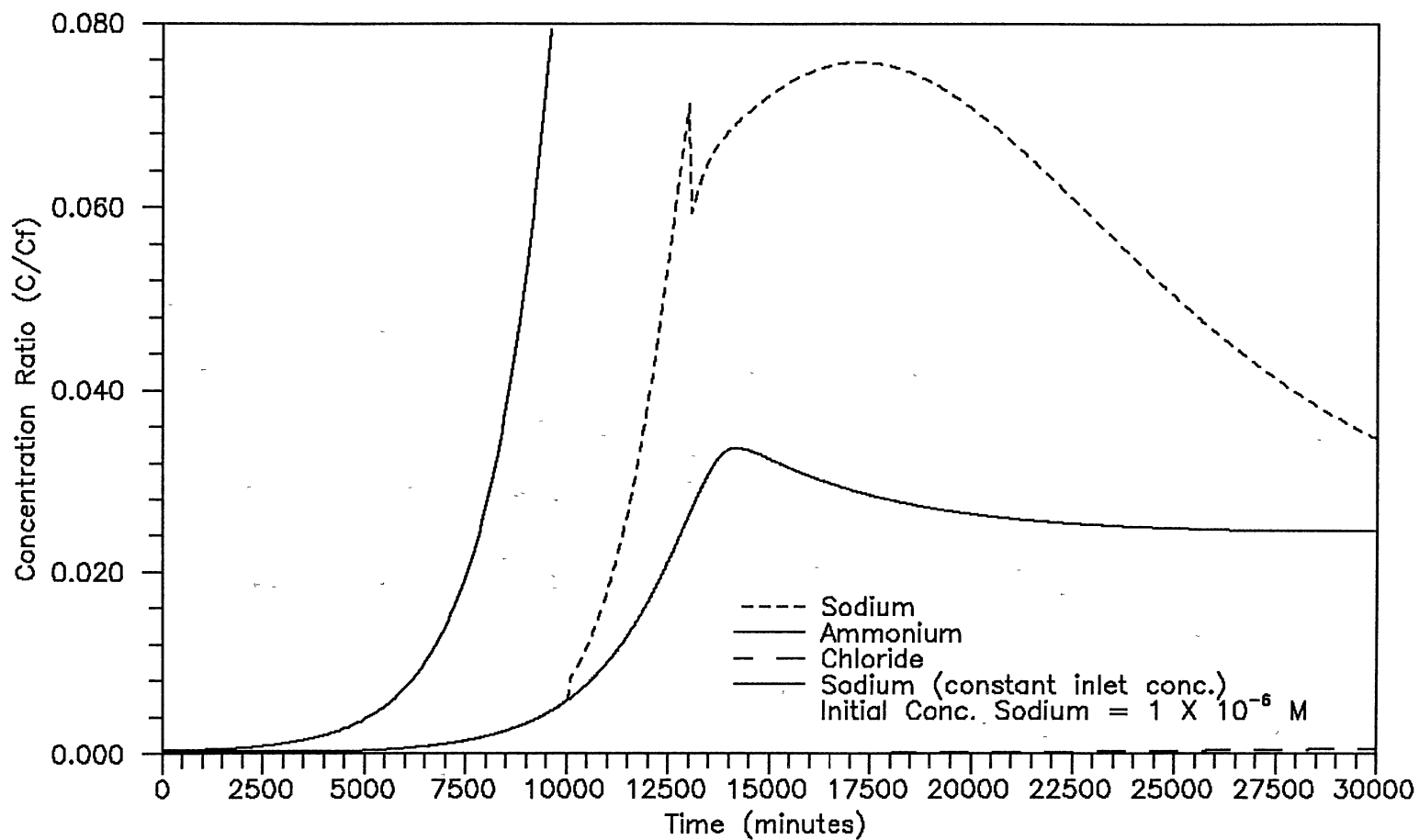


Figure 7. Ammonia Cycle Operation Past the Ammonia Break for pH 9.6 and Cation-to-Anion Resin Ratio of 1/1 with a Square Wave Inlet Concentration Change

system is more complicated than that since the concentration of morpholine is considerably greater than that for sodium within the bed. The net effect is a lower elution of sodium off of the bed than was seen for the presence of ammonia.

Figure 8 shows the outlet concentrations for morpholine as the pH additive for the same column conditions as in Figure 2. The fact that the selectivity coefficient for sodium over morpholinium is greater than one removes the transient "bump" that was evident when ammonium was present. The lower dissociation constant for morpholine also contributes to the sharpness of the morpholine break and the initial leakage. Comparing Figure 2 with Figure 8 shows lower initial leakage for sodium with a slower rise to the equilibrium value. The behavior of the outlet sodium concentration with the presence of morpholine is as expected.

Figure 9 shows the variation in the outlet pH for the same conditions as Figure 8. The conditions also correspond to those used for Figures 2 and 3 with ammonia replaced with morpholine. The initial outlet pH is significantly lower than the inlet pH due to the water neutralization reaction. Comparing Figure 9 and Figure 3 shows a higher outlet pH for the presence of morpholine. The higher pH in the hydrogen cycle is caused by the higher total morpholine (undissociated plus dissociated) concentration and the below one selectivity for morpholinium over hydrogen. These factors combine to yield a lower rate of hydrogen release that causes a higher outlet pH. The higher pH is desirable since morpholine was added to the water stream in order to elevate the pH.



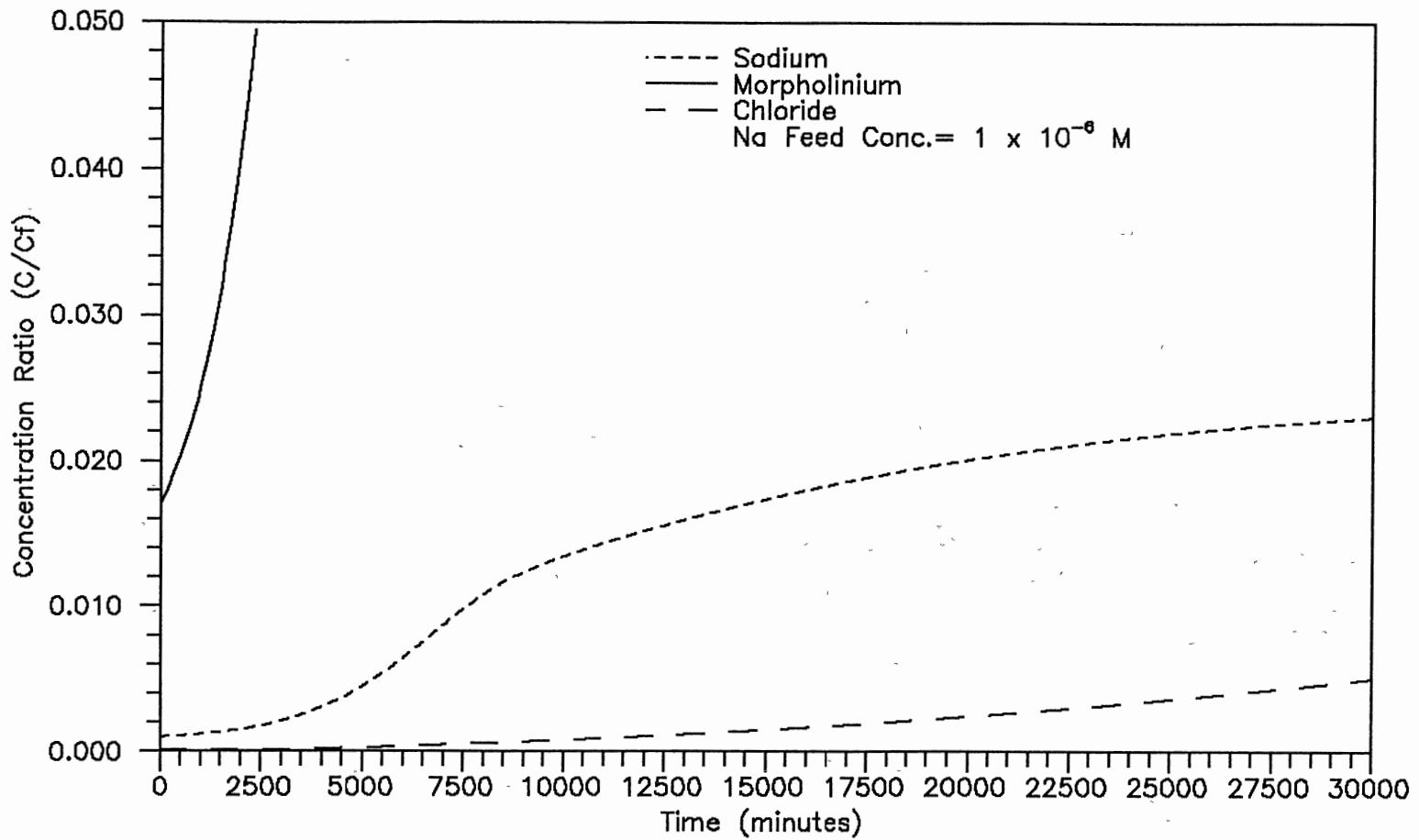


Figure 8. Hydrogen Cycle Operation Past the Morpholine Break for pH 9.6 and Cation-to-Anion Resin Ratio of 1/1

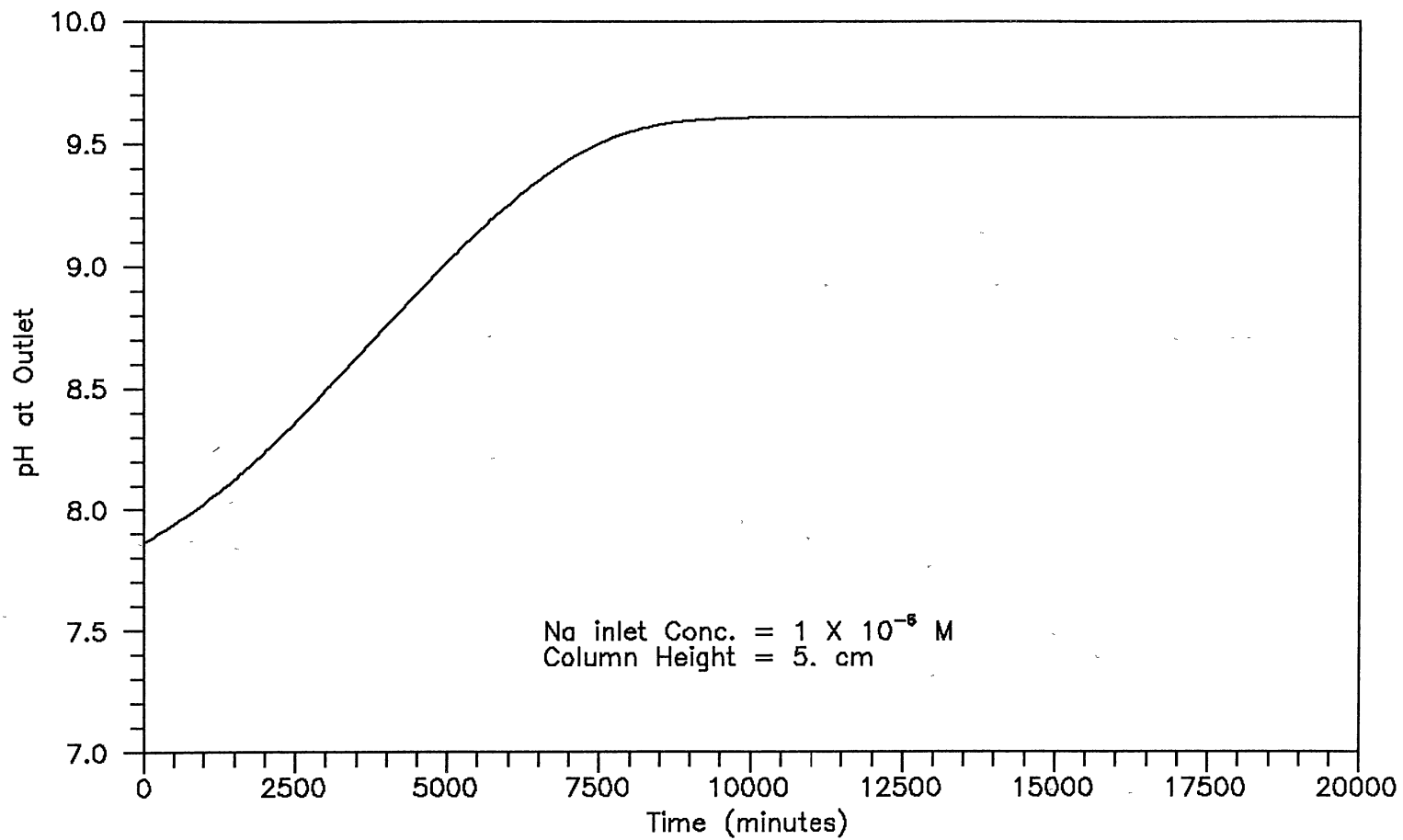


Figure 9. Outlet pH for Hydrogen Cycle Operation Past the Morpholine Break for pH Inlet 9.6 and Cation-to-Anion Resin Ratio of 1/1

Figures 10 and 11 show the effect of increasing the cation-to-anion resin ratio for the same inlet conditions as Figure 8. The initial leakage levels are lower, as expected, since there is a greater cation exchange capacity. The relatively high selectivity for chloride over hydroxide causes the chloride breakthrough to lag significantly behind the sodium breakthrough, as was seen with ammonia. The near overlap of the sodium and chloride outlet concentrations for a ratio of 2/1 is caused by the increased removal of sodium due to a higher capacity. The higher capacity equalizes the tremendous difference in the selectivity coefficients for the cation and anion resins. The additional effect of a higher selectivity for sodium over morpholinium than for sodium over hydrogen also aids the exchange process. The drawback of a higher cation-to-anion resin ratio is that the removal of morpholinium is also enhanced. The decrease in outlet morpholinium concentration will require the addition of more make up morpholine, which is an added cost.

Figure 12 shows the effect of a square wave inlet concentration surge with morpholine. Figure 12 corresponds to the same conditions as were used in Figure 7. The same type of behavior seen with ammonium is again seen in Figure 12 when it is compared with the base line leakage. The base line leakage is the outlet concentration profile for no change in inlet concentration. The surge results in a slight transient bump due to the change in inlet concentration, and the beds removal capacity for long term use is reduced. The cycle is able to reduce the impact of the change, as it was for ammonium, which was the desired result.

The presence of morpholine was evaluated on AMBERSEP 252

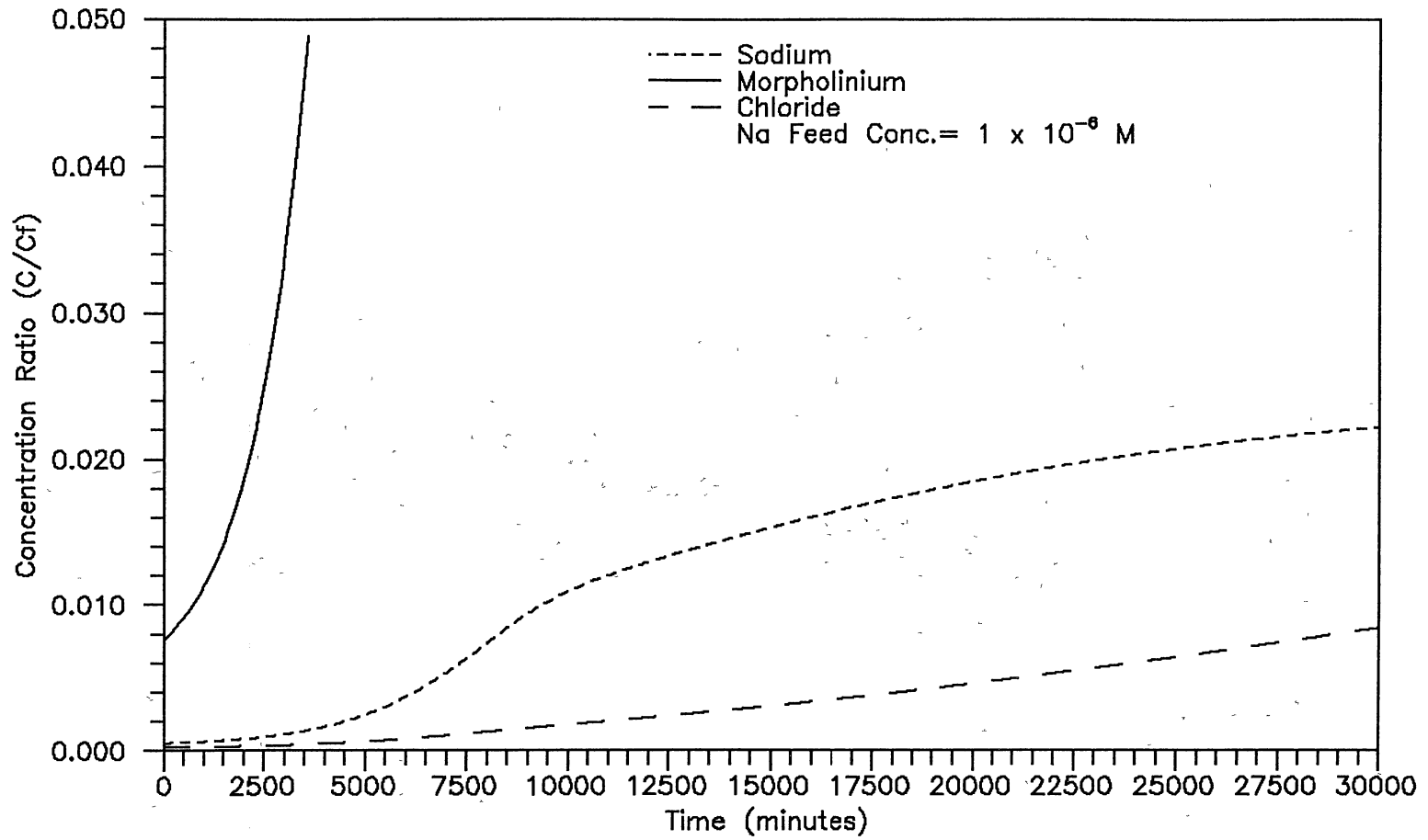


Figure 10. Hydrogen Cycle Operation Past the Morpholine Break for pH 9.6 and Cation-to-Anion Resin Ratio of 1.5/1

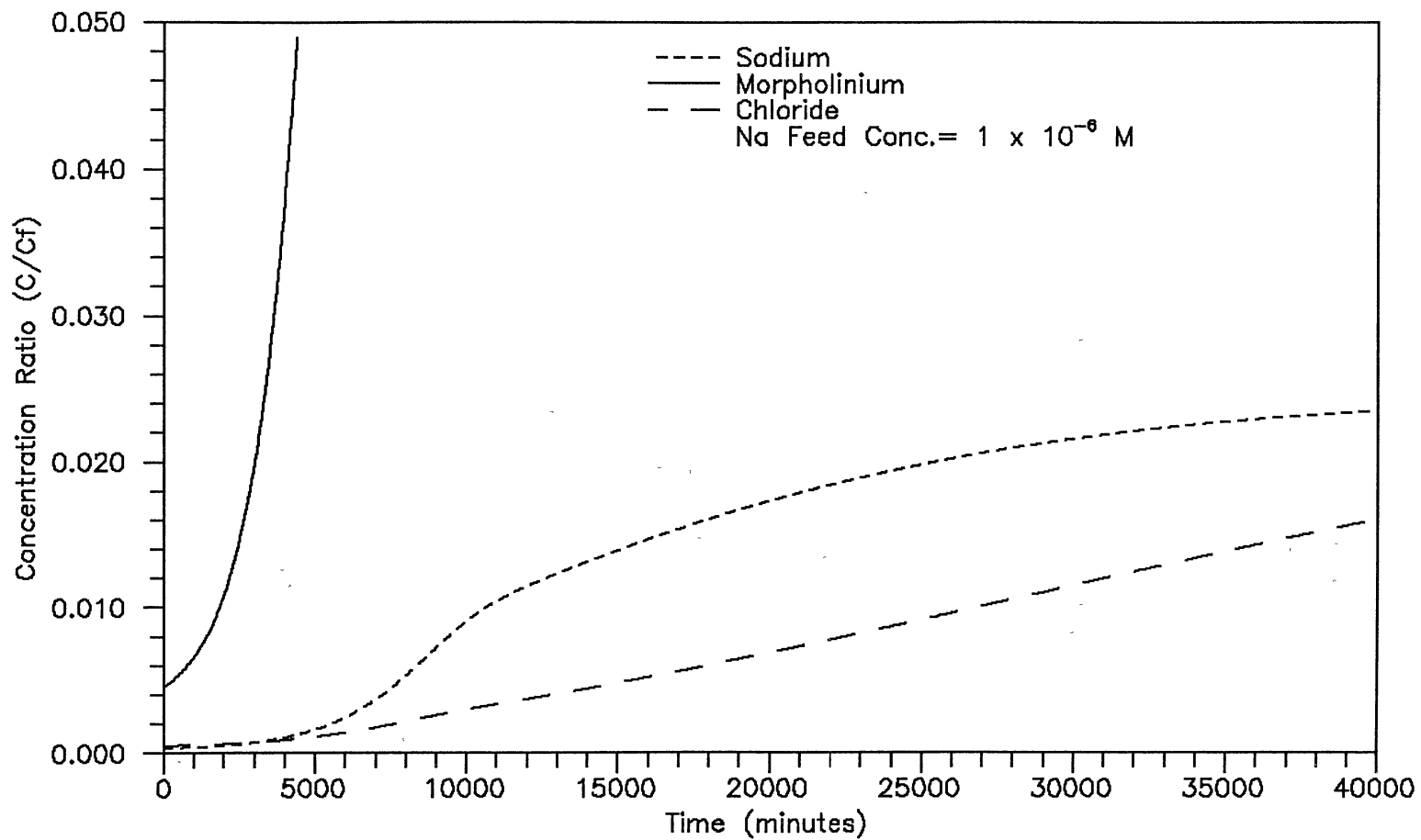


Figure 11. Hydrogen Cycle Operation Past the Morpholine Break for pH 9.6 and Cation-to-Anion Resin Ratio of 2/1

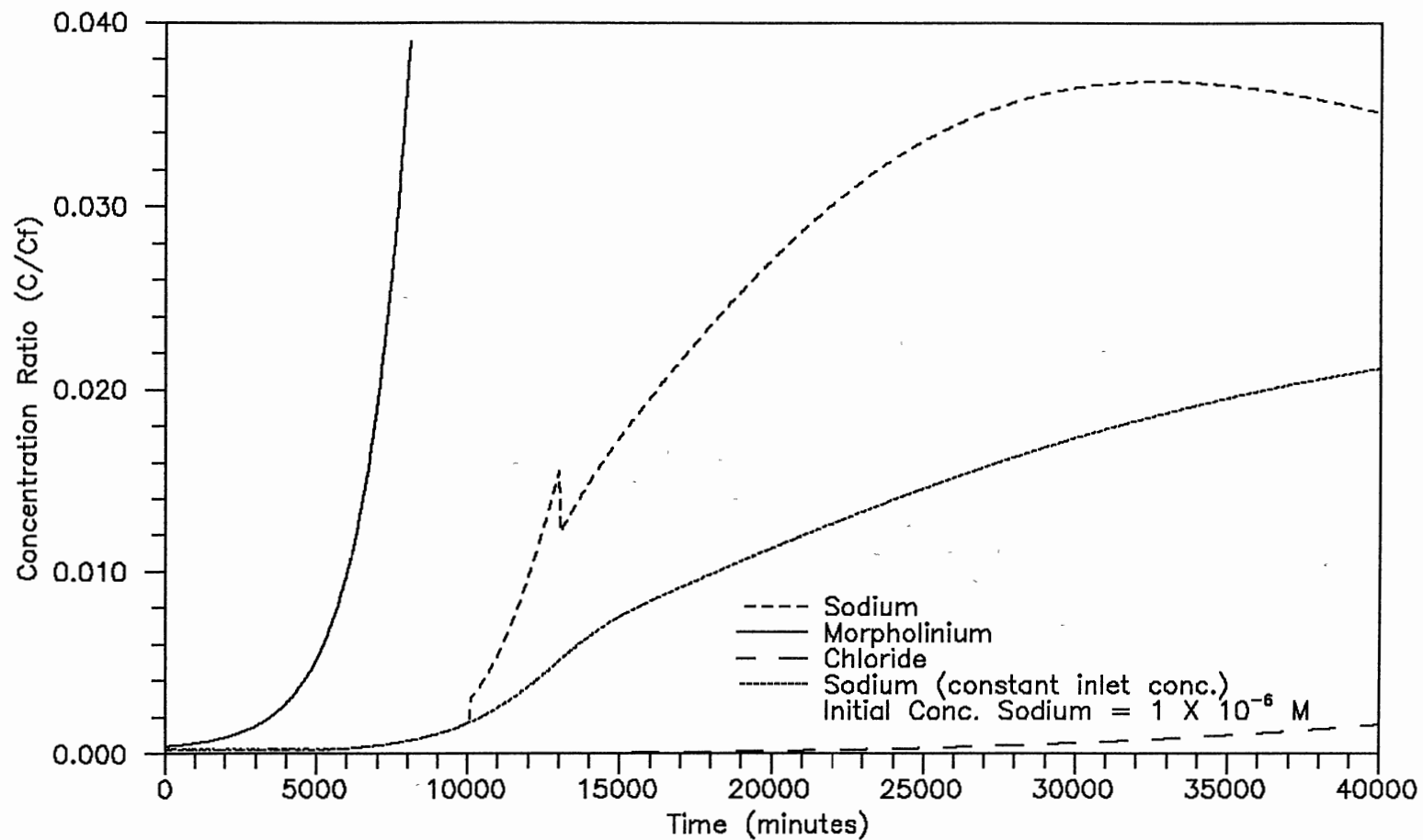


Figure 12. Hydrogen Cycle Operation Past the Morpholine Break for pH 9.6 and Cation-to-Anion Resin Ratio of 1/1 with a Square Wave Inlet Concentration Change

cation exchange resin, since this is the prevalent resin choice. Considering AMBERSEP 200 which has a significantly higher selectivity coefficient for sodium over morpholinium should result in even longer times for breakthrough. Unfortunately, many power facilities using amines to control pH can no longer operate in the hydrogen cycle past the amine break. This is due to the decrease in allowable outlet concentrations for MBIE units. The ability of the amine cycle to achieve lower than three ppb outlet concentrations while reducing the amount of redosing required (and thereby the possibility of external contamination) has lead to using amine cycles instead of the hydrogen cycle.

#### Conclusions and Recommendations

The model developed in this article addresses an area that has previously not been considered. Hydrogen cycle exchange past the amine break requires that the complex equilibria be handled and that ternary exchange be addressed. Previous work (this dissertation, Chapter 3) developed a model for multi-component uni-valent exchange. The incorporation of ternary exchange capabilities and amine equilibrium resulted in a model that can predict MBIE performance for aminated waters.

The model was evaluated for two different pH control additives, ammonia and morpholine. Past experiences with ammonium (Emmett, 1983) presented quantitative comparisons for the outlet-concentration profiles predicted by the model. The transient sodium "blip" was predicted and the ability to operate past the ammonia break demonstrated. The model was evaluated for morpholine.

exchange with fairly high inlet concentrations (compared to those observed industrially). The bed consumption of morpholine was quickly overcome by the inlet sodium concentration. Industrially, inlet concentrations could be two orders of magnitude lower than those considered here. The lower inlet sodium concentration results in much of the bed capacity being consumed by morpholinium and thereby reducing the beds sodium removal efficiency (Darvill, 1986). The inability of hydrogen form resin to maintain pH and remove sodium has led to industrial acceptance of amine cycles. The increased costs associated with hydrogen form operation significantly restrict its application.

The model was compared with the outlet profiles described in the literature (Emmett, 1983). The qualitative agreement is very good, much the same as reported earlier (this dissertation, Chapter 3). The complete lack of experimental data in multi-component aminated systems restricted the comparisons to a qualitative basis. There is a tremendous need for experimental data in low concentration ranges, for model evaluation and design purposes. Resin manufacturers only have any of this type of data, and it is proprietary. Additional factors, such as temperature and concentration dependence of selectivity coefficients is necessary to extend the models ability to accurately describe industrial MBIE units.



## References

- Darvill, M.R., Bates, A.J., Bates, J.C., Ellis, G.W., Gardner, D.J., and Sadler, M.A., CEGB report SWR/SSD/0842/N/86, 1986.
- Emmett, J.R., and Water Trmt. J., 507, 1983.
- Gottlieb, M.C., Ultra Pure Water, 61, March, 1990.
- Haub, C.E., M.S. Thesis, Oklahoma State University, 1984.
- Kataoka, T, Yoshida, H., and Yamada, T., J. Chem Eng. Jpn., 5, 132, 1972.
- Kataoka, T, Yoshida, H., and Shibahara, Y., J. Chem Eng. Jpn., 9, 130, 1976.
- Salem, E., Proc. Amer. Power Conf., 31, 669, 1969.
- Wildhagen, G.R.S., Qassim, R.Y., Rajagopal, K., and Rahman, K., Ind. Eng. Chem. Fund., 24, 423, 1985.

## CHAPTER V

### CONCLUSIONS AND RECOMMENDATIONS

A series of chapters have been presented with each addressing specific concerns in mixed bed ion exchange (MBIE) modeling. The chapters were ordered so that each could draw on the developments presented earlier. The overall structure was to proceed from simpler to more complex model applications and developments. The models developed described MBIE in the film diffusion controlled regime for uni-valent exchange with bulk-phase reaction. Previous work by Haub (1984) has been extended to address non-neutral and multi-component systems.

Chapter 2 presented a model for amine cycle exchange. The model was able to describe the experimental results presented by Bates and Johnson (1984), and compared favorably with the AMMLEAK model they developed. Previous models, with the exception of Haub (1984), considered MBIE as a single salt removing process and used only one resin phase, or equilibrium calculations to describe the process. Haub (1984) showed that the MBIE unit is not a single salt removing process and that the diffusion limited nature of ion exchange must be accounted for. The amine cycle model uses film diffusion controlled exchange accompanied by bulk-phase reaction. The model is the first to examine amine cycle exchange from a diffusion limited viewpoint. Two different pH control agents were

evaluated, ammonia and morpholine. Temperature effects were also included within the model with the exception of the temperature dependence of the selectivity coefficients. A comparison of the results between ammonia and morpholine show, that from an ion exchange view, morpholine is preferable to ammonia. Longer bed run times and superior sodium removal were demonstrated by model evaluations of both systems. The major drawbacks to morpholine are; its high degradation rate and its lower dissociation constant, when compared with ammonia. Further consideration of two possible resin selections for morpholine, AMBERSEP 200 and AMBERSEP 252, were conducted. AMBERSEP 200 has extremely favorable selectivities and results in significantly extended run times. Industrially, though, AMBERSEP 252 is the predominant resin. This is because of past experiences with that resin. The complete lack of experimental data on morpholine systems allowed only a qualitative evaluation of the model. There is a need for accurate experimental data for morpholine form MBIE operation.

The third chapter presented a model for multi-component MBIE in uni-valent systems. A pseudo single coion approach was implemented to determine the system effective diffusivities and thereby determine outlet-concentration profiles for an ion exchange column. The approach leads to a discontinuity in the area of zero exchange rate that must be avoided by forcing the rate to zero in that area. The resulting model was compared with the existing experimental data of Omatete et al. (1980b) and Dranoff and Lapidus (1961). The model qualitatively predicted the ternary exchange data presented by Omatete, but was unable to accurately represent the data of Dranoff and Lapidus. The inability to describe Dranoff and Lapidus's data

could stem from the shallow bed technique used leading to kinetic leakage, which the present model cannot describe. The model was then extended to five and six component uni-valent systems to determine stability and predict breakthrough curves. The model predicts transient and fully developed outlet concentration surges and can be used for qualitative consideration of many multi-component systems. At present, this is the only model designed for MBIE evaluation in multi-component systems. The effluent concentrations for MBIE could not be compared with existing experimental data because there are none. Consideration of operating temperatures other than 25°C were not done since the selectivity coefficients were not available. It is known that the selectivity coefficients are functions of temperature, but how the resulting binary coefficients relate was not available. Therefore, model evaluations at other than 25°C would be more misleading than informative. The total lack of experimental data in multi-component film diffusion controlled ion exchange needs to be remedied. Model comparisons with experimental data should yield specific areas where further work is necessary.

The fourth chapter developed a model for hydrogen cycle exchange operating through the amine break. This model is an extension of the one presented in chapter 3 to consider pH adjusted waters. The model qualitatively predicts the known properties of ammonia in the hydrogen cycle. Further evaluations for morpholine were conducted, and again from an ion exchange viewpoint, morpholine performs better. The same general conclusions made in Chapter 2 apply to the systems considered in Chapter 4. The total lack of experimental data for MBIE at low concentrations excludes the

possibility of experimental comparisons. The model is the only one developed specifically for MBIE in non-neutral systems.

The point that each of the chapter conclusions stresses is the total lack of experimental data. A model is only useful if it can predict actual behavior. Without the ability to compare model predictions with experimental data the quantitative abilities of the model cannot be known. The models developed in this dissertation addressed a specific form of ion exchange that has been well applied industrially but totally untouched theoretically. Once the models quantitative abilities are confirmed, reduced costs in plant operations and improved resins will result.

There are certain areas in which improvements need to be made to the models presented here. The inclusion of di and tri-valent species must be the first. Sulfate is an anionic species that is of extreme interest to industry. The present model is, unfortunately, restricted to uni-valent exchange processes. The temperature dependent properties of the selectivity coefficients must be addressed. Typically industrial scale ion exchange units operate in the 40°C to 60°C range. Incorporating temperature dependent properties will extend the models flexibility. Kataoka et al (1980) showed that ternary interactions of selectivity coefficients can be important. Developing a better system than binary selectivity coefficients will further improve the range of applications of the present model. Numerically, a method that uses a variable step size should be implemented. The reason for this is that the majority of the exchange process occurs in a thin band within the bed where unreacted solution contacts unreacted resin. The step size in this

region should be very small so that the large changes in concentration within this narrow section can be followed. The multi-component case would require this to be modified for a series of zones. The exchange process occurs in four different zones for the six component case, and each of these zones needs to be considered.

The models developed in this dissertation represent the first step towards a general multi-component MBIE model. There is a definite need for further model development as well as accurate experimental data for model evaluation.

## BIBLIOGRAPHY

- Ahmad, H.S., M.S. Thesis, Oklahoma State University, 1989.
- Bajpai, R.K., Gupta, A.K., and Rao, M.G., A.I.Ch.E. J., 20, 989, 1974.
- Bates, J.C. and Johnson, T.D., Society of Chem. Ind., Int. Conf. on Ion Exchange, Cambridge, GB, 1984.
- Bird, R.B., Stewart, W.E., and Lightfoot, E.N., Transport Phenomena, John Wiley and Sons, N.Y., 1960.
- Boyd, G.E., Adamson, A.W., and Myers, L.S., Jr., J. Am. Chem. Soc., 69, 2836, 1947.
- Carberry, J.R., A.I.Ch.E. J., 4, 460, 1960.
- Cobble, J.W. and Turner, P.J., EPRI report NP-4209, 1985.
- Dadgar, A.M., Ph.D. Qualifying Exam, Oklahoma State University, 1986.
- Darvill, M.R., Bates, A.J., Bates, J.C., Ellis, G.W., Gardner, D.J., and Sadler, M.A., CEGB report SWR/SSD/0842/N/86, 1986.
- Davis, N.S., paper given at Ion Chromatography Symposium for the Power Industry, Atlanta, 1990.
- Divekar, S.V., Foutch, G.L., and Haub, C.E., Ind. Eng. Chem. Res., 26, 1906, 1987.
- Dranoff, J.S. and Lapidus, L., Ind. Eng. Chem. Fund., 49, 1297, 1957.
- Dranoff, J.S. and Lapidus, L., Ind. Eng. Chem. Fund., 50, 1648, 1958.
- Dranoff, J.S. and Lapidus, L., Ind. Eng. Chem., 53, 71, 1961.
- Dwyer, R.E., Zoppoli, I.E., Crits, G.J., and Tamaki, D.T., Proc. Amr. Power Conf., 38, 941, 1976.
- Erickson, K.L. and Rase, H.F., Ind. Eng. Chem. Fund., 18, 312, 1979.
- Emmett, J.R., Water Chem. Nucl. React. Syst., Proc. Int. Conf., Paper No. 4, 1977.
- Emmett, J.R., Wastewater and Water Trmt. J., 507, 1983.
- EPRI Report, NP-5056, 1987.

- EPRI Report, NP-5594, 1988.
- Gilbert, R., Lamarre, C., and Dundar, Y., paper given at CNA/CNS Annual Conf., 1989.
- Glaski, F.A. and Dranoff, J.S., A.I.Ch.E. J., 9, 426, 1963.
- Gottlieb, M.C., Ultra Pure Water, 61, March, 1990.
- Grahm, F.E. and Dranoff, J.S., Ind. Eng. Chem. Fund., 21, 360, 1982.
- Green S.J., Chem. Eng. Prog., 31, July, 1987.
- Haub, C.E., M.S. Thesis, Oklahoma State University, 1984.
- Haub, C.E. and Foutch, G.L., Ind. Eng. Chem. Fund., 25, 373, 1986a.
- Haub, C.E. and Foutch, G.L., Ind. Eng. Chem. Fund., 25, 381, 1986b.
- Helffferich, F.G. and Plesset, M.S., J. Chem. Phys., 28, 418, 1958.
- Helffferich, F.G., J. Phys. Chem., 69, 1178, 1965.
- Helffferich, F.G., in Ion Exchange, Vol. 1, J. Marinsky (ed.), 65, Marcel-Dekker Inc., N.Y., 1966.
- Helffferich, F.G., Ind. Eng. Chem. Fund., 6, 352, 1967.
- The Holy Bible, Revised Standard Edition, Exodus, 15:22-25, Melton Book Co., 1952.
- Hwang, Y-L., and Helffferich, F.G., Reactive Polymers, 5, 237, 1987.
- Kataoka, T, Sato, N., and Ueyama, K., J. Chem Eng. Jpn., 1, 38, 1968.
- Kataoka, T, Yoshida, H., and Yamada, T., J. Chem Eng. Jpn., 5, 132, 1972.
- Kataoka, T, Yoshida, H., and Yamada, T., J. Chem Eng. Jpn., 6, 172, 1973.
- Kataoka, T, Yoshida, H., and Shibahara, Y., J. Chem Eng. Jpn., 9, 130, 1976a.
- Kataoka, T, and Yoshida, H., J. Chem Eng. Jpn., 9, 383, 1976b.
- Kataoka, T, Yoshida, H., and Ozasa, Y., Chem Eng. Sci., 32, 1237, 1977.
- Kataoka, T, and Yoshida, H., J. Chem Eng. Jpn., 13, 328, 1980.
- Kataoka, T, and Yoshida, H., A.I.Ch.E. J., 21, 1020, 1988.



- King, D., M.S. Report, Oklahoma State University, 1988.
- Klein, G., Tondeur, D., and Vermeulen, T., Ind. Eng. Chem. Fund., 6, 339, 1967.
- McNulty, J.T., Personal Communication, 1990.
- Nernst, W., Z. Physik. Chem., 47, 52, 1904.
- Omatete, O.O., Clazie, R.N., and Vermeulen, T., Chem. Eng. J., 19, 229, 1980a.
- Omatete, O.O., Clazie, R.N., and Vermeulen, T., Chem. Eng. J., 19, 241, 1980b.
- Pan, S.H., and David, M.M., A.I.Ch.E. Symp. Ser., 74, 74, 1978.
- Pieroni, L.J., and Dranoff, J.S., A.I.Ch.E. J., 9, 42, 1963.
- Plesset, M.S., Helfferich, F.G., and Franklin, J.N., J. Chem Phys., 29, 1064, 1958.
- Rao, M.G., and David, M.M., A.I.Ch.E. J., 10, 213, 1964.
- Robinson, R.A., and Stokes, R.H., Electrolyte Solutions, Butterworths: England, 1959.
- Salem, E., Proc. Amer. Power Conf., 31, 669, 1969.
- Sawochka, S.G., Power, 67, April, 1988.
- Shallcross, D.C., Herrman, C.C., and McCoy, B.J., Chem. Eng. Sci., 43, 279, 1988.
- Sisson, A.B., Baker, M.M., Wirth, L.F. Jr., and Selby, K.A., Combustion, 6, July, 1968.
- Smith, T.G., and Dranoff, J.S., Ind. Eng. Chem. Fund., 3, 195, 1964.
- Strauss, and Kunin
- Streat, M. and Bringal, W.J., Trans. Inst. Chem. Eng., 48, T151, 1970.
- Tittle, K., Proc. Amer. Power Conf., 43, 1126, 1981.
- Tondeur, D. and Klein, G., Ind. Eng. Chem. Fund., 6, 351, 1967.
- Turner, J.C.R., Church, M.R., Johnson, A.S.W., and Snowdon, C.B., Chem. Eng. Sci., 21, 317, 1966.
- Van Brocklin, L.P., and David, M.M., Ind. Eng. Chem. Fund., 11, 91, 1972.

- Van Brocklin, L.P., and David, M.M., A.I.Ch.E. Symp. Ser., 71, 191, 1975.
- Wagner, J.D., and Dranoff, J.S., J. of Phys. Chem., 71, 4551, 1967.
- Wildhagen, G.R.S., Qassim, R.Y., Rajagopal, K., and Rahman, K., Ind. Eng. Chem. Fund., 24, 423, 1985.
- Wilke, C.R. and Chang, P., A.I.Ch.E. J., 1, 264, 1955.
- Yoon, T.Y., Ph.D. Dissertation, Oklahoma State University, 1990.
- Yoshida, H., and Kataoka, T., Ind. Eng. Chem. Res., 26, 1179, 1987.
- Zecchini, E.J., and Foutch, G.L., paper given at A.I.Ch.E. National Meeting, Session #65, San Francisco, 1989.

APPENDIX

## APPENDIX A

### ANION FLUX EXPRESSIONS

The anion resin flux expressions will be derived in general form for binary exchange. The equations developed will apply equally as well for the case of multiple homo valent coions. The necessary assumptions and conditions will be applied and explained at the appropriate junctures.

Binary film diffusion controlled ion exchange was addressed in detail by Haub (1984) for application in MBIE. The derivations presented here will follow the same nomenclature and similar logic structure. Modifications are made as necessary because of the different situations to which they apply.

The Nernst-Planck expression is used to describe the flux of a given species within the static film that is assumed to surround the resin bead under consideration. Assuming that the curvature of the film can be neglected, this expression is:

$$J_i = D_i \left[ \frac{\partial C_i}{\partial r} + Z_i \frac{FC}{RT} \left( \frac{\partial \phi}{\partial r} \right) \right]$$

Where  $\phi$  is the electrical potential and  $Z_i$  is the charge on ion  $i$ . This applies for each ion present in the film. Making use of the pseudo steady state assumption, which says that changes with position are much more important than changes with time, allows the partial derivatives to be replaced by ordinary derivatives.

The flux expressions can be considered from two different view points. First, that any neutralization or equilibrium reactions will take place in the bulk phase. This will be referred to as bulk phase neutralization. Second, that the reactions take place at a reaction plane located within the actual film surrounding the anion resin. This will be referred to as film neutralization. Film neutralization applies specifically to systems where hydrogen ions are present and allowed to diffuse into the anion film.

#### Bulk Neutralization

There are certain conditions that must be satisfied within the film surrounding the anionic resin. These are:

$$\sum_i Z_i C_i = 0 \quad (\text{electro-neutrality}),$$

$$J_{\text{coions at surface}} = 0 \quad (\text{no coion flux into resin}),$$

this yields an expression for the summation of the fluxes within the film as;

$$\sum_i Z_i J_i = 0 \quad (\text{no net current flow}),$$

since the film is assumed to be very thin and curvature can be neglected then the surface condition can be relaxed to include the whole film as;

$$J_{\text{coions}} = 0 \quad (\text{no coion flux}).$$

Rewriting these in terms of a five component system with three cations and univalent exchange yields:

$$J_n + J_h + J_x = J_c + J_o \quad (\text{no net current flow}),$$

$$J_n = J_h = J_x = 0 \quad (\text{no coion flux}),$$

$$C_n + C_h + C_x = C_c + C_o \quad (\text{electro-neutrality}).$$

Applying the no net coion flux expression to the Nernst-Planck expression for each of the cations yields an expression for the electrical potential  $\phi$  as:

$$\frac{d\phi}{dr} = \frac{-RT}{F C_n} \frac{dC_n}{dr} = \frac{-RT}{F C_h} \frac{dC_h}{dr} = \frac{-RT}{F C_x} \frac{dC_x}{dr}.$$

Thus a relation between each of the cation concentration gradients is determined. Differentiating the electro-neutrality condition with respect to  $r$  yields:

$$\frac{dC_n}{dr} + \frac{dC_h}{dr} + \frac{dC_x}{dr} = \frac{dC_c}{dr} + \frac{dC_o}{dr}.$$

Solving for each of the cation concentration gradients in terms of the sodium gradient ( $C_n$ ) and inserting into the above expression yields:

$$\frac{dC_n}{dr} + \frac{C_h}{C_n} \frac{dC_n}{dr} + \frac{C_x}{C_n} \frac{dC_n}{dr} = \frac{dC_c}{dr} + \frac{dC_o}{dr}.$$

The left hand side can be manipulated to give:

$$\frac{1}{C_n} \frac{dC_n}{dr} (C_n + C_h + C_x) = \frac{dC_c}{dr} + \frac{dC_o}{dr}.$$

But the electro-neutrality condition gives the term in the parenthesis as the sum of the counter ion concentrations. This fact, combined with the previous expression for the electrical potential gradient give a more useful result as:

$$\frac{d\phi}{dr} = \frac{-RT}{F} \left( \frac{1}{C_c + C_o} \right) \left( \frac{dC_c}{dr} + \frac{dC_o}{dr} \right) \quad (\text{eq. A-1}).$$

This allows  $\phi$  to be eliminated from the flux expressions for hydroxide and chloride. The fluxes become:

$$J_o = -D_o \left( \frac{dC}{dr}^o + \frac{C}{C_c + C_o} \left( \frac{dC}{dr}^o + \frac{dC}{dr}^c \right) \right) \quad \text{and}$$

$$J_c = -D_c \left( \frac{dC}{dr}^c + \frac{C}{C_c + C_o} \left( \frac{dC}{dr}^o + \frac{dC}{dr}^c \right) \right).$$

Using the no net current flow condition with the no net coion flux:

$$D_o \left( \frac{dC}{dr}^o + \frac{C}{C_c + C_o} \left( \frac{dC}{dr}^o + \frac{dC}{dr}^c \right) \right) + D_c \left( \frac{dC}{dr}^c + \frac{C}{C_c + C_o} \left( \frac{dC}{dr}^o + \frac{dC}{dr}^c \right) \right) = 0$$

Collecting terms and multiplying through by  $C_o + C_c$  yields:

$$(2D_o C_o + D_o C_c + D_c C_c) \frac{dC}{dr}^o + (2D_c C_c + D_o C_c + D_c C_o) \frac{dC}{dr}^c = 0$$

so:

$$\frac{dC}{dr}^o = -\frac{dC}{dr}^c \left( \frac{2D_o C_c + D_o C_c + D_c C_c}{2D_c C_c + D_o C_c + D_c C_o} \right) \quad (\text{eq. A-2}).$$

This allows the hydroxide derivative to be replaced by the chloride derivative in the flux expressions. Also, the following result can be obtained:

$$\frac{d}{dr} \left[ (D_o C_o + D_c C_c) (C_o + C_c) \right] = 0.$$

Therefore the term enclosed in the parenthesis is a constant. This determines a relationship between the bulk phase concentrations and the film concentrations of the form:

$$(D_o C_o + D_c C_c) (C_o + C_c) = (D_o C_o^o + D_c C_c^o) (C_o^o + C_c^o) = \text{RHS},$$

where the superscript,  $^o$ , denotes the bulk phase, this is eq. A-3.

The quantity on the right hand side will be abbreviated as RHS for convenience. This can be expanded and the resulting expression solved using the quadratic formula to determine the relationship between hydroxide and chloride concentration.

$$D_o C_o^2 + (D_o C_c + D_c C_c) C_o + (D_c C_c^2 - \text{RHS}) = 0$$

Thus:

$$C_o = \frac{-C_c(D_o + D_c) + (C_c^2(D_o + D_c)^2 - 4D_o(D_c C_c^2 - \text{RHS}))^{1/2}}{2D_o}$$

The positive square root is used since the concentration of a species can never be less than zero. Substituting the previous expressions into the Nernst-Planck equation for chloride yields:

$$J_c = -D_c \left[ \frac{dC}{dr} c + \frac{C}{C_c + C_o} \left( 1 - \left( \frac{2D_o C_c + D_o C_o + D_c C_o}{2D_o C_o + D_o C_c + D_c C_c} \right) \right) \frac{dC}{dr} c \right],$$

where  $C_o$  is given in the preceding equation. The right hand side of the chloride flux expression can be rearranged into a much more convenient form by replacing  $C_o$  and canceling like factors.

$$J_c = -D_c \frac{dC}{dr} c \left( 1 + \frac{D_o^2 C_c - D_o C_c C_o - D_c C_c C_o}{(C_c + C_o)(2D_o C_o + D_o C_c + D_c C_c)} \right)$$

Putting the entire expression over a common denominator:

$$J_c = -D_c \frac{dC}{dr} c \left( \frac{2D_o C_c^2 + 4D_o C_c C_o + 2D_o C_o^2}{(C_c + C_o)(2D_o C_o + D_o C_c + D_c C_c)} \right).$$

This reduces to:

$$J_c = -D_c \frac{dC}{dr} c \left( \frac{2D_o(C_o + C_c)}{2D_o C_o + D_o C_c + D_c C_c} \right) \quad (\text{eq. A-4}),$$

Now  $C_o$  can be replaced and the final expression simplified. Expanding the right hand side:

$$\begin{aligned} & \frac{2D_o C_c \left[ \frac{-C_c(D_o + D_c)}{2D_o} + \frac{(C_c^2(D_o + D_c)^2 - 4D_o(D_c C_c^2 - \text{RHS}))^{1/2}}{2D_o} + C_c \right]}{2D_o \left[ \frac{-C_c(D_o + D_c)}{2D_o} + \frac{(C_c^2(D_o + D_c)^2 - 4D_o(D_c C_c^2 - \text{RHS}))^{1/2}}{2D_o} \right] + D_o C_c + D_c C_c} \\ &= \frac{\left[ \frac{-D_c D_o C_c - D_c^2 C_c + D_c (C_c^2(D_o + D_c)^2 - 4D_o(D_c C_c^2 - \text{RHS}))^{1/2} + 2D_c D_o C_c}{-D_o C_c - D_c C_c + (C_c^2(D_o + D_c)^2 - 4D_o(D_c C_c^2 - \text{RHS}))^{1/2} + D_o C_c + D_c C_c} \right]}{2D_o} \end{aligned}$$



$$D_c + \left( \frac{D_c C_c (D_o - D_c)}{(C_c^2 (D_c + D_o)^2 - 4D_o (D_c C_c^2 - \text{RHS}))^{1/2}} \right) =$$

$$D_c + \left( \frac{D_c C_c (D_o - D_c)}{(C_c^2 (D_o - D_c)^2 + 4D_o \text{RHS})} \right).$$

This result is significantly simpler than the preceding expression.

Now this can be placed in the flux expression for chloride. The flux expression can be separated and integrated once the pseudo-steady state assumption is applied. This results in:

$$\frac{dJ}{dr} = 0 \text{ or } J_c = \text{constant.}$$

This allows for the flux expression to be separated and integrated with the boundary conditions:

$$C_c = C_c^o \text{ at } r = r_o + \delta \quad \text{and}$$

$$C_c = C_c^* \text{ at } r = r_o.$$

With the aid of a change of variable, the right hand side of the flux expression can be converted to (after separation):

$$u = C_c (D_o - D_c)$$

$$\int J_c dr = \frac{D_c}{(D_o - D_c)} \int \left( \frac{u}{(u^2 + a)} \right) du + \int D_c dC_c.$$

This has an analytical solution of the form:

$$-J_c \delta = \left[ \frac{D_c}{(D_o - D_c)} (C_c^2 (D_o - D_c)^2 + 4D_o \text{RHS})^{1/2} + D_c C_c \right] \Bigg|_{C_c^*}^{C_c^o}$$

Applying the limits of integration and simplifying the resulting expression yields:

$$-J_c \delta = \frac{2D_o D_c}{(D_o - D_c)} \left[ C_o^o + C_c^o - C_o^* - C_c^* \right] \quad (\text{eq. A-5}).$$

This was the expected result analogous to the that derived by Haub (1984). The static film model can now be used in conjunction with the above result to predict the particle rate.

#### Film Neutralization

This is employed due to the differing mobilities of the hydrogen and hydroxide ions. When there is a surplus of one component in the bulk phase, the reaction front, which was originally assumed to be at the film-bulk interface, will shift into the film surrounding the appropriate resin. This is limited to the binary exchanges where the cation resin is in the hydrogen form. The approach applies specifically to binary exchange at near neutral pH. The derivation was carried out in depth by Haub (1984) and since the preceding derivation resulted in the expected form, the derivation of the film neutralization model will highlight the earlier derivation.

The film is broken down into two distinct regions, counter ion diffusion and coion diffusion. These are separated by the location of the reaction plane,  $\delta_r$ . The location of the reaction plane within the film is found by equating the non-reacting counter ion flux at the reaction plane. In the case of hydrogen and hydroxide, the concentrations at the reaction plane are fixed by the dissociation constant of water. This coupled with the flux expressions allows for the location of the reaction plane to be determined.

The two zones under consideration have different conditions that must be satisfied within the film. The counter ion diffusion

region is located between the resin surface and the reaction plane,  $\delta_r$ , the conditions that must be satisfied are the same as for bulk-phase neutralization with the outer limit of the film being  $\delta_r$  instead of  $\delta$ . The hydrogen flux in this region can still be accounted for, so the flux will not be set equal to zero.

The coion diffusion region lies between the reaction plane and the film-bulk interface. The conditions that must be satisfied in this region relate the flux of the hydrogen coion and the chloride ion. This results in an expression between the concentration gradients of the diffusing species as:

$$\frac{dC_c}{dC_h} = \left[ \frac{2D_c K_w + 2D_c C_c C_h - D_c C_h^2 + D_h C_h^2}{2D_h K_w + D_h C_c C_h + D_c C_c C_h} \right]$$

the resulting flux expression for the chloride ion is:

$$J_c = - \frac{dC_c}{dr} \left[ \frac{2D_c D_h (C_c C_h + K_w)}{2D_h K_w + D_h C_c C_h + D_c C_c C_h} \right] \quad (\text{eq. A-6})$$

The hydrogen ion concentration at the reaction plane is fixed due to the water equilibrium. Pseudo steady state exchange gives the chloride flux as a constant so eq. A-6 can be numerically integrated. Since the chloride flux must be equal across the reaction plane, the zone between the resin and the reaction plane can be combined with the chloride flux expression.

The result is an expression for the relative position of the reaction plane within the film as:

$$h = \frac{\delta_r}{\delta} = \frac{2D_o D_c C_c^o (C_o^r / C_c^o + C_c^r / C_c^o - Y)}{-I(D_c - D_o) + 2D_o D_c C_c (C_o^r / C_c^o + C_c^r / C_c^o - Y)}$$

where I is the numerical result of the integration of the chloride

flux expression, and  $Y$  is the result of the resin to bulk concentration relation using the selectivity coefficients. The above equations must be solved numerically for each evaluation of the rate of exchange. The resulting expression for the effective diffusivity is:

$$D_e = \frac{I}{(1-h)(C_c^o)(1-C_c^*/C_c^o)} \quad (\text{eq. A-7}).$$

The relationship between the coion and counter ion concentration gradients is solved using Simpson's rule and then an interpolation routine is called to determine intermediate values for the solution of the flux equations. This results in the determination of the effective diffusivity based on a linear driving force. These results will be coupled with the particle rates and column material balances to determine column performance.

This approach is limited to binary exchange because of the inability of the static film model to give an actual value for the film thickness. The method also requires that the concentrations of the reacting species be specified at the reaction plane. Thus, an additional reactant cannot be accounted for in this case.

## APPENDIX B

### TERNARY EXCHANGE EQUATIONS

The equations and relations needed to define the case of ternary exchange with bulk phase neutralization will be developed. The major considerations are to obtain an expression for the interface concentrations in terms of bulk phase concentrations and to determine the appropriate flux expression, which will be used to obtain the effective diffusivity.

The development will follow similar to that already conducted for binary exchange but will be extended to three components. The conditions that must be satisfied within the thin static film surrounding the particle are:

$$C_n + C_x + C_h = C_o + C_c \quad (\text{electro-neutrality}),$$

$$J_n + J_x + J_h = J_o + J_c \quad (\text{no net current flow}), \text{ and}$$

$$J_o = J_c = 0 \quad (\text{no coion flux}).$$

The no coion flux arises from the surface condition of no electrolyte sorption being relaxed between the surface and the reaction plane. The reaction plane is assumed to be the bulk-film interface since bulk-phase neutralization is the only case that can be addressed. These relations apply only within the film around the exchange particle. The Nernst-Planck expression is used to describe the fluxes of the species through the film. The electrical potential,  $\phi$  can be

eliminated by using the no coion flux relation:

$$\frac{\partial \phi}{\partial r} = \frac{RT}{F C_c} \frac{\partial C}{\partial r} = \frac{RT}{F C_o} \frac{\partial C}{\partial r} \quad \text{and} \quad \frac{\partial C}{\partial r} = \frac{C_o}{C_c} \frac{\partial C}{\partial r}$$

Using this and differentiating the charge balance condition with respect to  $r$  yields:

$$\frac{\partial \phi}{\partial r} = \frac{RT}{F} \left( \frac{1}{C_n + C_x + C_h} \right) \left( \frac{\partial C}{\partial r} + \frac{\partial C}{\partial r} + \frac{\partial C}{\partial r} \right) \quad (\text{eq. B-1}).$$

This allows the electrical potential to be eliminated by the concentration gradients of the cations and the sum of their concentrations. The pseudo steady state assumption allows for the formality of the partial derivatives to be dropped, since they become ordinary derivatives under that condition. Making use of pseudo steady state and the no net current flow coupled with no coion flux yields:

$$D_n \frac{dC}{dr} + D_n \left( \frac{C}{C_n + C_x + C_h} \right) \nabla C_i + D_h \frac{dC}{dr} + D_h \left( \frac{C}{C_n + C_x + C_h} \right) \nabla C_i + D_x \frac{dC}{dr} + D_x \left( \frac{C}{C_n + C_x + C_h} \right) \nabla C_i = 0,$$

where the subscript  $i$  denotes all of the cations. Expanding this and collecting derivatives yields:

$$\begin{aligned} & \frac{dC}{dr} \left( 2 D_n C_n + D_n C_h + D_n C_x + D_h C_h + D_x C_x \right) + \\ & \frac{dC}{dr} \left( 2 D_h C_h + D_h C_n + D_h C_x + D_n C_n + D_x C_x \right) + \\ & \frac{dC}{dr} \left( 2 D_x C_x + D_x C_h + D_x C_n + D_h C_h + D_n C_n \right) = 0. \end{aligned}$$

Letting  $\alpha_h = D_h/D_n$  and  $\alpha_x = D_x/D_n$  and rearranging the above expression the following is obtained:

$$\frac{d}{dr} \left[ (C_h + C_n + C_x) (\alpha_h C_h + C_n + \alpha_x C_x) \right] = 0.$$

This says that in the film surrounding the resin that the quantity contained within the brackets is a constant. Solving this elementary differential equation with the boundary conditions:

$$\begin{aligned} C_h &= C_h^o @ r = r_o + \delta & C_h &= C_h @ r_o < r < r_o + \delta , \\ C_n &= C_n^o @ r = r_o + \delta & C_n &= C_n @ r_o < r < r_o + \delta , \\ C_x &= C_x^o @ r = r_o + \delta & C_x &= C_x @ r_o < r < r_o + \delta . \end{aligned}$$

The relationship between the film concentrations and the bulk phase is given by:

$$(C_h + C_n + C_x)(\alpha_h C_h + C_n + \alpha_x C_x) = (C_h^o + C_n^o + C_x^o)(\alpha_h C_h^o + C_n^o + \alpha_x C_x^o),$$

This is equation B-2. The previous expression that was solved for the film concentration relation can also be used to eliminate one of the concentration gradients from the flux expressions. This is of the form:

$$\frac{dC_h}{dr} = \frac{-1}{A} \left( B \frac{dC_n}{dr} + C \frac{dC_x}{dr} \right) \quad (\text{eq. B-3}),$$

where:

$$A = 2\alpha_h C_h + \alpha_h C_n + \alpha_h C_x + C_n + \alpha_x C_x ,$$

$$B = 2C_n + C_h + C_x + \alpha_h C_h + \alpha_x C_x , \text{ and}$$

$$C = 2\alpha_x C_x + \alpha_x C_h + \alpha_x C_n + \alpha_h C_h + C_n .$$

The pseudo steady state assumption also gives that the fluxes are constants within the film, so with this substitution the three component flux expressions are simplified. Unfortunately, there is no relation between the sodium and x concentration gradients so they can not be solved directly in this form. If the film thickness were known, then a trial and error approach could be used to obtain the

concentration gradients. The draw back of the static film model is that it does not allow for the film thickness to be found expressly.

A slightly different approach can be used, based on a fractional concentration within the film and a pseudo single coion. This approach will be used in order to obtain an expression for the effective diffusivity of each species within the film. The binary case for film diffusion control and bulk phase neutralization has been addressed earlier, some of those results will be used here.

The approach is to apply the continuity equation to the film surrounding the resin. It must be satisfied within this region and some of the films properties allow for an improved expression for the effective diffusivity within the film. This approach is similar to the one recommended by Wildhagen, et. al. (1985). The concept of a pseudo single coion applies for exchange where the coions are homo-valent, ie. they all have the same valence. The restriction also extends to incorporate the counter ions of interest, they must also be a homo-valent matrix. The case of non-uniform valence will have to be addressed in some other manner, such as by a series of binary pairs.

The pseudo coion has properties similar to those of the original system of coions. This component is defined as:

$$C_p = C_c + C_o \quad (\text{eq. B-4}).$$

This development applies regardless of the number of coions involved as long as they are homo-valent, so this expression could be generalized as the sum over all coions. After applying the Nernst-Planck equation for each of the coions:

$$J_c = D_c \left[ \frac{dC}{dr} - \frac{F}{R T} C \nabla \phi \right] = 0 ,$$



and,

$$J_o = D_o \left[ \frac{dC}{dr} - \frac{F-C}{RT} \nabla \phi \right] = 0 .$$

These equations can be replaced by the pseudo component equation:

$$J_p = 0 = D_p \left[ \frac{dC}{dr} - \frac{FC}{RT} \nabla \phi \right] \quad (\text{eq. B-5}).$$

This can be seen to be the Nernst-Plank expression for the pseudo component p. Thus, the properties of the actual system are retained through the introduction of this new component. The charge balance and the no net current flow terms still apply as:

$$C_n + C_h + C_x = C_p , \text{ and,}$$

$$J_n + J_h + J_x = J_p .$$

The continuity equation within the film can be written as:

$$\frac{\partial C_i}{\partial t} + U C_i + \nabla \cdot J_i = 0 ,$$

where the reactions that take place are restricted to the bulk phase, due to the bulk phase neutralization assumption. This can be simplified by the application of a few of the earlier assumptions. The accumulation within the film can be neglected since pseudo steady state has been assumed. The convective term can be neglected due to the assumption that there is a stagnant film surrounding the particle. This results in the previously applied assumption that the fluxes are constant due to the pseudo steady state assumption:

$$\frac{d J_i}{d r} = 0 .$$

Applying the continuity equation to each of the counter ions and the pseudo coion and adding the following relation results:

$$\frac{d^2 C_n}{dr^2} + \frac{d^2 C_h}{dr^2} + \frac{d^2 C_x}{dr^2} + \frac{d^2 C_p}{dr^2} + \frac{F}{RT} \left[ \nabla \cdot \left( (C_n + C_h + C_x - C_p) \frac{d\phi}{dr} \right) \right] = 0.$$

The term in the parentheses is another way of expressing the charge balance equation, so it is equal to zero.

This results in the equation:

$$\frac{d^2}{dr^2} \left( C_n + C_h + C_x \right) + \frac{d^2 C_p}{dr^2} = 0.$$

This can be simplified from the charge balance condition to:

$$2 \frac{d^2 C_p}{dr^2} = 0.$$

This simplified expression can be integrated to give the concentration profile of the pseudo component within the film:

$$\frac{d C_p}{dr} = K_1, \text{ and, } C_p = K_1 r + K_2 \quad (\text{eq. B-6}).$$

This is a linear profile for the coion concentration within the film.

The constants of integration can be evaluated by applying the boundary conditions at the film-bulk interface and at the resin surface:

$$C_p = C_p^* \quad @ \quad r = 0 \quad \text{and,} \quad C_p = C_p^o \quad @ \quad r = \delta.$$

This results in the following expression for  $C_p$ :

$$C_p = \frac{C_p^o - C_p^*}{\delta} r + C_p^* \quad (\text{eq. B-7}).$$

Thus, the pseudo coion is defined at any point within the film surrounding the particle. This result can now be used to obtain the flux of counter ion  $i$  within the film.

The electrical potential term is eliminated by using the no coion flux condition as:

$$\frac{d\phi}{dr} = \frac{RT}{FC_p} \frac{d C_p}{dr}.$$

The derivative of  $C_p$  with respect to  $r$  is given by the linear relation within the film as  $K_1$ . Rewriting the flux expression for component  $i$ .

$$J_i = D_i \left[ \frac{dC_i}{dr} + K_1 C_i / C_p \right].$$

Defining a new variable:

$$Y_i = C_i / C_p \quad (\text{eq. B-8}).$$

Substituting this into the flux expression yields:

$$J_i = D_i \left[ C_p \frac{dY_i}{dr} + 2 K_1 Y_i \right] \quad (\text{eq. B-9}).$$

$J_i$  is a constant as shown by the earlier applied continuity equation.

Thus, the previous expression can be separated and integrated to obtain an expression for the flux.

$$J_i / D_i + 2 K_1 Y_i = -C_p \frac{dY_i}{dr}.$$

Substituting the known value for  $C_p$ :

$$-dr / (K_1 r + K_2) = dY_i / (J_i / D_i + 2 K_1 Y_i).$$

This can readily be integrated within the limits given by the boundary conditions:

$$Y_i = Y_i^* \quad @ \quad r = 0 \quad \text{and}, \quad Y_i = Y_i^o \quad @ \quad r = \delta.$$

$$\int_0^\delta -dr / (K_1 r + K_2) = \int_{Y_i^*}^{Y_i^o} dY_i / (J_i / D_i + 2 K_1 Y_i),$$

or:

$$\left[ -2 \ln (K_1 r + K_2) \right]_0^\delta = \ln (J_i / D_i + 2 K_1 Y_i) \Big|_{Y_i^*}^{Y_i^o}.$$

Evaluating within the limits and exponentiating both sides yields:

$$\left( \frac{K_1 \delta + K_2}{K_2} \right)^2 = \frac{J_i / D_i + 2 K_1 Y_i^o}{J_i / D_i + 2 K_1 Y_i^*}.$$

The squared expression can be simplified to:

$$\left( \frac{C_p^{\circ}}{C_p^*} \right)^2.$$

Therefore:

$$J_i/D_i \left[ \left( \frac{C_p^{\circ}}{C_p^*} \right)^2 - 1 \right] = 2 \text{ Kl} \left[ \left( \frac{C_p^{\circ}}{C_p^*} \right)^2 Y_i^{\circ} - Y_i^* \right].$$

This leads directly to an expression for the flux of species i as:

$$J_i = 2 D_i \text{ Kl} \left[ \frac{\left( \frac{C_p^{\circ}}{C_p^*} \right)^2 Y_i^{\circ} - Y_i^*}{\left( \frac{C_p^{\circ}}{C_p^*} \right)^2 - 1} \right].$$

Simplifying this expression and substituting for Kl:

$$J_i = 2 D_i \left[ \frac{\left( \frac{C_p^{\circ}}{C_p^*} \right) \left( C_p^{\circ 2} Y_i^{\circ} - C_p^{*2} Y_i^* \right)}{\delta \left( C_p^{\circ} + C_p^* \right) \left( C_p^{\circ} - C_p^* \right)} \right] \quad (\text{eq. B-10}).$$

This yields the desired expression for the flux times the film thickness:

$$\delta J_i = 2 D_i \left[ \frac{C_p^{\circ 2} Y_i^{\circ} - C_p^{*2} Y_i^*}{C_p^{\circ} + C_p^*} \right].$$

Remembering the original definition of  $Y_i$  and converting to fractional concentrations:

$$\delta J_i = 2 D_i \left[ \frac{1 - \left( \frac{C_p^*}{C_p^{\circ}} \right) \left( \frac{C_i^*}{C_i^{\circ}} \right)}{\left( 1 + \frac{C_p^*}{C_p^{\circ}} \right)} \right] \quad (\text{eq. B-11}).$$

The flux expression for any counter ion i is specified by the previous expression. This expression can be used in conjunction with the static film model rate expression to determine the effective diffusivity for the exchange process.

## APPENDIX C

### PARTICLE RATES

The flux expressions derived in the previous Appendixes were developed so that the particle rates could be determined. The rate of change of the resin phase compositions require that a model for the liquid film surrounding the resin be specified. The static film model will be used in preference to other available models due to its simplicity and less than a few percent deviation from the other film models (Kataoka et. al. 1976).

The static film model results in an expression of the form:

$$\frac{\partial \langle C_i \rangle}{\partial t} = K_i' a_s (C_i^o - C_i^*) \quad (\text{eq. C-1}).$$

The driving force for exchange is of a simple linear nature. The non-linearity of the exchange process is introduced in the determination of the mass transfer coefficient  $K_i'$ . This coefficient is defined as:

$$K_i' = D_{ei} / \delta .$$

The reason that  $D_{ei}$  is used instead of the typical  $D_e$  is that for multi-component exchange the value for the effective diffusivity is species dependent. The rate of exchange is related to the flux of the species by:

$$\frac{\partial \langle C_i \rangle}{\partial t} = K_i' a_s (C_i^o - C_i^*) = -J_i a_s \quad (\text{eq. C-2}).$$

This demonstrates why the flux expressions are so important in determining the rate of exchange. A more convenient form of the resin phase concentration  $\langle C_i \rangle$  is:

$$\langle C_i \rangle = y_i Q ,$$

where  $Q$  is the capacity of the particular resin of interest and  $y_i$  is the fraction of the resin in that form. This gives an expression for the rate of exchange as:

$$\frac{\partial y_i}{\partial t} = \frac{K_i'}{Q} a_s (C_i^o - C_i^*) = \frac{-J_i}{Q} a_s \quad (\text{eq. C-3}).$$

Substituting for the flux from previous developments and the effective diffusivity from the definition of  $K_i'$  allows for  $D_{ei}$  to be found.

This expression is:

$$D_{ei} = -J_i \delta / (C_i^o - C_i^*) \quad (\text{eq. C-4}).$$

This expression can be combined with the relation for  $R_i$  as defined by Pan and David (1978):

$$R_i = \left[ \frac{D_{ei}}{D_i} \right]^{2/3} = K_i' / K_i \quad (\text{eq. C-5}).$$

The right hand portion of eq. C-5 has been shown to correlate well by Kataoka et al. (1973). This allows the non-ionic mass transfer coefficient in the packed bed to be used in the rate expression. The correlations of Carberry (1960) or Kataoka (1973) can be used to determine the non-ionic mass transfer coefficients based on the particle Reynolds number and the species Schmidt number. The final rate expression is:

$$\frac{\partial y_i}{\partial t} = K_i R_i \frac{a_s}{Q} (C_i^o - C_i^*) \quad (\text{eq. C-6}),$$

where  $K_i$  is the non-ionic mass transfer coefficient for species  $i$ .

Now the concept of the selectivity coefficient can be introduced to provide a relation between the resin phase fraction and the interfacial concentration. The selectivity coefficient is a constant for a given resin that relates the equilibrium concentrations of two exchanging species. It is defined as:

$$K_B^A = (\bar{C}_B C_A) / (\bar{C}_A C_B) ,$$

where the bar denotes resin phase concentration. The selectivity coefficient can be concentration dependent but expressions for this dependence are not available. The assumption applied here is that the coefficient is constant and that the binary selectivities can be used to describe ternary exchange. The previous expression can be rewritten in terms of the resin phase fractions as:

$$K_B^A = (y_B C_A^*) / (y_A C_B^*)$$

since the resin phase is assumed to be in equilibrium with the concentrations at the particle surface. The sum of the fractions of all species on the resin must be one, so there are n-1 independent expressions that can be derived from the selectivity coefficients. If the previously derived expressions relating film and bulk phase concentrations are combined with this definition of the selectivity coefficient, a relationship between the resin phase and the bulk phase concentrations can be found. The fractions of species on the resin for ternary cation exchange is given by:

$$y_x + y_h + y_n = 1 ,$$

or;

$$y_h = 1 - y_x - y_n .$$

Thus there are only two unknowns and the hydrogen fraction can be

eliminated as its concentration was previously. The film concentration relation can be applied to determine the interfacial concentrations:

$$\left( C_h^* + C_n^* + C_x^* \right) \left( D_h C_h^* + D_x C_x^* + D_n C_n^* \right) =$$

$$\left( C_h^o + C_n^o + C_x^o \right) \left( D_h C_h^o + D_n C_n^o + D_x C_x^o \right) = \text{RHS}$$

The selectivities can be used to eliminate  $C_h^*$  and  $C_x^*$  leaving only  $C_n^*$  in the equation. Solving for  $C_n^*$  yields:

$$C_n^* = y_n \left[ \text{RHS} / \left( (1-K_h^n) y_n + (K_x^n - K_h^n) y_x + K_h^n \right) \right. \\ \left. \left( (1-\alpha_h K_h^n) y_n + (\alpha_x K_x^n - \alpha_h K_h^n) y_x + \alpha_h K_h^n \right) \right]^{1/2}$$

Reapplying the definition of the selectivity coefficient allows for all of the interfacial concentrations to be defined as:

$$C_x^* = C_n^* K_x^n (y_x / y_n)$$

$$C_h^* = C_n^* K_h^n (1 - y_n - y_x) / y_n$$

The same expression can be obtained for binary exchange, in a slightly simpler mode. This relation allows for the resin phase and the bulk phase to be related. This will be paramount in the determination of MBIE performance.

The above expressions can now be used with the particle rates to describe the exchange process. This relationship is extremely valuable when coupled with the soon to be presented material balance frame work. The combination of these, with the expressions for the



effective diffusivities derived earlier, determine the exchange characteristics of any given particle.

## APPENDIX D

### COLUMN MATERIAL BALANCES

The simulation of an ion exchange packed bed requires the implementation of column material balances to determine the effluent concentration history. These material balances will use the previously derived rate expressions and the effective diffusivities to predict outlet concentrations. The overall material balance for species  $i$  is given by:

$$\frac{u_s}{\epsilon} \frac{\partial C}{\partial z} n + \frac{\partial C}{\partial t} n + \frac{(1-\epsilon)}{\epsilon} \frac{\partial q}{\partial t} n = 0 \quad (\text{eq. D-1}),$$

where:

$u_s$  = superficial velocity, and

$\epsilon$  = void fraction.

This is not in the most useful form, so some change of variables are in order. Dimensionless time and distance will be implemented to simplify the above equation. These are defined as:

$$\tau = \frac{K_i C_T^f}{d_p Q} \left( t - \frac{\epsilon z}{u_s} \right) \quad (\text{eq. D-2}),$$

and,

$$\xi = \frac{K_i (1-\epsilon)}{u_s} \frac{z}{d_p} \quad (\text{eq. D-3}).$$

$K_i$  is the non-ionic mass transfer coefficient for species  $i$ ,  $d_p$  is the particle diameter,  $Q$  is the resin capacity and  $C_T^f$  is the total

cationic feed concentration. Transforming the material balance equation requires that the intermediate derivatives be determined.

These are:

$$\frac{\partial \tau}{\partial t} = \frac{K_i C_T^f}{d_p Q}, \quad \frac{\partial \tau}{\partial z} = \frac{-K_i C_T^f \epsilon}{d_p Q u_s}$$

$$\frac{\partial \xi}{\partial t} = 0 \quad \text{and} \quad \frac{\partial \xi}{\partial z} = \frac{K_i (1-\epsilon)}{u_s d_p}$$

So now the original derivatives can be expressed in terms of the new variables as:

$$\frac{\partial C_i}{\partial t} = \frac{\partial C_i}{\partial \tau} \left( \frac{\partial \tau}{\partial t} \right) + \frac{\partial C_i}{\partial \xi} \left( \frac{\partial \xi}{\partial t} \right) = \frac{K_i C_T^f}{d_p Q} \frac{\partial C_i}{\partial \tau} + 0 \frac{\partial C_i}{\partial \xi}$$

$$\frac{\partial C_i}{\partial z} = \frac{\partial C_i}{\partial \xi} \left( \frac{\partial \xi}{\partial z} \right) + \frac{\partial C_i}{\partial \tau} \left( \frac{\partial \tau}{\partial z} \right) = \frac{K_i (1-\epsilon)}{u_s d_p} \frac{\partial C_i}{\partial \xi} - \frac{K_i C_T^f \epsilon}{d_p u_s Q} \frac{\partial C_i}{\partial \tau}$$

$$\frac{\partial q_i}{\partial t} = \frac{\partial q_i}{\partial \tau} \left( \frac{\partial \tau}{\partial t} \right) + \frac{\partial q_i}{\partial \xi} \left( \frac{\partial \xi}{\partial t} \right) = \frac{K_i C_T^f}{d_p Q} \frac{\partial q_i}{\partial \tau} + 0 \frac{\partial q_i}{\partial \xi}$$

Replacing these into the material balance yields:

$$\frac{\partial C_i}{\partial \xi} + \frac{C_T^f}{Q} \frac{\partial q_i}{\partial \tau} = 0 \quad (\text{eq. D-4}).$$

This is a significantly easier to handle equation. Transforming the dependent variables into a more useful form:

$$x_i = C_i / C_T^f, \quad \text{and} \quad q_i = Q y_i,$$

yields an expression for the material balance of the form:

$$\frac{\partial x_i}{\partial \xi} + \frac{\partial y_i}{\partial \tau} = 0 \quad (\text{eq.D-5}).$$

The new variables are dependent upon which species is chosen as the basis since all of the material balances need to be solved using the

same steps in  $\tau$  and  $\xi$ . Implementation of the mixed bed is achieved by modifying the resin phase portion of the material balance to reflect the fractions of the resin that are cationic and anionic. This is done through the introduction of the constants FCR and FCA which must be specified for any given column. The case of ternary cation exchange and binary anion exchange will be developed with the basis for the dimensionless variables on the third cation species  $x$  and the cation resin. This gives expressions for  $\tau$  and  $\xi$  as:

$$\tau = \tau_x = \frac{K_x Q_T^f}{d_{pc} Q_c} \left( t - \frac{\epsilon z}{u_s} \right), \text{ and}$$

$$\xi = \xi_x = \frac{K_x (1-\epsilon)}{u_s d_{pc}} z,$$

where the additional subscript  $c$  denotes the cation resin. This requires that the material balance for each species be written. These are:

$$\frac{\partial x}{\partial \xi^n} = \frac{\partial x}{\partial \xi_x^n} \left( \frac{\partial \xi_x}{\partial \xi} \right) = \frac{K_x}{K_n} \frac{\partial x}{\partial \xi_x^n},$$

$$\frac{\partial y_n}{\partial \tau} = \frac{\partial y_n}{\partial \tau_x} \left( \frac{\partial \tau_x}{\partial \tau} \right) = \frac{K_x}{K_n} \frac{\partial y_n}{\partial \tau_x}, \text{ and}$$

$$\frac{\partial x}{\partial \xi^c} = \frac{\partial x}{\partial \xi_x^c} \left( \frac{\partial \xi_x}{\partial \xi} \right) = \frac{K_x d_{pa}}{K_c d_{pc}} \frac{\partial x}{\partial \xi_x^c},$$

$$\frac{\partial y_c}{\partial \tau} = \frac{\partial y_c}{\partial \tau_x} \left( \frac{\partial \tau_x}{\partial \tau} \right) = \frac{K_x d_{pa} Q_a}{K_c d_{pc} Q_c} \frac{\partial y_c}{\partial \tau_x}.$$

Replacing into the general material balance equation and introducing the cation (FCR) and anion (FCA) resin volume fractions within the bed:

$$\frac{\partial x_x}{\partial \xi_x} + FCR \frac{\partial y_x}{\partial \tau_x} = 0 \quad (\text{eq. D-6}),$$

$$\frac{\partial x_n}{\partial \xi_x} + FCR \frac{\partial y_n}{\partial \tau_x} = 0 \quad (\text{eq. D-7}),$$

$$\frac{\partial x_c}{\partial \xi_x} + FCA \frac{\partial y_c}{\partial \tau_x} = 0 \quad (\text{eq. D-8}).$$

The rate equations that were developed earlier need to be modified to incorporate the dimensionless variables that have been introduced. This involves changing from  $t$  to  $\tau$  as the basis for the equations. The same principles apply as were used to modify the material balance equations. Ternary cation exchange, with binary anion exchange, yields two equations for the cation resin phase rates and one for the anion resin phase as:

$$\frac{\partial y_i}{\partial t} = K_i \left( \frac{D_{ei}}{D_i} \right)^{2/3} \frac{a_s C_i^o}{Q} \left( 1 - \frac{C_i^*}{C_i^o} \right)$$

Changing from  $t$  to  $\tau$  yields:

$$\frac{\partial y_i}{\partial \tau} = d_p a_s R_i \left( \frac{C_i^o}{C_T^f} - \frac{C_i^*}{C_T^f} \right) \quad (\text{eq. D-9}),$$

where  $R_i$  is equal to the two thirds power of the diffusivity ratio. It is useful to note that the product  $d_p a_s$  is equal to six, so:

$$\frac{\partial y_i}{\partial \tau} = 6 R_i \left( \frac{C_i^o}{C_T^f} - \frac{C_i^*}{C_T^f} \right)$$

Changing to the same basis for  $\tau$  or  $\tau_x$  yields three rate equations (assume: cations = n,h and x; anions = :c and o):

$$\frac{\partial y_x}{\partial \tau_x} = 6 R_x (x_x^o - x_x^*) \quad (\text{eq. D-10}),$$

$$\frac{\partial y_n}{\partial \tau_x} = \frac{K_n}{K_x} 6 R_n (x_n^o - x_n^*) \quad (\text{eq. D-11}), \text{ and}$$

$$\frac{\partial y_c}{\partial \tau_x} = \frac{K_c d_{pc} Q_c}{K_x d_{pa} Q_a} (x_c^o - x_c^*) \quad (\text{eq. D-12}).$$

This represents the rate equations that describe the exchange process. These coupled with the previously derived material balance equations need to be solved simultaneously to determine the effluent concentration history. The six component system is an extension of the previous equations to incorporate a third anionic species. Fortunately, solution methods for these types of systems are fairly well documented. They can be solved by the method of characteristics. The general approach is described briefly in Appendix E.

## APPENDIX E

### NUMERICAL TECHNIQUES

The material balance equations presented in Appendix D are a system of partial differential equations that need to be solved in order to determine the effluent concentration history for the MBIE column. The equations have been transformed to be of the form:

$$\frac{\partial X}{\partial \xi} = - \frac{\partial Y}{\partial \tau} = - R$$

Where R is the rate equation and the dependent variables are vectors. This system can be readily addressed by the method of characteristics. This method involves the solution of the system by evaluating it along curves of constant  $\tau$  and  $\xi$ . The evaluation along these lines reduces the system of partial differential equations to a system of ordinary differential equations where, the other independent variable is held constant. The method defines a grid structure for the calculation procedure. Solving these equations requires a technique for systems of differential equations.

There are a large number of methods that can be employed to solve systems of differential equations. In previous work, Omatete (1980b) compared three different single step methods; Runge-Kutta-Fehlberg, explicit Euler and modified Euler. All three methods converged to the same solution but the modified Euler method was the fastest of the three. Dranoff and Lapidus (1961) employed

Milne's method to solve the material balance equations. They found that towards the end of the exchange process, the instability that can be present in Milne's method occurred. The MBIE modeling efforts of Haub and Foutch (1986a,b) employed the modified Euler method in  $\xi$  and the explicit Euler method in  $\tau$ . This method has been improved upon by using an implicit method that does not suffer from the same instabilities that Milne's method does. The increased accuracy and proven stability of the Adams-Bashforth-Moulton implicit method led to its adoption for the solution of the material balance equations in  $\xi$  and the explicit Adams-Bashforth method in  $\tau$ .

Adams-Bashforth (fourth order) method employs a Newton-Gregory interpolating polynomial applied to the previous four points, which is then integrated. This extends the functions influence from just the previous step, as in Euler, to the previous four steps. The resulting formula for the calculation of the next variable value is:

$$y_{n+1} = y_n + \frac{h}{24} \left( 55 f_n - 59 f_{n-1} + 37 f_{n-2} - 9 f_{n-3} \right)$$

This is used as the predictor equation in the Adams-Bashforth-Moulton method. The corrector, or fourth order Adams-Moulton equation, introduces the implicit portion of the method as:

$$y_{n+1} = y_n + \frac{h}{24} \left( 9 f_{n+1} + 19 f_n - 5 f_{n-1} + f_{n-2} \right)$$

These equations are both employed when using the implicit method, and only the predictor is used for the explicit method. The value of  $f_{n+1}$  in the corrector equation is evaluated with the value obtained for  $y_{n+1}$  from the predictor equation. This method can be applied as many times as is necessary to achieve the desired accuracy.

The error in employing the explicit Euler's method is on the



order of the step size (global). The modified (or implicit) Euler's method has a global error on the order of the step size squared. Runga-Kutta-Fehlberg has a global error on the order of the step size to the fifth power. The Adams-Bashforth explicit method is order step size to the third and the implicit Adams-Bashforth-Moulton is on the order of the step size to the fourth. Table I summarizes the global error that each of these methods causes plus the number of function evaluations required per step. The Runga-Kutta-Fehlberg requires six function evaluations per step, this emphasizes the trade off between accuracy and speed. The Adams-Bashforth-Moulton (ABM) method requires only two evaluations per step once the initial four steps have been completed and is considerably more accurate than Euler's method. Since the implicit ABM method requires the previous four points, a modified Euler's method is employed to determine the first four function values in  $\xi$  and explicit Euler in  $\tau$ .

Table I

## Comparison of Numerical Techniques

Technique	Function Evaluations Per Step	Local Error	Global Error
Euler	1	$O(h^2)$	$O(h)$
Modified Euler	2	$O(h^3)$	$O(h^2)$
Runga- Kutta- Fehlberg	6	$O(h^6)$	$O(h^5)$
Adams- Bashforth	1	$O(h^4)$	$O(h^3)$
ABM	2	$O(h^5)$	$O(h^4)$

## APPENDIX F

### MODEL PARAMETER VALUES

The actual numeric value used in the different model evaluations are summarized here. The parameters used that were not included within the individual chapters are; particle diameters, void fraction, volumetric flow rate, column diameter, column height, and resin capacities.

The values used for the variables in Chapter II are:

Cation Particle Diameter: 0.0825 cm ,

Anion Particle Diameter: 0.06 cm ,

Void Fraction: 0.35 ,

Volumetric Flow Rate: 50.0 ml/s ,

Column Diameter: 5.0 cm ,

Column Height: 100.0 cm ,

Cation Resin Capacity: 2.1 meq/ml ,

Anion Resin Capacity: 1.4 meq/ml .

These values were used to evaluate ammonia cycle and morpholine cycle exchange.

The values used for Chapter III vary because of the comparisons with experimental data. The values used to compare with Omatete et al. are:

Cation Particle Diameter: 0.071 cm ,  
Void Fraction: 0.40 ,  
Volumetric Flow Rate: 0.5 ml/s ,  
Column Diameter: 2.5 cm ,  
Column Height: 55.0 cm ,  
Cation Resin Capacity: 1.94 meq/ml .

The values used to compare with Dranoff and Lapidus are:

Cation Particle Diameter: 0.0225 cm ,  
Void Fraction: 0.42 ,  
Volumetric Flow Rate: 1.24 ml/s ,  
Column Diameter: 1.5 cm ,  
Column Height: 2.5 cm ,  
Cation Resin Capacity: 1.94 meq/ml .

The values used in the Five and Six component calculations are:

Cation Particle Diameter: 0.0825 cm ,  
Anion Particle Diameter: 0.06 cm ,  
Void Fraction: 0.42 ,  
Volumetric Flow Rate: 1.0 ml/s ,  
Column Diameter: 2.54 cm ,  
Column Height: 5.0 cm ,  
Cation Resin Capacity: 1.94 meq/ml ,  
Anion Resin Capacity: 1.4 meq/ml .

Values used for the model evaluations in Chapter IV are the same as those used for the five and six component model except for using a column height of 10.0 cm.

APPENDIX G

COMPUTER SOURCE CODE LISTING FOR CHAPTER III

\*  
 \* This program was developed to model multi-component mixed  
 \* bed ion exchange with two anions and three cations. The model  
 \* can be readily modified for amine cycle exchange or hydrogen  
 \* cycle exchange past the amine break.  
 \*

\* The variables used within the code are defined as follows  
 \*

\* Print Control (1=Print, 0=No Print)  
 \*

\* KPBK When KPBK=1 and Time=0, effluent breakthrough is  
 \* printed at different time.  
 \* KPPR When KPPR=1, the concentration profiles for all ionic  
 \* species in the column are printed during the first  
 \* program iteration in which the time elapsed from feed  
 \* introduction exceeds the value of TIME in minutes.  
 \*

\* State of Regeneration  
 \*

\* YCO initial fraction of chloride on the anionic resin  
 \* YNO initial fraction of sodium on the cationic resin  
 \* YXO initial fraction of species x on the cationic resin  
 \*

\* Resin Characteristics  
 \*

\* PDC cation resin particle diameter (cm)  
 \* PDA anion resin particle diameter (cm)  
 \* VD bed void fraction  
 \* FCR cation resin volume fraction (cation resin/total resin)  
 \* FCA anion resin volume fraction (anion resin/total resin)  
 \*

\* Bed and System Variables  
 \*

\* CF total feed solution concentration (meq/cm<sup>3</sup>)  
 \* FR volumetric flow rate (cm<sup>3</sup>/sec)  
 \* DIA column diameter (cm)  
 \* CHT height of packed resin (cm)  
 \* AREA column cross-sectional area (cm<sup>2</sup>)  
 \* VS superficial liquid velocity (cm/sec)  
 \* TMP system temperature (C)  
 \*

\* Resin Constants  
 \*

\* QC cation resin capacity (meq/cm<sup>3</sup>)  
 \* QA anion resin capacity (meq/cm<sup>3</sup>)  
 \* TKCO selectivity coefficient for chloride-hydroxide exchange  
 \* TKNH selectivity coefficient for sodium-hydrogen exchange  
 \* TKXH selectivity coefficient for x-hydrogen exchange  
 \* TKNX selectivity coefficient for sodium-x exchange  
 \*

\* Numeric Constants  
 \*

\* TAU dimensionless time increment  
 \* XI dimensionless distance increment  
 \*

```

*
* Fluid Properties
*
*   CP   solution viscosity (cp)
*   DEN  solution density (g/cm3)
*
* Dimensionless numbers
*
*   REi  Reynolds number for ion i
*   SCi  Schmidt number for ion i
*   Di   Ionic diffusion coefficient for species i
*   KLi  Non-ionic mass transfer coefficient for species i
*   Ri   R value for species i
*
* Program Limits
*
*   TMAX time limit for column operation (min)
*   XNMAX effluent sodium concentration limit (Cn/Cn )
*
* All real variables will be double precision
*
* IMPLICIT INTEGER (I-N), REAL*8 (A-H,O-Z)
*
* Variable and array declaration
*
* REAL KLN, KLX, YNC(4,1100), XNC(4,1100), XXC(4,1100), RATEN(10),
1  RATN(4,1100), YXC(4,1100), RATEX(10), RATX(4,1100), XHC(4,1100),
2  RATC(4,1100), RATEC(4), YCA(4,1100), XCA(4,1100), XOA(4,1100),
3  KLA, XCAD(2)
*
* Function statements for determining non-ionic mass transfer
* coefficients based on system parameters
*
*   Carberry's Correlation
*
*       
$$F1(R,S) = 1.15*VS/(VD*(S**(2./3.))*(R**0.5))$$

*
*   Kataoka's Correlation
*
*       
$$F2(R,S) = 1.85*VS*((VD/(1.-VD))**(1./3.))/$$

1      
$$(VD*(S**(2./3.))*(R**(2./3.)))$$

*
* Open files output file
*
*   OPEN (6, FILE='O2.DAT', STATUS='NEW')
*
* Initial Conditions and Bed Properties
*
* DATA KPBK, KPPR, TIME/ 1, 0, 0.0D0/
* DATA YNO, YXO, YCO/ 0.00001, 0.00001, 0.00001/
* DATA PDC, PDA, VD/ 0.0825D0, 0.060, 0.42D0/

```

```

DATA CF, FR, DIA, CHT/ 1.0D-5, 1.0D0, 2.54D0, 10.0D0/
DATA TAU, XI, FCR, TKCO/ 0.005D0, 0.005D0, 0.4, 16.5/
DATA DEN, QC, QA, FCA/ 1.0D0, 1.94D0, 1.4, 0.6/
DATA TMAX, XNMAX, TMP/ 8.5D4, 0.99D0, 25.0D0/
DATA FNF, FXF, FHF/ 0.50, 0.50, 0.0/

```

```

*
*
*

```

Output system parameters

```

WRITE (6,10)
WRITE (6,11)
WRITE (6,12) YXO, YNO
WRITE (6,13) PDC, VD
WRITE (6,14) QC
WRITE (6,15) CF, FR, DIA, CHT

```

```

*

```

CP = 0.9004D0

```

*
*
*

```

Concentrations and Dissociation constant

```

CF1 = CF
DISS = 1.D-14
CF = CF+1.0D-7
DIV = CF/CF1

```

```

*
*
*
*

```

Calculation of Ionic Diffusion Coefficients based on Temperature using limiting ionic conductivities (Robinson and Stokes (1959))

```

RTF = (8.931D-10)*(TMP+273.16)
XLAMH = 221.7134+5.52964*TMP-0.014445*TMP*TMP
XLAMX = 1.40549*TMP+39.1537
XLAMN = 23.00498+1.06416*TMP+0.0033196*TMP*TMP
XLAMO = 104.74113+3.807544*TMP*TMP
XLAMC = 39.6493+1.39176*TMP+0.0033196*TMP*TMP
DN = RTF*XLAMN
DX = RTF*XLAMX
DO = RTF*XLAMO
DC = RTF*XLAMC
DH = RTF*XLAMH

```

```

*
*
*

```

Output Calculated Ionic Diffusion Coefficients

```

WRITE (6,16) DX, DN, DH, DC, DO
WRITE (6,17) CP, DEN, TMP

```

```

*
*
*
*

```

Calculate Reynolds numbers, Schmidt numbers and Non-ionic mass transfer coefficients

```

AREA = 3.1415927*(DIA**2)/4.
VS = FR/AREA
REC = PDC*100.*VS*DEN/((1.-VD)*CP)
REA = PDA*100.*VS*DEN/((1.-VD)*CP)
SCX = (CP/100.)/DEN/DX
SCN = (CP/100.)/DEN/DN
SCA = (CP/100.)/DEN/DC

```



```

      IF (REC.LT.20.) THEN
        KLN = F2(REC,SCN)
        KLX = F2(REC,SCX)
      ELSE
        KLN = F1(REC,SCN)
        KLX = F1(REC,SCX)
      ENDIF
      IF (REA.LT.20.) THEN
        KLA = F2(REA,SCA)
      ELSE
        KLA = F1(REA,SCA)
      ENDIF
*
*   Calculated total number of steps in distance (NT)
*
      CHTD = KLX*(1.-VD)*CHT/(VS*PDC)
      NT = CHTD/XI
*
*   Output calculated parameters
*
      WRITE (6,18)
      WRITE (6,19)
      WRITE (6,20)
      WRITE (6,21) TAU,XI,NT
      WRITE (6,22) REC,KLN,KLX,KLA
      WRITE (6,23) VS
*
*   Output breakthrough curve headings
*
      IF (KPBK.NE.1) GO TO 50
      WRITE (6,24)
      WRITE (6,25)
      WRITE (6,26)
      WRITE (6,27)
      WRITE (6,28)
50 CONTINUE
*
*   Output concentration profile headings
*
      T = 0.
      TAUPR = KLX*CF*(TIME*60.)/(PDC*QC)
      IF (KPPR.NE.1) GO TO 60
      WRITE (6,30)
      WRITE (6,31) TIME
      WRITE (6,32)
      WRITE (6,33)
      WRITE (6,34)
60 CONTINUE
*
*   Set initial fractions for the resin phase
*
      MT = NT + 1
      DO 100 M=1,MT
        YNC(1,M)=YNO

```

```

      YXC(1,M)=YXO
      YCA(1,M)=YCO
100 CONTINUE
*
*   Calculate dimensionless program time limit
*   based on inlet conditions (Z=0)
*
      TAUMAX = KLX*CF*(TMAX*60.)/(PDC*QC)
*
      J = 1
      JK = 1
      TAUTOT = 0.
      JFLAG = 0
      XNC(JK,NT) = 0.
      KK = 1
*
*   Time stepping loop within which all column calculations are
*   implemented, time is increment and outlet concentrations checked
*
1 CONTINUE
  IF (TAUTOT.LT.TAUMAX.AND.XNC(JK,NT).LT.XNMAX) THEN
*
*   Correction of time step value for Adams-Bashforth Method
*
      IF (J.EQ.4) THEN
          JD = 1
      ELSE
          JD = J + 1
      ENDIF
*
*   Set inlet liquid phase fractional concentration for each
*   species in the matrix
*
      XNC(J,1) = FNF/DIV
      XXC(J,1) = FXF/DIV
      XHC(J,1) = 1.0D-7/CF
      XOA(J,1) = 1.0D-7/CF
      XCA(J,1) = (FNF+FXF)/DIV
*
*   Calculation for bed length at a fixed time
*
      DO 400 K=1,NT
*
*   Define bulk phase concentrations for subroutines
*
      CXO = XXC(J,K)*CF
      CNO = XNC(J,K)*CF
      CHO = XHC(J,K)*CF
      COO = XOA(J,K)*CF
      CCO = XCA(J,K)*CF
      CCT2 = CCO
      CNT2 = CNO
      CXT2 = CXO
      CH1 = CHO

```

```

CO1 = COO
YN = YNC(J,K)
YX = YXC(J,K)
YC = YCA(J,K)
XNL = XNC(J,K)
XXL = XXC(J,K)
XCL = XCA(J,K)
*
*   Solve the tau constant material balance equation in xi
*
DO 300 L=1,2
*
*   Call subroutines to calculate RN, RX, CNI, CXI
*
IF (YX .LT. 1.0) THEN
  CALL CR (CHO,CNO,CXO,DH,DN,DX,YN,YX,CNI,CXI,RN,RX,CTI)
  XXI = CXI/CF
  XNI = CNI/CF
ELSE
  XXI = 1.0
  XNI = 0.0
  RN = 0.0
  RX = 0.0
ENDIF
*
*   Call subroutine to find RIA and CCI
*
IF (YC .LT. 1.0) THEN
  CALL BULK (TKCO,COO,CCO,YC,DO,DC,RIA,XCI)
ELSE
  XCI = 1.0
  RIA = 0.0
ENDIF
XCAD(1) = XCA(J,K)
XCI = XCI*XCAD(L)
*
*   Evaluate the rate of exchange
*
RATEN(L) = 6.*RN*(XNL - XNI)*KLN/KLX
RATEX(L) = 6.*RX*(XXL - XXI)
RATEC(L) = 6.*RIA*(XCL - XCI)*KLA*PDC/KLX/PDA
IF (L .EQ. 2) GO TO 310
*
*   First step calculation across bed inlet
*
IF (K .EQ. 1) THEN
  RATN(J,1) = RATEN(1)
  RATX(J,1) = RATEX(1)
  RATC(J,1) = RATEC(1)
  YNC(JD,1) = ABS(YNC(J,1)+TAU*RATN(J,1))
  YXC(JD,1) = ABS(YXC(J,1)+TAU*RATX(J,1))
  YCA(JD,1) = ABS(YCA(J,1)+TAU*RATC(J,1)*QC/QA)
  IF ((YNC(JD,K+1)+YXC(JD,K+1)).GT.1.0) THEN
    YYY= YNC(JD,K+1)+YXC(JD,K+1)
  
```

```

      YNC(JD,K+1) = YNC(JD,K+1)/YYY
      YXC(JD,K+1) = YXC(JD,K+1)/YYY
    ENDIF
  ENDIF
*
*   Use Modified Euler's method to obtain the first four function
*   values, then change to Adams-Bashforth
*
      IF(K.LE.3) THEN
        XN2 = XNC(J,K) - XI*RATEN(L)*FCR
        XX2 = XXC(J,K) - XI*RATEX(L)*FCR
        XC2 = XCA(J,K) - XI*RATEC(L)*FCA
      ELSE
        COEN=55.*RATEN(L)-59.*RATN(J,K-1)+37.*RATN(J,K-2)-9.*RATN(J,K-3)
        XN2 = ABS(XNC(J,K)-XI/24.*COEN*FCR)
        COEX=55.*RATEX(L)-59.*RATX(J,K-1)+37.*RATX(J,K-2)-9.*RATX(J,K-3)
        XX2 = ABS(XXC(J,K)-XI/24.*COEX*FCR)
        COEC=55.*RATEC(L)-59.*RATC(J,K-1)+37.*RATC(J,K-2)-9.*RATC(J,K-3)
        XC2 = ABS(XCA(J,K)-XI/24.*COEC*FCA)
      ENDIF
*
*   Determine intermediate concentrations and calculate
*   equilibrium hydrogen and hydroxide concentrations
*
        XCAD(2) = XC2
        CNO2 = XN2 * CF
        CXO2 = XX2 * CF
        CCO2 = XC2 * CF
        CHT = CHO - CXO2+CXO-CNO2+CNO
        COT = COO - CCO2+CCO
        CALL EQB(DISS,CHT,COT)
*
*   Redefine bulk phase concentrations for subroutines...
*
        CNO = CNO2
        CXO = CXO2
        CHO = CHT
        CCO = CCO2
        COO = COT
        YX = YXC(J,K+1)
        YN = YNC(J,K+1)
        YC = YCA(J,K+1)
        XNL = XN2
        XXL = XX2
        XCL = XC2
300 CONTINUE
310 CONTINUE
*
*   Impliment Implicit Portion of the Adams-Bashforth-Molton
*   method provided that the previous function values are known
*
      IF (K.LE.3) THEN
        XNC(J,K+1) = XNC(J,K) - (XI/2.)*(RATEN(1) + RATEN(2))*FCR
        XXC(J,K+1) = XXC(J,K) - (XI/2.)*(RATEX(1) + RATEX(2))*FCR

```

```

XCA(J,K+1) = XCA(J,K) - (XI/2.)*(RATEC(1) + RATEC(2))*FCA
ELSE
COEN=9.*RATEN(2)+19.*RATEN(1)-5.*RATN(J,K-1)+RATN(J,K-2)
XNC(J,K+1) = ABS(XNC(J,K) - (XI/24.)*COEN*FCR)
COEX=9.*RATEX(2)+19.*RATEX(1)-5.*RATX(J,K-1)+RATX(J,K-2)
XXC(J,K+1) = ABS(XXC(J,K) - (XI/24.)*COEX*FCR)
COEC=9.*RATEC(2)+19.*RATEC(1)-5.*RATC(J,K-1)+RATC(J,K-2)
XCA(J,K+1) = ABS(XCA(J,K) - (XI/24.)*COEC*FCA)
ENDIF
*
* Determine concentrations for next distance step and recalculate
* bulk phase equilibria
*
CXO = XXC(J,K+1) * CF
CNO = XNC(J,K+1) * CF
CCO = XCA(J,K+1) * CF
CHO = CH1 - CNO - CXO + CXT2 + CNT2
COO = CO1 - CCO + CCT2
CALL EQB(DISS,CHO,COO)
XHC(J,K+1) = CHO/CF
XOA(J,K+1) = COO/CF
*
* Call subroutines to determine rates at constant xi for solution
* of the tau material balance
*
IF (YX.LT.1.0) THEN
CALL CR (CHO,CNO,CXO,DH,DN,DX,YN,YX,CNI,CXI,RN,RX,CTI)
XXI = CXI/CF
XNI = CNI/CF
ELSE
XXI = 1.0
XNI = 0.0
RN = 0.0
RX = 0.0
ENDIF
IF (YC .LT. 1.0) THEN
CALL BULK (TKCO,COO,CCO,YC,DO,DC,RIA,XCI)
ELSE
XCI = 1.0
RIA = 0.0
ENDIF
XCI = XCI*XCA(J,K+1)
*
RATN(J,K+1) = 6.*RN*((XNC(J,K+1)) - XNI)*KLN/KLX
RATX(J,K+1) = 6.*RX*((XXC(J,K+1)) - XXI)
RATC(J,K+1) = 6.*RIA*PDC*KLA*((XCA(J,K+1)) - XCI)/PDA/KLX
*
* Determine Y using adams-bashforth
*
IF (KK.LE.1) THEN
YNC(J,K+1) = YNC(J,K+1) + TAU*RATN(J,K+1)
YXC(J,K+1) = YXC(J,K+1) + TAU*RATX(J,K+1)
YCA(J,K+1) = YCA(J,K+1) + TAU*RATC(J,K+1)*QC/QA
ELSE

```

```

      IF(J.NE.1) GOTO 201
      J1=4
      J2=3
      J3=2
      GOTO 209
201  IF (J.NE.2) GOTO 202
      J1=1
      J2=4
      J3=3
      GOTO 209
202  IF (J.NE.3) GOTO 203
      J1=2
      J2=1
      J3=4
      GOTO 209
203  J1=3
      J2=2
      J3=1
209  COEN=55.*RATN(J,K+1)-59.*RATN(J1,K+1)
      COEN = COEN +37.*RATN(J2,K+1)-9.*RATN(J3,K+1)
      YNC(JD,K+1)=ABS(YNC(J,K+1)+(TAU/24.)*COEN)
      COEX =57.*RATX(J,K+1)-59.*RATX(J1,K+1)
      COEX = COEX +37.*RATX(J2,K+1)-9.*RATX(J3,K+1)
      YXC(JD,K+1)=ABS(YXC(J,K+1)+(TAU/24.)*COEX)
      COEC=55.*RATC(J,K+1)-59.*RATC(J1,K+1)
      COEC = COEC +37.*RATC(J2,K+1)-9.*RATC(J3,K+1)
      YCA(JD,K+1)=ABS(YCA(J,K+1)+(TAU/24.)*COEC*QC/QA)
      ENDIF
      IF ((YNC(JD,K+1)+YXC(JD,K+1)).GT.1.0) THEN
      YYY= YNC(JD,K+1)+YXC(JD,K+1)
      YNC(JD,K+1) = YNC(JD,K+1)/YYY
      YXC(JD,K+1) = YXC(JD,K+1)/YYY
      ENDIF
*
*   Output concentration profiles
*
      IF (KPPR.NE.1) GO TO 350
      IF (TAUTOT.LT.TAUPR) GO TO 350
      JFLAG = 1
      ZA = FLOAT(NT)
      ZB = FLOAT(K-1)
      Z = ZB*CHT/ZA
      KOUNT = KOUNT+1
      IF (KOUNT.NE.(KOUNT/10*10)) GOTO 350
      WRITE (6,35) Z,XNC(J,K),XXC(J,K),XHC(J,K),YNC(J,K),YXC(J,K)
350 CONTINUE
400 CONTINUE
*
*   Output breakthrough curves
*
      IF (KPBK.NE.1) GO TO 450
      KK = KK+1
      TAUTIM = TAUTOT*PDC*QC/(KLX*CF*60.)
      T = TAUTIM

```

```

WRITE (6,29) TAUTIM,XNC(J,NT),XXC(J,NT),XHC(J,NT),XCA(J,NT),
1      XOA(J,NT),YNC(J,NT),YXC(J,NT)
450 CONTINUE
   JK = J
   IF (J.EQ.4) THEN
       J = 1
   ELSE
       J = J+1
   ENDIF
*
   IF (JFLAG.EQ.1) STOP
   TAUTOT = TAUTOT + TAU
*
*   End of loop, return to beginig and step in time
*
   GOTO 1
   ENDIF
*
*   Output formats Statements
*
10 FORMAT ('1MIXED BED SYSTEM PARAMETERS:')
11 FORMAT ('0')
12 FORMAT ('ORESIN REGENERATION',7X,' : YXO=',F5.3,8X,'YNO=',F5.3)
13 FORMAT ('ORESIN PROPERTIES',9X,' : PDC=',F6.4,6X,'VD  =',F6.4,6X)
14 FORMAT ('ORESIN CONSTANTS',10X,' : QC =',E10.4)
15 FORMAT ('OCOLUMN PARAMETERS',8X,' : CF =',E10.4,'   FR =',F7.3,5X,
1      'DIA =',F5.2,7X,'CHT =',F5.1)
16 FORMAT ('OIONIC CONSTANTS',10X,' : DX =',E10.4,'   DN =',E10.4,
1      '2X,'DH  =',E10.4,2X,'DC =',E10.4,2X,'DO =',E10.4)
17 FORMAT ('OFLUID PROP.', ' : CP =',F7.5,' DEN=',F6.4,' TEMP=',F6.3)
18 FORMAT ('0')
19 FORMAT ('OCALCULATED PARAMETERS')
20 FORMAT ('0')
21 FORMAT ('OINTEGRATION INCREMENTS   : TAU=',F7.5,5X,'XI =',F7.5,
1      '5X,'NT  =',I6)
22 FORMAT ('OTRANSFER COEFFICIENTS     : REC=',E10.4,
1      '   KLN =',E10.4,'   KLX =',E10.4,'KLA =',E10.4)
23 FORMAT ('OSUPERFICIAL VELOCITY      : VS =',F7.3)
24 FORMAT ('1')
25 FORMAT ('OBREAKTHROUGH CURVE RESULTS:')
26 FORMAT ('0')
27 FORMAT ('0',6X,'T(MIN)',9X,'XNC',11X,'XXC',11X,'XHC',11X,'XCA',
1      '11X,'XOA',11X,'YNC',11X,'YXC')
28 FORMAT ('0')
29 FORMAT ('0',8(2X,E12.5))
30 FORMAT ('1')
31 FORMAT ('OCONCENTRATION PROFILES AFTER ',F5.0,' MINUTES')
32 FORMAT ('0')
33 FORMAT ('0',9X,'Z',11X,'XNC',11X,'XXC',11X,'XHC',11X,'YNC',
1      '11X,'YCA')
34 FORMAT ('0')
35 FORMAT ('0',6(2X,E12.5))
138 STOP
    END

```

```

*
* Subroutines
*
SUBROUTINE CR (CHO, CNO, CXO, DH, DN, DX, YN, YX, CNI, CXI, RN, RX, CTI)
*
* Subroutine to calculate Ri and interfacial concentrations
* for ternary exchange
*
IMPLICIT REAL*8 (A-H,O-Z)
*
TKNH = 1.5D0
TKXH = 2.4D0
TKNX = TKNH/TKXH
AH = DH/DN
AX = DX/DN
S = (CHO+CNO+CXO)*(AH*CHO+CNO+AX*CXO)
*
DENOM1 = TKNH+(1-TKNH)*YN+(TKNX-TKNH)*YX
DENOM2 = AH*TKNH+(1-AH*TKNH)*YN+(AX*TKNX-AH*TKNH)*YX
*
* Calculate Interfacial Concentrations
*
CNI = YN*(ABS(S/DENOM1/DENOM2)**0.5)
CXI = ABS(CNI*TKNX*YX/YN)
CHI = ABS(CNI*TKNH*(1-YN-YX)/YN)
CTI = CNI+CHI+CXI
CTO = CXO+CHO+CNO
CTR = CTI/CTO
CNR = CNI/CNO
CXR = CXI/CXO
BBB = 1.+ CTR
*
* Calculate Ternary Effective Diffusivities
*
IF (CNI.NE.CNO) GOTO 57
DEN = 0.0
GOTO 58
57 DEN = 2.*(CTR*CNR-1.)
CCC = 1.- CNR
DEN = DEN/(BBB*CCC)
58 IF (CXI.NE.CXO) GOTO 59
DEX = 0.0
GOTO 61
59 DEX = 2.*(CTR*CXR-1.)
BBX = 1.- CXR
DEX = DEX/(BBX*BBB)
61 CONTINUE
*
* Calculate Ri's for components
*
EPN = 2./3.
RN = (ABS(DEN))**(EPN)
RX = (ABS(DEX))**(EPN)
*

```



```

RETURN
END

*
*
SUBROUTINE BULK (TKNA,CAO,CNO,YN,DA,DN,RIC,XNI)
*
*   Subroutine to calculate Ri and the interface concentration
*   using the bulk phase neutralization model for binary exchange
*
IMPLICIT REAL*8 (A-H,O-Z)
A = DA/DN
Y = CAO/CNO
IF (YN.GT.1.0) YN = 1.0
IF (YN.LT.0.0001) THEN
    YP = ((CAO/CNO + 1./A) * (CAO/CNO + 1.))**0.5
    DE = 2.*A*(YP - CAO/CNO - 1.) / (1.-A)
    XNI = 0.0
ELSE
    S = TKNA*(1. - YN)/YN
    XNI = (((A*Y+1.)*(Y+1.))/((A*S+1.)*(S+1.)))**0.5
    DE = 2.*A*(S*XNI+XNI-Y-1.)/((1.-A)*(1.-XNI))
ENDIF
RIC = ABS((DE))**(2./3.)
RETURN
END

*
SUBROUTINE EQB(DISS,CAO,COO)
*
*   Subroutine to calculate bulk phase concentrations
*   based on water equilibrium
*
IMPLICIT REAL*8 (A-H,O-Z)
V=CAO*COO
IF (V.EQ.DISS) GOTO 57
V1=(COO-CAO)*(COO+CAO)+4.*DISS
X2=(CAO+COO-(V1**0.5))/2.
56 CAO=CAO-X2
COO=COO-X2
57 RETURN
END

```

2  
VITA

Edward J. Zecchini

Candidate for the Degree of  
Doctor of Philosophy

Dissertation: SOLUTIONS TO SELECTED PROBLEMS IN MULTI-COMPONENT  
MIXED-BED ION EXCHANGE MODELING

Major Field: Chemical Engineering

Biographical:

Personal Data: Graduated from Queensbury High School, Glens Falls, New York, June 1982; received Associate of Science in Engineering from Adirondack Community College, Glens Falls, New York, May 1983; received Bachelor of Science in Chemical Engineering from Rensselaer Polytechnic Institute, May 1985; received Master of Science in Chemical Engineering from Oklahoma State University, December 1986; Completed requirements for the Doctor of Philosophy Degree in Chemical Engineering at Oklahoma State University in July, 1990.

Professional Organizations: Student member of the American Institute of Chemical Engineers and Omega Chi Epsilon; Associate member of Sigma Xi; Engineering Intern as of June 1986; EI member of Oklahoma and National Society of Professional Engineers.

Professional Experience: Research Assistant, School of Chemical Engineering, Oklahoma State University, September 1985 to November 1986; Research Associate, School of Chemical Engineering, Oklahoma State University, December, 1986 to May, 1990; Instructor, School of Chemical Engineering, Oklahoma State University, August, 1989 to December 1989.